

INTRA-ANNUAL TO INTER-DECADAL VARIABILITY IN THE UPPER
COLORADO HYDROCLIMATOLOGY: DIAGNOSIS, FORECASTING AND
IMPLICATIONS FOR WATER RESOURCES MANAGEMENT

By

SATISH KUMAR REGONDA

B.Tech., Kakatiya University, India, 2000

M.Tech., Indian Institute of Technology Kanpur, India, 2002

A thesis submitted to the faculty of the Graduate School of the University of

Colorado in partial fulfillment of the requirement for the degree of

Doctor of Philosophy

Department of Civil, Environmental, and Architectural Engineering

2006

This thesis entitled:
Intra-annual to Inter-decadal Variability in the Upper Colorado Hydroclimatology:
Diagnosis, Forecasting and Implications for Water Resources Management
written by Satish Kumar Regonda
has been approved for the
Department of Civil, Environmental, and Architectural Engineering

Balaji Rajagopalan

Edith Zagona

Kenneth Strzepek

Date _____

The final copy of this thesis has been examined by the signatories, and we find that both the content and the form meet acceptable presentation standards of scholarly work in the above mentioned discipline.

Regonda, Satish Kumar (Ph.D., Civil, Environmental, and Architectural Engineering)

Intra-annual to Inter-decadal Variability in the Upper Colorado Hydroclimatology:

Diagnosis, Forecasting and Implications for Water Resources Management

Thesis directed by Professor Balaji Rajagopalan

This research analyzes hydrological variability in association with climate variability and climate change; and using this information it develops a statistical forecasting framework which is then integrated with a decision support system to manage water resources efficiently. This research has three major components: (i) Climate diagnostics of hydroclimate variables; (ii) Development of a statistical forecasting framework; and (iii) Evaluation of water resources decision strategies. As part of the first component, interannual variability of various hydroclimate variables is studied and large-scale climate features that drive the variability are diagnosed. The second component develops a framework for ensemble seasonal streamflow forecasts using the large-scale climate information obtained from the diagnostics. This uses nonparametric methods (assumption free and data driven) in association with an objective criterion, Generalized Cross Validation (GCV, selects a suite of best models) to issue ensemble forecasts of seasonal streamflow at several lead times (i.e., one month to five months at monthly intervals), and at several locations simultaneously. In the third component, forecasted streamflow ensembles drive a water resources Decision Support System (DSS) and the skills of various decision variables are evaluated. The DSS used is RiverWare, a flexible tool in which operational policies are easily incorporated.

The utility of this integrated climate diagnostics-to-DSS framework is demonstrated by successfully implementing it on the Gunnison River Basin, in Colorado, USA. This basin is in a semi-arid climate and has several competing water resources including agriculture, water supply, energy and environmental considerations. The framework can also be used for future planning and management of water resources in the basin. This offers an attractive tool for integrated water resources management and planning, especially in the western US, which is severely water stressed. Last, but not least, a methodology is proposed to generate realistic streamflow scenarios using paleo reconstructions (tree ring based reconstructions of past streamflows) in conjunction with the limited observational record. This approach provides the ability to generate a richer variety of drought and flood scenarios than those observed in recent history. It, thus, provides useful insight into streamflow variability, which is crucial for water resources management and planning in the basin.

DEDICATION

To my parents, brothers, late grandfather and late grandmother, friends, and teachers
who instilled values in me and shaped me who I am today.

ACKNOWLEDGEMENTS

I am highly indebted to my research advisor, Dr. Balaji Rajagopalan, for his valuable suggestions and constant guidance which influenced my academic and non-academic life. Discussions with him always enhanced my interest in research; his extraordinary patience and easy accessibility allowed me to effectively learn about many issues. His encouragement was pivotal to improving my abilities as a research scientist. I owe him more than words of thanks can ever convey.

My co-advisors, Dr. Edith Zagona and Dr. Martyn Clark, are very kind and taught me many issues with a lot of patience. Dr. Edith Zagona's valuable guidance improved various aspects of my professional skills, particularly in organizing thoughts and communicating effectively. Dr. Martyn Clark always encouraged new ideas and motivated me by inculcating independent thinking. Discussions with him broadened my horizons and exposed me to various interdisciplinary research areas. I am fortunate to have these advisors; their guidance inspired me and their unconditional freedom and encouragement motivated me to do my best.

I am very thankful to my committee members Dr. Shaleen Jain and Dr. Kenneth Strzepek for serving on my thesis committee and providing valuable insight.

Funding for this study by the NOAA Regional Integrated Sciences and Assessment Program, the Western Water Assessment (WWA) - NOAA cooperative agreement NA17RJ1229 is gratefully acknowledged. I also wish to give special thanks to Brad Udall, director, WWA for his constant support throughout the entire period.

Additional important funding from Center for Advanced Decision Support for Water and Environmental Systems (CADSWES) through logistical and

computational support and also Dr. Edith Zagona's valuable time is gratefully acknowledged – without which this research would not be possible.

Paul Davidson and Christopher Cutler of the USBR in Salt Lake City were greatly helpful and provided valuable information on the Gunnison River basin. The help of Brenda Alcorn, Jeff Smith and Steve Shumate of Colorado Basin River Forecast Center is also greatly appreciated. Research scientists of the CU *hydroclimate group*, particularly Dr. Andrew Slater, Dr. Subhrendu Gangopadhyay, Dr. Andy Barrett, and Dr. Andrea Ray, exposed me to different areas of research with their exciting work. Many other people provided valuable information on this research, and I appreciate their help.

I thank Dr. Ashu Jain, Dr. Krishna Kanikicharla, Dr. Hari Rajaram, Dr. Vijay Gupta, Dr. John Pitlick, and Dr. Sanaga Srinivasulu for their encouragement during my Ph.D. program. Also, I thank James Pasquotto, Bill Oakley, and Steve Setzer for their help with RiverWare model building. Special thanks to my friends, Veerender Garg and Sitara Nerella for proof reading this thesis.

I do thank all my friends in Boulder and Vani Cheruvu in particular who had taught me many things since my arrival in Boulder. The good hearted friendly nature of Katrina Grantz, Matt Grantz, and James Priarie made me feel at home. Discussion with Ravi Inampudi, a.k.a guru, helped me understand various aspects of life. Bruce Ward always encouraged me to push myself to give speeches in an effective way.

Special thanks to my academic friends, particularly, Carly Jerla, Somkiat Apipattanavis, John Emmert, Sarah Stapleton, Russell Callejo, and my non-academic friends, Sunil, Ashish, Krishna(s), Aditya(s), Prasad, Phani, Harish, Preeti, Balakishore, Hrishikesh, Aravind, Ajay, Amaranatha, Sandeep, Senthil, and Sundar. There are a large number of friends (especially cricket friends) who spiced things up,

and I thank each and every one of them. Also, it was very nice to work with CADSWESIANS, who made me feel comfortable being at CADSWES. In the fabulous company of these friends, the past four years were just melted like the snow of recent years (very fast!).

Friends from my Masters program Madhukar, Rajsekhar, Ravinder, Pijush (a.k.a dada), Uma, Deepak, and Balaji, and from my undergraduate studies Veerander, Sudhakar, Srikanth and Ramana, and my childhood friends Naveen, Anil, and Vamshidhar always encouraged me in what I am doing, and their support is greatly appreciated. Also, I express thanks to all my friends who encouraged me directly or indirectly to complete this research successfully.

I am greatly indebted to my uncle Gangadhar Motukuri who guided me in the early stages of my career. Thanks are due to my aunty Vijaya Motukuri, and to my late grandmothers, Narasamma Pulluri and Madhuramma Regonda, and to my uncles, particularly Satyanarayana Allenki and his family members, and to my cousins, particularly Santosh, Ganga, Sredevi, Shanti, Sridhar, Praveen, Prem, Pramod, Dr. Radhakrishna and Ramesh, for all their moral support and encouragement throughout my career. I wish to give special mention to my cousin Santosh Motukuri, from whom I learned many things in my life.

My deepest gratitude goes to my parents, Sulochana and Bhoomaiah, and brothers, Rajesh and Suresh, for their love, support, encouragement and understanding. My indebtedness to them is more than what I convey in words. My late grandfather, Rajesham Pulluri, was very influential and helped shape who I am today. Without all these people this thesis would not have been possible.

Satish Kumar Regonda

CONTENTS

CHAPTER 1	1
INTRODUCTION	1
1.1. Background.....	1
1.1.1. Water Management Challenges	1
1.1.2. Need for Forecasting.....	2
1.1.3. Current Forecast Framework	3
1.1.3.1. Limitations	5
1.1.4. Gunnison River Basin.....	6
1.1.4.1. Geographic Characteristics	6
1.1.4.2. Hydrologic Characteristics.....	6
1.1.5. San Juan River Basin	9
1.1.5.1. Geographic Characteristics	9
1.1.5.2. Hydrologic Characteristics.....	9
1.1.6. Decision Support System.....	11
1.1.7. Streamflow Scenarios for Long-term Planning	11
1.2. Proposed Research.....	12
1.3. Outline of the Thesis.....	13
CHAPTER 2	17
LARGE SCALE CLIMATE FEATURES AND THE WESTERN US HYDROCLIMATOLOGY	17
2.1. Interannual Variability.....	17
2.2. Hydroclimate Trends	20
CHAPTER 3	25
A MULTIMODEL ENSEMBLE FORECAST FRAMEWORK	25
3.1. Streamflow Forecasting Framework.....	25
3.1.1. Principal Component Analysis (PCA).....	26
3.1.2. Climate Diagnostics	27
3.1.3. Forecast Framework.....	27
3.1.4. Multimodel Selection.....	30
3.1.5. Multimodel Ensemble Forecast Algorithm.....	31

3.1.6. Links to Model Averaging Literature	32
3.1.7. Forecast Skill Evaluation	33
3.2. Data Sets	35
3.2.1. Streamflow	35
3.2.2. Snow	36
3.2.3. Large-scale Climate Variables	36
3.2.4. Palmer Drought Severity Index	37
3.3. Results.....	37
3.3.1. Gunnison River Basin.....	37
3.3.1.1. Streamflow characteristics: Principal Component Analysis.....	37
3.3.1.2. Climate Diagnostics - Predictor Selection	40
3.3.1.3. Multimodel Ensemble Forecast	43
3.3.2. San Juan River Basin	51
3.3.2.1. Streamflow characteristics - Principal Component Analysis.....	51
3.3.2.2. Climate Diagnostics-Predictor selection.....	55
3.3.2.3. Multimodel Ensemble Forecast	58
3.3.3. Comparison between multimodel ensemble and current framework	64
3.4. Summary and Discussions	70
CHAPTER 4	72
A NEW METHOD TO PRODUCE CATEGORICAL STREAMFLOW FORECASTS.....	72
4.1. Introduction.....	72
4.2. Methodology	76
4.2.1. Data.....	76
4.2.2. Forecast Method.....	77
4.2.2.1. Step 1: Principal Component Analysis (PCA).....	77
4.2.2.2. Step 2: Predictor Selection.....	78
4.2.2.3. Step 3: Categorical Forecast Framework - Logistic Regression.....	79
4.2.3. Forecast Evaluation.....	82
4.3. Results.....	83
4.4. Summary	85
CHAPTER 5	87

DECISION SUPPORT SYSTEM FOR GUNNISON RIVER BASIN FORECASTS	87
5.1. Introduction.....	87
5.2. Water Issues and Management Policies.....	88
5.3. The RiverWare Model	89
5.3.1. Taylor Park Reservoir Operations	93
5.3.2. Blue Mesa Reservoir Operations	93
5.3.3. Morrow Point Reservoir and Crystal Reservoir Operations	95
5.4. Methodology.....	95
5.4.1. Multimodel Ensemble Forecast Framework.....	95
5.4.2. Test Case.....	97
5.5. Results.....	100
5.5.1. Data.....	100
5.5.2. Streamflow Characteristics	100
5.5.3. Decision Variables	105
5.5.3.1. Taylor Park Reservoir	105
5.5.3.2. Blue Mesa Reservoir.....	106
5.6. Summary and Discussion.....	112
CHAPTER 6	114
A NEW FRAMEWORK TO SIMULATE STREAMFLOW SCENARIOS ON LONG TIME SCALES.....	114
6.1. Introduction.....	114
6.2. Paleo streamflow reconstructions	116
6.3. Proposed Approach.....	117
6.4. Application.....	119
6.5. Results.....	120
6.5.1. Performance Statistics.....	120
6.5.2. Sequent Peak Algorithm	124
6.6. Summary	125
CHAPTER 7	128
SUMMARY AND CONCLUSIONS	128
7.1. Summary.....	128
7.2. Conclusions.....	128

7.2.1. Multimodel ensemble forecast framework	128
7.2.2. Categorical Streamflow Forecast Framework.....	129
7.2.3. Decision Support System.....	131
7.2.4. Streamflow Scenarios for Long-term Planning	132
7.3. Future Work.....	133
REFERENCES	135

FIGURES

Figure 1: The annual streamflow of the Tomichi Creek at Gunnison, CO. The thick solid line corresponds to the average annual streamflow of all years at this location.....	2
Figure 2: Map of the Gunnison River Basin and six selected streamflow locations (detailed in the Table 1) shown as filled circles. Map was provided by James Pasquotto, University of Colorado, Boulder.....	7
Figure 3: Annual average hydrograph of the Gunnison River Basin. Monthly values (cms) are the average of streamflows at selected six locations (detailed in the Table 1).....	8
Figure 4: Map of the San Juan River Basin and selected two streamflow locations (detailed in the Table 2) shown as filled circles.....	10
Figure 5: Annual average hydrograph of the Animas River at Durango.....	10
Figure 6: Flow chart of the proposed decision support system that applied on the Gunnison River Basin.	16
Figure 7: (a) Percentage variance explained by the six Principal Components (PCs), (b) Time series of the first PC and, (c) Eigen loadings of the first PC at the six streamflow locations.....	38
Figure 8: (a) Scatter plot of first PC of spring flow and April 1st SWE along with the best fit linear regression line, and (b) Scatter plot of residuals of the first PC of spring flow from the regression fit in (a) with the preceding fall season PDSI – the thin line is the best fit line for the scatter and the solid line is the best fit line of the filled circle points.....	40
Figure 9: Correlation between the first PC of Spring flow and Nov-Mar large scale climate variables (a) Geopotential Height – 700 mb (b) Surface Air Temperature (C) Zonal wind - 700 mb (d) Meridional wind - 700 mb (e) Sea Surface Temperature. Maps were generated from NOAA’s Climate Diagnostic Center Website.	42
Figure 10: Composite maps of vector wind anomalies at 700 mb for (a) wet years and, (b) dry years. Maps were generated from NOAA’s Climate Diagnostic Center Website.	43
Figure 11: Using the LWP approach for $K=N$ and $p=1$, first PC flows are estimated as a function of (a) first PC SWE; (b) first PC SWE and PDSI; (c) first PC SWE and (MW-P1)-(MW-N1); and (d) first PC SWE and (MW-P1)-(MW-N2).	46
Figure 12: Boxplots of forecasted spring streamflow (million m ³) at Tomichi, issued on (a) January 1 st , and (b) April 1 st . The dashed horizontal lines represent the 33rd, 50th and 66th percentiles of the historical flow data which are shown as points connected by solid line.	48

Figure 13: Same as Figure 12 but for forecast of wet years issued on (a) January 1 st (b) April 1 st	48
Figure 14: Boxplots of forecasted spring streamflow (million m ³) at Tomichi for forecast of dry years issued on (a) January 1 st , and (b) April 1 st . The dashed horizontal lines represent the 33rd, 50th and 66th percentiles of the historical flow data which are shown as points connected by solid line.	49
Figure 15: Annual average hydrograph of McElmo Creek at CO-UT border line.....	52
Figure 16: Time series of the first PC of spring streamflows of SJRB.....	54
Figure 17: (a) Percentage variance explained by the five Principal Components (PCs), (b) Time series of the first PC and, (c) Eigen loadings of the first PC at the five SWE locations.	54
Figure 18: Scatter plot of first PC of, spring flow and April 1st SWE along with the best fit linear regression line.	55
Figure 19: Correlation between the first PC of Spring flow and Nov-Mar large scale climate variables (a) Geopotential Height – 500 mb (b) Surface Air Temperature (C) Zonal wind - 500 mb (d) Meridional wind - 500 mb (e) Sea Surface Temperature. Maps were generated from NOAA’s Climate Diagnostic Center Website.	57
Figure 20: Composite maps of vector wind anomalies at 500 mb for (a) wet years and, (b) dry years. Maps were generated from NOAA’s Climate Diagnostic Center Website.	58
Figure 21: Boxplots of forecasted spring streamflow (million m ³) for Animas River at Durango issued on (a) January 1 st , and (b) April 1 st . The dashed horizontal lines represent the 33rd, 50th and 66th percentiles of the historical flow data which are shown as points connected by solid line.	66
Figure 22: Same as Figure 21 but for forecasts of all years for McElmo Creek at CO-UT state borderline issued on (a) January 1st and (b) April 1st.....	66
Figure 23: Boxplots of forecasted spring streamflow (million m ³) for Animas River at Durango for forecast of wet years issued on (a) January 1 st , and (b) April 1 st . The dashed horizontal lines represent the 33rd, 50th and 66th percentiles of the historical flow data which are shown as points connected by solid line.....	67
Figure 24: Same as Figure 23 but for forecasts of dry years for Animas River at Durango issued on (a) January 1 st and (b) April 1 st	67
Figure 25: Boxplots of forecasted spring streamflow (million m ³) for McElmo Creek at CO-UT state borderline for forecast of wet years issued on (a) January 1 st , and (b) April 1 st . The dashed horizontal lines represent the 33rd, 50th and 66th percentiles of the historical flow data which are shown as points connected by solid line.	68

Figure 26: Same as Figure 25 but for forecasts of dry years for McElmo Creek at CO-UT state borderline issued on (a) January 1 st and (b) April 1 st	68
Figure 27: Comparison between multimodel ensemble streamflow forecast with CBRFC most probable forecast, for Blue Mesa reservoir inflows (a) January 1 st forecast; (b) April 1 st forecast. Boxplots corresponds to multimodel ensemble forecast; blue and red circles correspond to actual and most probable CBRFC forecast.	69
Figure 28: BSS of forecasts from the logistic regression (LR) framework (circles) and the “best model” (BM) ensemble of Regonda et al. [2006] (triangles), issued on 1 January (open circles and open triangles) and 1 April (solid circles and solid triangles) at the six locations in the GRB. Exceedance percentiles and BSS are plotted on x and y axes, respectively.	84
Figure 29: RiverWare workspace showing 24-month study model of the Gunnison River Basin.	92
Figure 30: Rules for operations of the reservoirs in the Gunnison River Basin.	96
Figure 31: Annual average hydrograph of four reservoir locations of the Gunnison Decision Support System (a) Taylor Park Reservoir, (b) Blue Mesa Reservoir, (c) Morrow Point Reservoir, and (d) Crystal Reservoir.	101
Figure 32: (a) Percentage variance explained by the four principal components (PCs), (b) time series of the first PC, and (c) eigen loadings of the first PC at the four reservoir locations.	102
Figure 33: Box plots of spring streamflow (KAF) at Blue Mesa Reservoir issued on (a) January 1st and (b) April 1st. The dashed horizontal lines represent the 33rd, 50th, and 66th percentiles of the historical flow data, which are shown as solid circles.	102
Figure 34: Boxplot of statistics for Blue Mesa Reservoir (a) mean, (b) standard deviation, (c) skew coefficient, (d) lag-1 correlation coefficient, (e) maximum flow and, (f) minimum flow. Left and right columns correspond to January 1st and April 1st forecasts.	104
Figure 35: Ranked Probability Skill Scores of decision variables of Taylor Park correspond to (a) spring (April through July) season and (b) winter (September though December) season. Circles, rectangles, and triangles represent all years, wet years, and dry year.	106
Figure 36: Ranked Probability Skill Scores of decision variables of Blue Mesa Reservoir for all months. First two left and last two right columns refer January 1 st and April 1 st issued forecasts respectively. Circles, rectangles, and triangles represent all years, wet years, and dry years respectively.	108
Figure 37: RPSS of decision variables of Blue Mesa Reservoir correspond to (a) spring (April through July) season and (b) winter (September though December) season. Circles, rectangles, and triangles represent all years, wet years, and dry year.	109

Figure 38: Probability Density Function (PDF) of decision variables of Blue Mesa Reservoir for year 1981 (dry year). Decision variables derived from forecasted and climatological streamflows are indicated with solid lines and dashed lines respectively. Solid vertical lines correspond to decision variables derived from actual streamflows. Black and blue lines correspond to the DSS that run on January 1 st and April 1 st respectively.....	110
Figure 39: Same as Figure 38, but for year 1985 (wet year).	110
Figure 40: RPSS of decision variables of Morrow Point Reservoir correspond to (a) spring (April through July) season and (b) winter (September through December) season. Circles, rectangles, and triangles represent all years, wet years, and dry year.	111
Figure 41: Same as Figure 40, but for Crystal Reservoir.	111
Figure 42: Time series of Paleo reconstructed streamflows (blue line) and natural streamflow estimates (red line) are shown. Mean of the natural streamflow estimates is plotted with thick solid line.	120
Figure 43: Boxplots of statistics of streamflow scenarios derived from KNN1 (left column) and proposed methods (right column). Solid triangles and solid circles correspond to the statistics computed for natural streamflow estimates and paleo reconstructed streamflows, respectively. Statistics are (a) mean, (b) standard deviation, (c) skew, (d) lag-1 correlation coefficient, (e) maximum, and (f) minimum.	122
Figure 44: Probability Density Function of annual streamflows generated from (a) traditional KNN method, and (b) KNN conditioned on paleo streamflows. Blue line corresponds to the natural streamflow estimates.	122
Figure 45: Boxplots of drought statistics (a) KNN1 – LS and LD, (b) proposed method – LS and LD, (c) KNN1 – MS and MD, and (d) proposed method – MS and MD.....	123
Figure 46: Boxplot of Yield-Storage of simulations from (a) Traditional KNN approach (b) KNN conditioned on paleo streamflows approach.....	125
Figure 47: The CDF of the storage values, derived from KNN1 (blue line) and proposed methods (red line), conditioned on yield of 2500 KAF. The vertical line corresponds to the storage value derived from natural streamflows.....	126

TABLES

Table 1: Gunnison River Basin streamflow data information.	8
Table 2: San Juan River Basin streamflow data information.	16
Table 3: Suite of predictors of GRB spring streamflow for April 1st forecast.....	44
Table 4: Multimodel combinations of GRB for April 1st forecast (presence and absence of predictors are indicated by “1” and “0”, respectively).....	45
Table 5: Ranked Probability Skill Scores of GRB forecasts at different lead times using ‘Climate and PDSI’ predictors and using ‘Climate, PDSI and SWE’ information.	51
Table 6: Teleconnection indices that are significantly correlated and corresponding seasons with their correlations are mentioned.	56
Table 7: Suite of predictors of SJRB spring streamflow for January 1 st forecast.....	59
Table 8: Suite of predictors of SJRB spring streamflow for April 1 st forecast.....	60
Table 9: Multimodel combinations of SJRB for January 1 st forecast (presence and absence of predictors are indicated by “1” and “0”, respectively).....	61
Table 10: Multimodel combinations of SJRB for April 1st forecast (presence and absence of predictors are indicated by “1” and “0”, respectively).....	62
Table 11: Ranked Probability Skill Scores of SJRB forecasts at different lead times using ‘Climate and PDSI’ predictors and using ‘Climate, PDSI and SWE’ information.....	69
Table 12: Correlation coefficients among actual observations, median of multimodel ensemble forecast and CBRFC's most probable forecast for two different lead times.	70
Table 13: Best predictor set for the Logistic Regression at different lead times.....	82
Table 14: Ranked Probability Skill Scores of Spring Streamflows Forecasts at Different Lead Times Using Climate and PDSI Predictors and Using Climate, PDSI, and SWE information.	103
Table 15: Probabilities of wet and dry conditions for paleo reconstructed streamflows and natural streamflow estimates. Wet years, if flow is greater than mean of natural flows, and vice versa for dry years.	121

CHAPTER 1

INTRODUCTION

1.1. Background

1.1.1. Water Management Challenges

Water resources play an important role in various socio-economic and environmental needs such as agriculture, industry, environmental preservation, energy production, and recreational purposes, and thus consequently, in the prosperity of society, environment and economy. The importance is further underscored in arid to semi-arid regions of the world where the water resources are variable in amount, quality, and demand. In addition, other variables such as competing water demands, societal development, population growth, future demand projections and climatic changes influence the planning and management of water resources. In recent years, several of these variables — in particular, increased development, population growth and climatic changes — have put great stress on the water resources around the world (e.g., Vorosmarty et al., 2000) and particularly in the western USA (e.g., Hamlet et al., 2002; Piechota et al., 2001). The recent 5-year long dry spell in the western USA, in association with increased demands, has generated many questions about the water resource system reliability, river basin planning and future management and robustness of current water compacts. In light of these concerns, careful planning and development is necessary to manage the competing water demands of the system (e.g., agricultural, municipal and industrial demand and releases required for ecological and environmental purposes), so as provide sustainable supplies.

1.1.2. Need for Forecasting

Hydrologic variability can be significant in the streamflows of river basins in the western US. For example, annual streamflows of Tomichi Creek (a tributary of the Gunnison River) at Gunnison, CO (Figure 1) indicates frequent wet and dry spells. Such variability leads to unreliable water availability to meet the diverse demands in the basin. To reduce the impacts of variability water, storage structures (e.g., reservoirs, canals) are developed which store water to ride out the dry spells and to provide a steady and reliable supply of water.

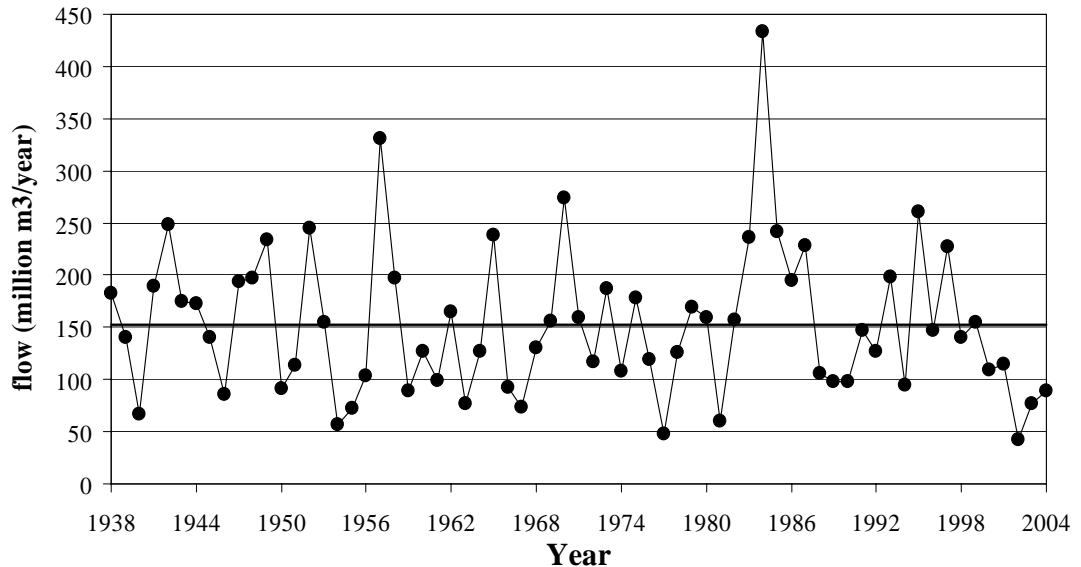


Figure 1: The annual streamflow of the Tomichi Creek at Gunnison, CO. The thick solid line corresponds to the average annual streamflow of all years at this location.

In the Gunnison River Basin, the study area of this research, the storage structures (i.e., reservoirs) have limited capacity, unlike the large reservoirs on the Colorado River. Furthermore, the demands on the basin are diverse and often in competition – e.g., the conflict between the amount of water stored and the timing of releases to meet agriculture, hydropower generation and environmental needs. Given these

challenges, skillful long lead forecast of streamflows (e.g., seasonal/monthly volume, timing of peak flow) are key to efficient and sustainable water resources development and management in this basin and in other such basins.

1.1.3. Current Forecast Framework

In the western USA, including the Gunnison and San Juan River basins (the study area of the research), most of the winter precipitation falls as snow, and in spring, the accumulated winter snow melts contributing a large amount to the annual flows. Therefore, winter snow pack is used as a predictor of the following spring runoff (Serreze et al., 1999). Currently, water managers use the basin snow water equivalent (SWE) during winter in a linear regression method for predicting the following spring streamflow. Additionally, a few large-scale climate patterns such as El Nino Southern Oscillation (ENSO) (Allan et al., 1996; Trenberth, 1997) and Pacific Decadal Oscillation (PDO) (Mantua et al., 1997) have also been used to predict streamflows in the western US. Hamlet and Lettenmaier (1999b) forecasted Columbia River streamflows using ENSO and PDO with several months lead-time. Clark et al. (2001) showed that including large-scale climate information together with SWE improved the overall skill of the streamflow predictions in the Columbia and Colorado River Basins. In almost all of these studies standard indices of ENSO and PDO have been used in conjunction with SWE. This is inadequate for several reasons. (1) Snow pack information is complete only by the start of snowmelt, thus limiting the lead time of the forecast. (2) Assumptions of linearity between the streamflows and predictors are not accurate. (3) Standard indices are not always well related to the streamflows because the surface climate is sensitive to minor shifts in large-scale atmospheric

patterns (e.g., Yarnal and Diaz, 1986). (4) The relationships are not stationary, as shown by McCabe and Dettinger (1999), who observed variation in the strength of ENSO teleconnections with precipitation in the western USA. Recently, Grantz et al. (2005) offered skillful predictions of spring streamflows on the Truckee and Carson Rivers in Nevada at two seasons ahead using large-scale climate information that alleviates some of these drawbacks.

In addition to the regression models, water managers in the Gunnison and San Juan River basins make operational decisions (e.g., daily, monthly) based on a 24-month operational forecast. In this, at the start of each month, streamflow forecasts/projections of the successive 24-month period are used to drive a simulation model of the river basin. The values of the system decision variables obtained from this 24-month outlook are used to make decisions such as reservoir releases and hydropower generation. The 24-month streamflow projection, issued by the U.S. Bureau of Reclamation (BOR), typically uses the Colorado Basin River Forecast Center's (CBRFC) April to July runoff forecast for the forecasts done in months January through July, and the CBRFC 3-month forecast for the remainder of the year, followed by climatology (monthly average flows) for the remaining months. CBRFC issues 10%, 50%, and 90% exceedance forecasts using primarily Extended Streamflow Prediction (ESP) and statistical regression that utilizes snow, streamflow, precipitation and climate indices (CBRFC scientists, personal communication, 2005). Thus, a single trace of the 24-month flows is developed combining all of the above information.

1.1.3.1. Limitations

In addition to the shortcomings of the SWE and standard climate indices based linear regression method for flow forecast, the key drawbacks of the BOR's forecast set up are: (i) a single 24-month trace does not quantify any uncertainty and (ii) the ESP method produces ensembles by driving a hydrologic model with past weather scenarios and current initial conditions, e.g., if there are 20 years of data available at a location the ESP method can only produce 20 ensembles. Although the input time series (i.e., past weather scenarios) of the ESP method is adjusted with monthly and seasonal forecasts of climate variables (e.g., temperature, precipitation, teleconnection indices), the range of uncertainty captured is still quite limited as it does not account for other sources of uncertainty (e.g., model structure and parameters).

Given these limitations in the current forecast framework and the increasing evidence that large-scale climate features (detailed in the Chapter 2) drive variability in regional hydrology at all time scales (sub-seasonal to decadal), a robust forecasting framework is proposed in this research. This new framework (described in the Chapter 3) incorporates predictive information from ocean-atmosphere-land system to generate spring seasonal ensemble streamflow forecasts at several lead times, providing a realistic representation of the uncertainty. The proposed method was applied to the Gunnison and San Juan River basins in the western USA.

1.1.4. Gunnison River Basin

1.1.4.1. Geographic Characteristics

The Gunnison River Basin (GRB) is located in the southwest part of Colorado (Figure 2). With a drainage area of approximately 7930 mi² (20,618 km²) and basin elevations ranging from 4,550 ft (1,387m) to 14,300 ft (4,359 m), the GRB extends from the continental divide to Grand Junction where it joins the Colorado River (McCabe, 1994). The Aspinall Unit is the major water development feature of the Colorado River Storage Project in the GRB. It consists of a series of three dams with associated storage reservoirs and hydroelectric plants, Blue Mesa, Morrow Point and Crystal, along a 40-mile (64 km) stretch of the river. The three reservoirs have a combined storage of approximately 1.1 million acre-feet (1,357 million m³) and hydropower generation capacity of 287 megawatts, and control one third of the total discharge of the river. The Gunnison tunnel, which is at the downstream of the Aspinall Unit, diverts water from the Gunnison River to the Uncompahgre Valley.

1.1.4.2. Hydrologic Characteristics

Climate in the GRB varies greatly due to its broad range of elevation; this is evident in the range of annual precipitation in the basin. The high mountains receive the highest precipitation of about 45-50 inches (1140-1270 mm) per year. The low elevated plains receive lowest precipitation of less than 10 inches (255 mm) per year (Ray, 2004). In addition to spatial variability, the precipitation also exhibits temporal variability. Stations at lower elevations have peak precipitation in summer whereas the high mountains have peak precipitation in the winter, with most of the annual

precipitation falling as snow. The annual hydrograph of the GRB (average of streamflows at selected six locations, detailed in Table 1) is shown in Figure 3. It can be seen that the majority (greater than 70 percent) of the annual flow occurs during the spring snowmelt (April – July). Consequently, spring flow plays a vital role in the decisions and management of the water, and several key decisions (e.g., fish releases) are made in January and February, hence long lead spring streamflow forecasts are crucial.

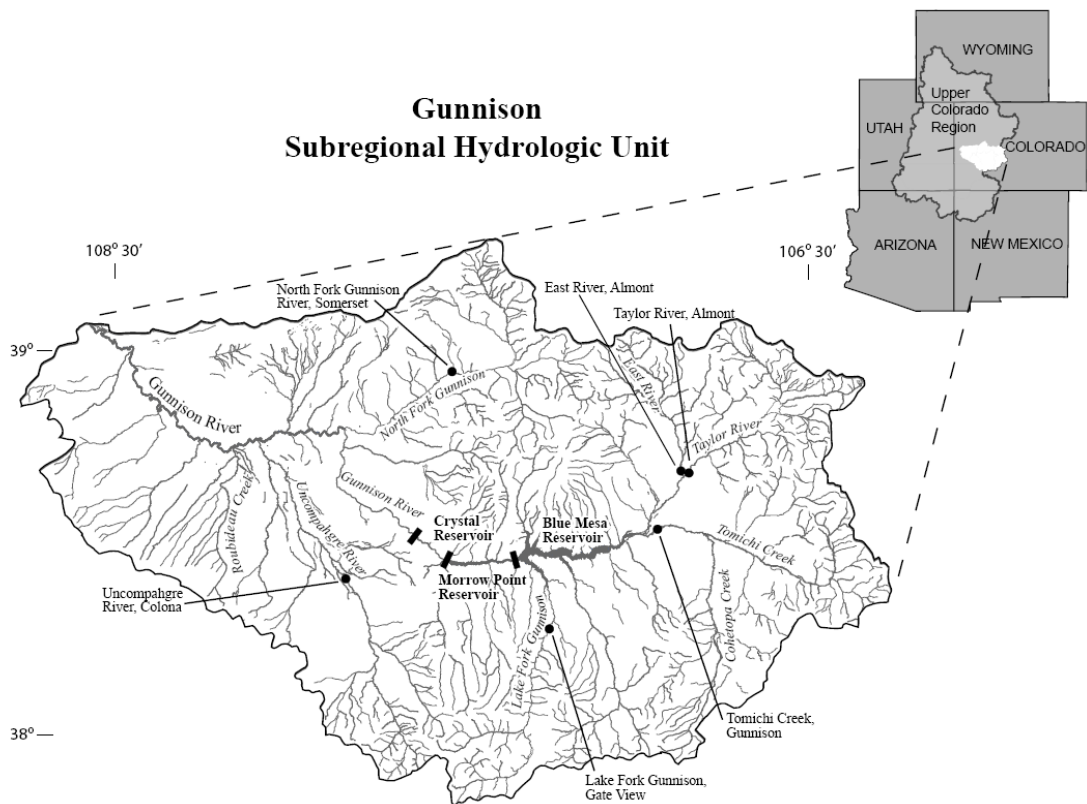


Figure 2: Map of the Gunnison River Basin and six selected streamflow locations (detailed in the Table 1) shown as filled circles. Map was provided by James Pasquotto, University of Colorado, Boulder.

Table 1: Gunnison River Basin streamflow data information.

Station Number	Site Number (USGS)	Site Name	Elevation (m)	Drainage Area (10^6 m ²)
1	09110000	Taylor River at Almont, CO	2442	1235
2	09112500	East River at Almont, CO	2440	749
3	09119000	Tomichi River at Gunnison, CO	2325	2748
4	09124500	Lake fork at Gate View, CO	2386	865
5	09132500	North fork Gunnison River near Somerset, CO	1914	1362
6	09147500	Uncompahgre River at Colona, CO	1926	1160

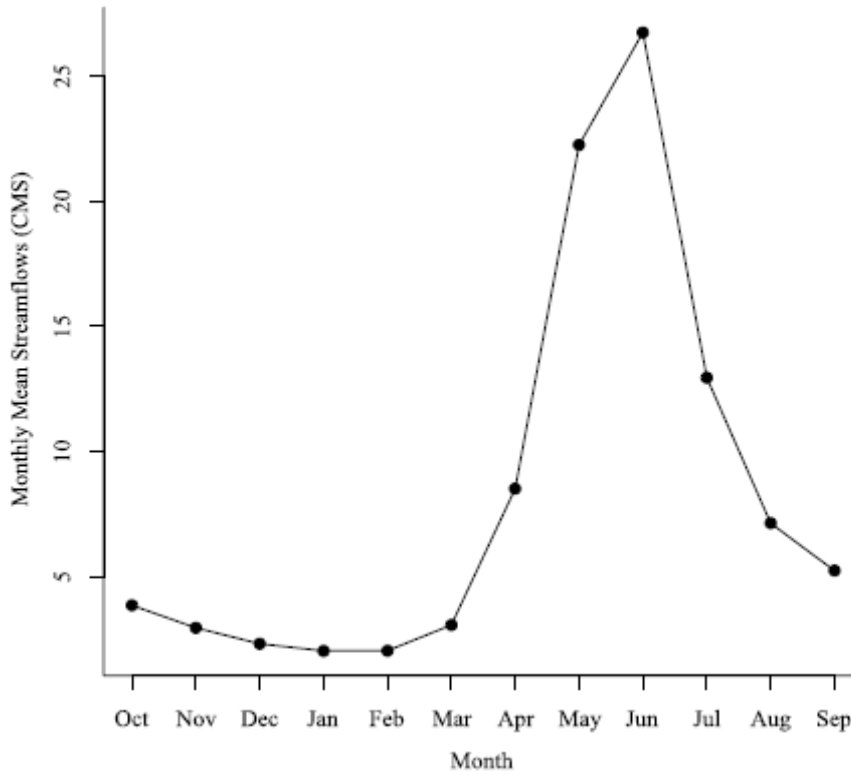


Figure 3: Annual average hydrograph of the Gunnison River Basin. Monthly values (cms) are the average of streamflows at selected six locations (detailed in the Table 1).

1.1.5. San Juan River Basin

1.1.5.1. Geographic Characteristics

The San Juan River Basin (SJRB) extends in four western United States (Figure 4) - Colorado, New Mexico, Arizona and Utah - draining approximately 24600 mi² (63,960 km²). Basin elevation ranges from 3700 feet (1110 m) at the confluence with Lake Powell to 14,000 feet (4200 m) at the crest of the San Juan Mountains. The one major water storage structure is Navajo Dam, situated at the Colorado-New Mexico border on the San Juan River. Navajo Reservoir is an important source of water supply for northwest New Mexico. It supplies the town of Farmington, NM, agricultural users and the Navajo Nation. In addition, it exports 100,000 acre-feet (123 million m³) water per year to the Rio Grande system through the San Juan-Chama Project.

1.1.5.2. Hydrologic Characteristics

Upstream of the basin is alpine whereas downstream of the basin is arid. Most of the basin precipitation falls in the upstream (San Juan) mountains as snow. In the lower elevations the precipitation is mostly supplied by summer monsoon rainfall. Annual precipitation varies greatly across the basin, from 60 inches (1520 mm) in small areas along the mountains, to less than 10 inches (255 mm) in extensive parts of the basin, to less than one-tenth inch in others. The annual streamflows in the upstream of the basin are spring driven, i.e., approximately 70% of the annual streamflows is contributed by the melting of snow (Figure 5) during spring and plays a key role in meeting various demands.

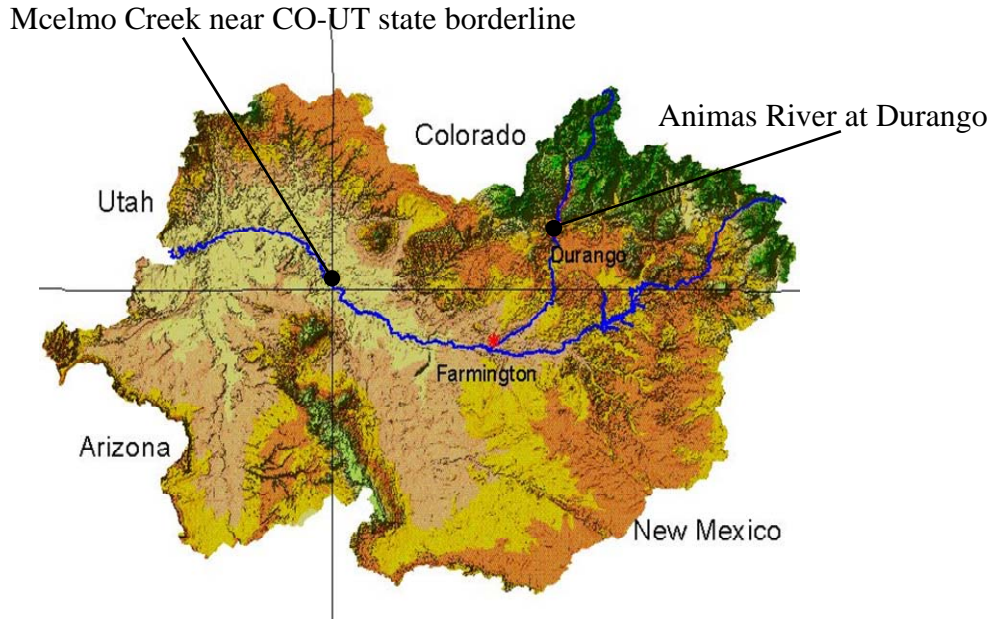


Figure 4: Map of the San Juan River Basin and selected two streamflow locations (detailed in the Table 2) shown as filled circles.

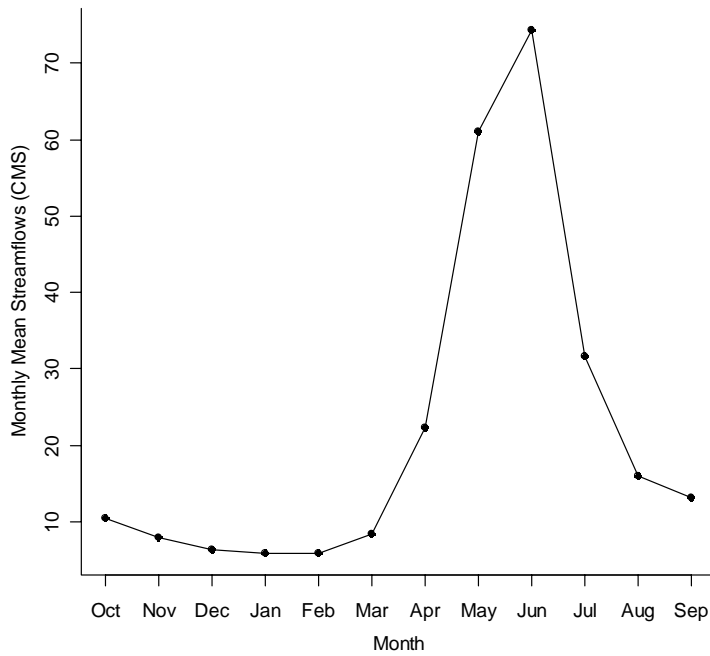


Figure 5: Annual average hydrograph of the Animas River at Durango.

1.1.6. Decision Support System

To meet the diverse and often conflicting water demands efficiently under varying hydrologic conditions, water development projects have been constructed and management policies have been formulated. However, increasing demands, climate change, extensive water laws, decrees and compacts made the system operations more complex. To enable efficient planning and operations of water resources under such a challenging environment, decision management tools such as RiverWare (Zagona et al., 2001) are developed. These are capable of integrating forecast information with operating policies and demands to forecast operational strategies. They also have the capability to analyze the efficacy of operational policies using risk and uncertainty metrics, and can derive optimal water management policies. However, the value of the output of these decision tools is limited by the accuracy of the forecast information that is input. To evaluate the utility and transferability of the skills in the input (streamflow forecasts) to output (water resources decision variables) of the decision tools, an experimental decision support system (DSS) for the water resources management of the GRB was developed. The DSS consists of a RiverWare model of the GRB coupled with the streamflow forecast framework mentioned earlier (described in Chapter 3).

1.1.7. Streamflow Scenarios for Long-term Planning

Long-term planning and development of water resources require plausible information on hydrologic variability, especially on extreme wet and drought conditions. Paleo reconstructions of streamflows are available on the GRB (C. Woodhouse, personal communication, 2006). These long flow records offer rich

information as to the potential variability of streamflows and complement the shorter observational flow data. Combining the observational and paleo reconstructed streamflows provides the ability to generate a richer variety of drought and flood scenarios than those in the observational record. Such variety will be of great use to water managers for long-term planning and development of basin water resources. To this end, a new methodology is proposed to simulate streamflow scenarios at decadal time scales that combines the paleo-reconstructed flows and the observational data.

1.2. Proposed Research

The motivation of the previous sections clearly compels the need for an integrated framework that seamlessly spans the physical climate system-to-water resources decision making, for sustainable and efficient management of water resources under high degree of hydrologic variability, competing and increasing demands, intricate water laws and procedures of management. Such an integrated framework, that is new, is developed in this research and demonstrated via application to the GRB (Figure 6). This is the most significant contribution of this research. The GRB acts as a good test basin as the water issues in the basin are a microcosm of those described earlier. The basin water resources play a key role in the economy by providing water supply for various competing socio-economic-environmental activities, e.g., water use for irrigation, municipal and industrial demands, hydropower generation, and for preservation of endangered fish habitat (detailed in the Chapter 5).

The proposed framework has three major components. (1) Understanding and identifying the drivers of interannual variability of GRB hydrology in the global land-ocean-atmospheric system. This involves analyzing the multivariate space-time data

of large-scale climate variables, and various basin attributes (e.g., soil moisture effects, topography). (2) Developing a robust statistical modeling approach for ensemble streamflow forecast. In this, a nonparametric functional estimation method was adapted to identify the best subset of predictors and multimodel ensemble forecast. (3) Evaluating the skill of streamflows forecast in the decision variables of the water resources system. Here, a decision support model, RiverWare, was adapted and improved to represent the water management and decision aspects in the basin.

The RiverWare model of the GRB, along with multimodel ensemble forecast framework, forms an experimental decision support system (DSS). The ensemble streamflow forecasts drive the RiverWare model resulting in ensembles of decision variables. In addition, future streamflow scenarios generated on long time scales (decadal or longer) using the paleo reconstructions can also be used with the RiverWare model to evaluate the system reliability and various management strategies for sustainable water resources.

1.3. Outline of the Thesis

The thesis is organized as follows.

Chapter 2 provides a comprehensive background from past literature on the role of large-scale climate features in the variability of western US hydroclimatology. The links between large-scale ocean-atmosphere patterns and hydrologic process at different temporal and spatial scales and their role in improving streamflow forecast is described. Also, literature on seasonal cycle shifts in hydroclimatology and the role of climate change is described. This background description makes a case for

including the large scale climate information in streamflow forecasting framework for improved skills.

Chapter 3 presents a new multimodel ensemble forecast framework for seasonal streamflows. In this predictors are identified from the large-scale ocean-atmosphere-land system. A nonparametric functional estimation method based on local polynomials in combination with principal component analysis is used to generate ensemble forecast of streamflows at six locations in the GRB (Table 1) and two locations in the San Juan basin (Table 2) simultaneously. The significant contribution is that ensemble forecasts are issued from several candidate models, which are then optimally combined to issue a multimodel ensemble forecast. The spring seasonal forecasts are issued at several lead times (as early as December, when the snow accumulation is partial at best). Significant long lead forecast skills have been demonstrated on these two basins. The forecast methodology and skill score estimation are described in detail in this chapter.

In Chapter 4 a new framework to produce categorical streamflow forecasts at multiple sites is developed. Often times water managers require the categorical streamflow forecasts. Typically, these are obtained by generating ensemble forecasts of streamflows as described in the Chapter 3 and counting the proportion of ensembles in the desired category. Alternatively, a simpler approach based on logistic regression can be devised to obtain the categorical forecasts directly – which is proposed in this chapter and applied to the six streamflow locations in GRB. This is a complementary approach to the multimodel ensemble forecast framework developed in the Chapter 3.

Chapter 5 develops an experimental decision support system (DSS) for the water resources management of the GRB. The DSS consists of a RiverWare model for water resources decision-making in the basin coupled with the multimodel ensemble forecast framework. The physical water resources system of the basin along with its operational rules and policies are represented in RiverWare. The ensemble streamflow forecasts (from chapter 3) drive the solution of the model to obtain ensembles of various decision variables. Significant skills in the decision variables were observed at long lead times, thus indicating the transferability of the streamflow forecast skills to the decision making context.

Chapter 6 provides a novel approach to simulating streamflow scenarios on long time scales (decadal or longer) combining the observational and paleo reconstructed streamflows. This approach provides the ability to generate a richer variety of drought and flood scenarios than those in the observational record. Such variety will be of great use to water managers for long-term planning and development of basin water resources. Application to paleo reconstruction streamflow data in the GRB demonstrates its utility and also insights into the system risk (reliability) for various demand levels.

Chapter 7 summarizes the results from this research and suggests potential improvements and extensions in future.

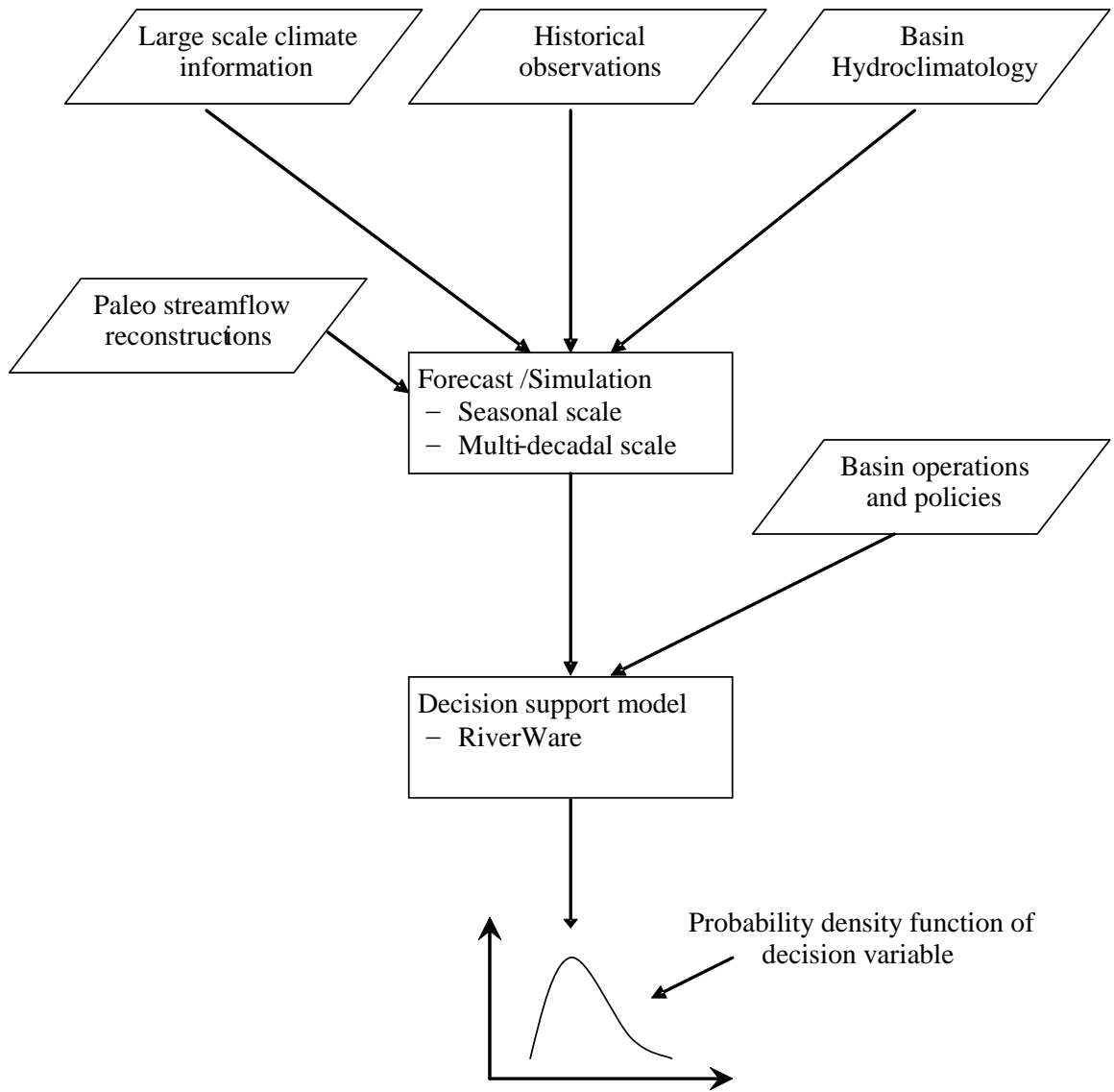


Figure 6: Flow chart of the proposed decision support system that applied on the Gunnison River Basin.

Table 2: San Juan River Basin streamflow data information.

Station Number	Site Number (USGS)	Site Name	Elevation (m)	Drainage Area (10^6 m ²)
1	09361500	Animas River at Durango , CO	1981	1792
2	09372000	McElmo Creek near CO-UT state line, CO	1490	896

CHAPTER 2

LARGE SCALE CLIMATE FEATURES AND THE WESTERN US

HYDROCLIMATOLOGY

There is increasing evidence that variability at interannual to interdecadal time scales in the western US hydroclimatology is driven largely by large-scale ocean-atmospheric patterns, especially of the Pacific Ocean. In this chapter a description of these connections from previous studies is provided and the need to incorporate these features in any hydrologic forecasting framework is discussed.

2.1. Interannual Variability

Western US hydroclimatology is strongly modulated by several of the large-scale climate patterns such as ENSO¹, PNA² and PDO³, and the literature is rich in documenting the teleconnections of the climate patterns in association with various hydrologic processes. ENSO, an ocean-atmospheric phenomenon in the tropical Pacific Ocean, exerts the most influence on the interannual variability of hydroclimatology in the western US. During the El Niño years (i.e., warm ENSO events), increase in sea surface temperatures and consequent convection in the central and eastern tropical Pacific Ocean deepen the Aleutian Low pressure in the North Pacific Ocean - this amplifies the northward branch of the tropospheric wave train over North America and strengthens the subtropical jet over the Southwestern US (Bjerknes, 1969; Horel and Wallace, 1981; Rasmussen, 1985). This teleconnection

¹ ENSO: El Niño Southern Oscillation

² PNA: Pacific North American Pattern

³ PDO: Pacific Decadal Oscillation

due to El Niño results in above-normal and below-normal precipitation patterns in the desert southwest and Pacific Northwest regions, respectively (e.g., Ropelewski and Halpert, 1986; Redmond and Koch, 1991; Cayan and Webb, 1992; Dettinger et al., 1998; Cayan et al., 1998, 1999). Generally opposing signals are evident in La Niña years (i.e., cold ENSO events), but some non-linearities are present (Hoerling et al., 1997; Clark et al., 2001). Similar ENSO teleconnection patterns have been observed in the interannual variability of winter snow water equivalent (Clark et al., 2001; Cayan, 1996), surface temperatures (Redmond and Koch, 1991; Higgins et al., 2002; Gershunov and Barnett, 1998), and streamflows (Kahya and Dracup, 1993, 1994; Dracup and Kahya, 1994; Piechota et al., 1997; Maurer et al., 2004).

Decadal variability of sea surface temperatures in the Northern Pacific (Mantua et al., 1997), described as PDO, is being identified as a primary driver of the western US hydroclimate variability on decadal time scales (McCabe and Dettinger, 1999, 2002; Hidalgo and Dracup, 2003; Brown and Comrie, 2004) – even though there is a debate on the independence of PDO from ENSO (Newman et al., 2003). In addition to inter-annual and inter-decadal variability, recent studies also indicate a significant shift in the seasonal cycle of hydroclimatology in the western US (Cayan et al., 2001; Regonda et al., 2005a; Stewart et al., 2005) modulated by ENSO and the general warming trend, especially, the early occurrence of spring warming and consequent early spring time peak flows due to early snowmelt.

The large-scale forcings, particularly ENSO and consequently PNA and the teleconnection patterns described above are highly persistent and thus have enabled long-lead hydroclimate predictions over the North America and western US in

particular. Higgins et al. (2004) forecasted surface temperatures across the United States using tropical Pacific Sea Surface Temperatures at 6-12 months lead-time. Hamlet and Lettenmaier (1999b) forecasted Columbia River streamflows using ENSO and PDO with several months lead-time. Clark et al. (2001) showed that combining large-scale climate information together with Snow Water Equivalent (SWE) improves the overall skill of the streamflow predictions in the Columbia and Colorado River Basins. Recently, Grantz et al. (2005) offered skillful predictions of spring streamflows on the Truckee and Carson Rivers in Nevada for two seasons ahead, using large-scale climate information.

Although much of the western US is strongly associated with large-scale climate patterns, interior west exhibited a weaker relationship because of the persistent winter storms of several different types in the region (Cayan, 1996). For example, unlike much of the western US, streamflows in the eastern central part of the western US (i.e., Rocky Mountains and the Great basin) are weakly correlated with upper level geopotential height anomalies (e.g., Cayan and Peterson, 1989; Klein et al., 1965; Weare and Hoeschele, 1983). Influence of various attributes of basin such as topography (i.e., irregular terrain), surface heating, and surface friction on winter precipitation are considered the potential causes for the observed weak correlations (e.g., Cayan and Roads, 1984). Also, there is a substantial variability in the strength of teleconnections from one river basin to another (McCabe and Dettinger, 2002) even in the regions that have strong teleconnections. Relatively minor shifts in large-scale atmospheric patterns can result in large differences in surface climate (e.g., Yarnal and Diaz, 1986). Therefore, the typical indices (e.g., ENSO, PNA) that

capture large-scale climate patterns may not be useful in explaining the variability of the hydroclimatology, establishing a need for the development of nonstandard indices (e.g., Grantz et al., 2005).

This is particularly the case in the Gunnison River Basin (GRB) and San Juan River Basin (SJR) which are situated in the interior west between the Pacific Northwest and desert Southwest; the region lying outside the areas that are strongly affected by ENSO variability (e.g., Cayan and Peterson, 1989; Klein et al., 1965; Weare and Hoeschele, 1983; Cayan et al., 1998; Dettinger et al., 1998). Also, the climate signal of the region is not characterized by well known phenomena (e.g., Cayan, 1996; Clark et al., 2001; Klein, 1963; Klein and Bloom, 1987; McCabe and Legates, 1995). However, there are few circulation features, i.e., categorized/clustered geopotential height anomalies (e.g., Changnon et al., 1993; McCabe, 1994, 1996; McCabe and Legates, 1995; Robertson and Ghil, 1999), which modulate the winter snow pack and consequently the spring streamflows in the interior west. These circulation features vary with region and can not explain more than 50% of the variance of the hydrologic processes (e.g., Klein, 1963; McCabe, 1994; McCabe and Legates, 1995). Also, these features are quite different from the typical standard indices such as ENSO and PNA patterns. This background motivates the need to identify the appropriate large-scale climate information that modulates the streamflows in the GRB and SJR.

2.2. Hydroclimate Trends

Changes in regional hydroclimatology can have substantial economic and environmental impacts. Increasing winter temperatures reduce the amount of snow in

a basin (e.g., more precipitation falling as rain than snow). This has been observed in several parts of the western USA (Aguado et al., 1992; Dettinger and Cayan, 1995). Also, higher spring temperatures initiate earlier runoff and peak streamflows in snowmelt-dominated basins (Aguado et al., 1992; Cayan et al., 2001). These can have significant impacts on water resources management – e.g., negative impacts on irrigation, non-firm energy, recreation, flood control, and instream flow for fish (Hamlet and Lettenmaier, 1999a). Knowing these shifts in advance can help water managers to optimize reservoir operations to meet competing demands such as irrigation, environmental needs, and power generation.

Observations suggest an advancement of the seasonal cycle in the Northern Hemisphere, especially, early occurrence of spring, which Thomson (1995) attributed to increased atmospheric CO₂ concentrations. Shifts in the seasonality of precipitation (Bradley, 1976; Rajagopalan and Lall, 1995) and streamflows (Roos, 1987, 1991; Aguado et al., 1992; Wahl, 1992; Lins and Michaels, 1994; Dettinger and Cayan, 1995; Cayan et al., 2001; Regonda et al., 2005a; Stewart et al., 2004; Stewart et al., 2005) have been observed across several regions of the western USA. Mote (2003) computed trends in snow water equivalent (SWE) in the Pacific Northwest and observed strong declines in SWE, in spite of increases in precipitation, which is consistent with an increase in spring temperatures. Recent research (Regonda et al., 2005a) indicates early occurrence of spring warming and as a result an early spring peak over most of the western US – corroborating all of the earlier studies mentioned above. Enhanced ENSO activity in recent decades and the general warming trend were argued as potential causes for these shifts. In an analysis of hydrologic impacts

of climate change over west-central Canada, Burn (1994) found a strong shift towards the early occurrence of the spring runoff events, especially in the last 30 years. Dettinger and Cayan (1995) observed early flows in association with warmer winters in California. Cayan et al. (2001) documented the early onset of spring in the western US by examining changes in the blooming of plants and the timing of spring snowmelt pulses. McCabe and Wolock (2002) observed a step increase in streamflow in the conterminous United States over the period 1941-99, with pronounced increases in the eastern United States after 1970.

Climate model simulations under CO₂ doubling show a strong seasonal shift in the snow accumulation and ablation seasons, leading to increased winter runoff and decreased spring runoff (Lettenmaier and Gan, 1990). Nash and Gleick (1991) used conceptual hydrological models to simulate streamflow response to changes in temperature and precipitation in the Colorado River basin. Increases in temperature of 2-4°C decreased mean annual runoff by 4 to 20%, whereas changes in annual precipitation of +/-10-20% result in corresponding changes in mean annual runoff of 10 to 20%. Seasonal shifts in flow were observed and attributed to an increase in the ratio of rain to snow. The potential effects of climate change (i.e., increased winter precipitation and warmer winter temperature) are quite pronounced in the Pacific Northwest region, where significant increases in winter flow, and corresponding decreases in summer flow, are shown under a range of different climate models (Hamlet and Lettenmaier, 1999a). The transitions in winter and summer flow volumes occur because of increased winter temperature and winter precipitation with resulting reductions in snow pack (see also Mote, 2003).

Recently a group of researchers evaluated future climate change impacts on western US water resources management as part of the Accelerated Climate Prediction Initiative (ACPI) (<http://www.csm.ornl.gov/ACPI>). The climate change scenarios of projected “Business as Usual” (BAU) greenhouse gas emissions were simulated using NCAR/DOE’s Parallel Climate Model (PCM). The BAU scenarios exhibited an average warming of about 1-2°C and both decrease and increase in precipitation across the western US. Downscaling these scenarios to the Colorado River basin, Christensen et al. (2004) find a significant decrease in April SWE (-30%), annual runoff (-17%), total basin storage (-40%), and reservoir levels (-33%) by the end of the 21st century. Furthermore, Barnett et al. (2004), find that these climate impacts can potentially drive the Colorado compact to the brink of failure. In the Pacific Northwest region (Wood et al., 2004) and on the Columbia River basin in particular, Payne et al. (2004) and Leung et al. (2004) find that the climate change scenarios lead to a decrease in SWE, more frequent rain on snow events, changes in SWE accumulation/melting period and consequently, increased likelihood of winter flooding and an earlier refill of reservoirs. This increases the competition of instream releases for hydropower generation and endangered species allocation (Payne et al., 2004; Barnett et al., 2004). Similar impacts of reduced winter and spring precipitation coupled with early spring warming and peak flows are seen in the Sacramento-San Joaquin basin (Vanrheenen et al., 2004) and several basins in the Sierra Nevada region (Dettinger et al., 2004). In general, climate change due to 1-2°C warming and shifts in spring streamflows (Dettinger et al., 2004; Stewart et al., 2004) were found

to significantly impact water resources in the western US by the end of the 21st century (Barnett et al., 2004; Leung et al., 2004).

From the research efforts discussed above it is clear that the western US hydroclimatology is impacted significantly by large-scale climate features at all the time scales. Thus, a credible forecasting framework should include information of the large-scale climate system in order to provide skilful forecasts. This motivates the present research as can be seen in the forecasting framework developed in the following chapter.

CHAPTER 3

A MULTIMODEL ENSEMBLE FORECAST FRAMEWORK

As motivated in the preceding chapters, here, in this chapter a new framework for multi-site ensemble forecast of seasonal streamflows, incorporating large-scale climate information is presented. The method is demonstrated by application to streamflows in the Gunnison River Basin (GRB) and San Juan River Basins (SJR).

3.1. Streamflow Forecasting Framework

Short-term decision-making requires skillful forecast of streamflow attributes, such as seasonal/monthly volume, timing of peak flow, at single/several locations. Streamflow forecasts at multiple locations act as points of release of water satisfying various basin needs (e.g., agricultural, municipal, and trans-basin diversions). Therefore, streamflow forecasts at all locations need to be generated simultaneously so as to capture the spatial dependence among locations. As noted in the chapter 3, large-scale climate forcings modulate the streamflow characteristics and hence, this also has to be included in the forecasting framework.

To this end, a new modeling integrated framework is proposed that produces an ensemble of spring streamflow forecasts at multiple locations and at different monthly lead times incorporating large-scale climate information. The proposed methodology consists of four broad components: (i) Principal Component Analysis (PCA) of the (spring season) streamflows at the locations to identify the dominant modes of variability; (ii) climate diagnostics to obtain the large-scale ocean-atmosphere predictors of the dominant modes; (iii) statistical model and multimodel

selection objective criterion to select a suite of models from the predictor set based on the Generalized Cross Validation (GCV); and (iv) multimodel ensemble streamflow forecast algorithm, in which ensembles of the dominant modes are predicted from the multimodels, and then combined, and translated into the original flow space to obtain the streamflow forecasts. These components will be described in detail in the following sections.

3.1.1. Principal Component Analysis (PCA)

Principal Component Analysis is widely used in climate research. This method decomposes a space-time random field (i.e., a multivariate dataset such as the seasonal streamflows at the six locations in the GRB) into orthogonal space and time patterns using Eigen decomposition (Von Storch and Zwiers, 1999). The patterns are ordered according to the percentage of variance captured, i.e., the first space-time pattern (also called “mode”) captures the most variance present in the data and so on. The temporal patterns are called principal components (PCs). Typically, the first few modes (PCs) capture most of the variance present in the data. This can also be thought of as a dimension reduction technique, where a large multivariate data set is effectively represented by a few PCs (i.e., smaller dimension). Furthermore, since the PCs are orthogonal they can be analyzed independently and combined to reconstruct the original data.

The mathematical formulation is as follows:

$$[\bar{Z}]_{NXM} = [Y]_{NXM} [\bar{E}]_{MXM} \quad \dots \quad 3.1$$

$$[Y]_{NXM} = [\bar{Z}]_{NXM} [\bar{E}]^T_{MXM} \quad \dots \quad 3.2$$

Where, Z is the original flows, Y is the Principal Components, E is the Eigen vectors, M is the number of streamflow locations, and N is the length of the data. Hence E can be considered a transformation matrix.

The decomposition is obtained by minimizing the error $\varepsilon_i = E[Z - Z E_i]^2$ (this maximizes variance) such that $EE^T = 1$ (Ortho normal criteria)

3.1.2. Climate Diagnostics

The next step is to search for indices that can be used to predict the dominant streamflow PCs. The leading PCs are correlated with global ocean and atmospheric circulation variables (i.e., Surface Temperatures, Geopotential heights, Winds) from preceding seasons. In this case, the leading PCs of the spring streamflows will be correlated with circulation variables from the preceding fall and winter months. From the resulting correlation maps, regions that exhibit strong correlations are used to develop potential predictors. These are typically the area-averaged values of the variables. Thus, a suite of potential predictors can be obtained. Composite analysis will be performed to identify the physical mechanisms driving the variability of the streamflows and also the consistency of the predictors.

3.1.3. Forecast Framework

The leading PCs and their potential predictors are incorporated into a statistical model, which is typically of the form:

$$y = f(x_1, x_2, x_3, \dots x_R) + e \quad \dots 3.3$$

Where f is a function fitted to the R predictor variables (x_1, x_2, \dots, x_R) , y is the dependent variable (in this case the leading PC of the spring streamflows) and e is the

errors assumed to be normally (or Gaussian) distributed with a mean of 0 and variance σ^2 . Traditional statistical methods fit a linear function that minimizes the squared errors, known as linear regression. The theory behind this approach, the procedures for parameter estimation, and hypothesis testing are very well developed (e.g., Helsel and Hirsch, 1995; Rao and Toutenburg, 1999) and are widely used. However, they do have some drawbacks: (i) the assumption of a Gaussian distribution of the errors and the variables and (ii) fitting a global relationship (e.g., a linear equation in the case of linear regression) between the variables. If the linear model is found inadequate, higher order models (quadratic, cubic, etc.) have to be considered, which can be difficult to fit in the case of short data sets. Also if the variables are not normally distributed, which is often the case in practice, suitable transformations have to be obtained to transform them to normal distribution. All of this can make the process unwieldy. Thus, a more flexible framework would be desirable.

Local estimation methods (also known as nonparametric methods) provide an attractive alternative. In this, the function f is fitted to a small number of neighbors in the vicinity of the point at which an estimate is required. This is repeated at all the estimation points. Thus, instead of having a single equation that describes the entire data set, there are several 'local fits', each capturing the local features. This provides the ability to model any arbitrary features (linear or nonlinear) that the data exhibits.

There are several approaches for local functional estimation applied to hydrologic problems (see Lall, 1995). Of these, the Locally Weighted Polynomial regression (LWP) is simple and robust, and has been used in a variety of hydrologic and hydroclimate applications with good results - for streamflow forecasting on the

Truckee and Carson river basins (Grantz et al., 2005), salinity modeling on the upper Colorado river basin (Prairie et al., 2005), forecasting of Thailand summer rainfall (Singhrattna et al., 2005), and spatial interpolation of rainfall in a watershed model (Hwang, 2005). Given these experiences, the LWP method is adopted in this research.

A brief description of the method is provided here and for specific details readers are referred to Loader (1999) and Grantz et al. (2005). In the LWP method a small number, $K = \alpha * N$ (where $\alpha = (0,1]$ and $N =$ number of observations) neighbors of the point of estimate, \mathbf{x}^* are identified from the data set. To the K neighbors, a polynomial of order p is fitted (equation 3) by a weighted least squares method where the K observations are weighted inversely to their distances to \mathbf{x}^* using a weight function. The fitted polynomial is then used to obtain the mean estimate for the dependent variable, y^* at the point of estimate. The standard regression theory also provides an estimate of the error variance (σ_{le}^2) corresponding to the predicted value of the dependent variable, y^* (Loader, 1999). Random normal deviates with this variance and zero mean, when added to predicted value, y^* , provide an ensemble. This assumes that the errors are normally distributed around the predicted value. Prairie et al. (2006a) developed a residual resampling approach to generate ensembles. In this the residuals of the LWP fit are resampled and added to the mean estimate. This can better capture the local error structure without assuming normality, but on short data sets the variety of ensembles produced is limited. Note that the LWP approach collapses to a traditional linear regression, when α is set to 1, p is set to 1, and each observation is weighted the same.

The two key parameters in this method, the size of the neighborhood, K , and the order of the polynomial, p are obtained by minimizing an objective criterion, Generalized Cross Validation (GCV) which is a good estimate of predictive risk of the model, unlike other functions which are goodness of fit measures (Craven and Whaba, 1979). This is given as:

$$GCV(K, p) = \frac{\sum_{i=1}^N \frac{e_i^2}{N}}{\left(1 - \frac{v}{N}\right)^2} \quad \dots \quad 3.4$$

Where e_i is the model residual, N is the number of data points, v is the degrees of freedom in the local polynomial model. Typically, several combinations of (K, p) are used and the combination that results in a minimum GCV value is selected.

3.1.4. Multimodel Selection

The predictor variables used in the regression equations tend to be highly correlated. If all the correlated predictors are used in the model, it can lead to overfitting and poor skill in prediction; this is known as ‘multicollinearity’. Thus, the ‘best’ subset of predictors needs to be identified. Typically, this is done using stepwise regression (e.g., Rao and Toutenburg, 1999; Walpole et al., 2002) where in, an objective function such as Mallows’s C_p statistic or adjusted R^2 or AIC (Akaike Information Criteria) or an F-test, is calculated from the fitted model to several predictor combinations. The best subset is then selected based on the combination that gives the optimal value for the chosen objective function. For noisy data (i.e., most real data) the values of the objective functions for several predictor combinations tend to be very close, suggesting that several combinations (i.e.,

candidate models) might be admissible. Thus selecting the ‘best’ subset might not be a good strategy, which warrants a multimodel approach. Recent studies show that multimodel ensemble forecasts tend to perform much better than a single model forecast (Hagedorn et al., 2005; Krishnamurti et al., 1999, 2000; Rajagopalan et al., 2002).

Here, the use of GCV for multimodel selection is proposed. The approach is as follows:

- (i) GCV is computed for all the possible combinations of the predictor set and parameter set (K, p).
- (ii) All combinations with GCV values within a prescribed threshold are selected as admissible – constituting the pool of candidate models, i.e., multimodels.
- (iii) Combinations with predictor variables significantly correlated amongst each other (i.e., multicollinear) are removed from the multimodel pool.

3.1.5. Multimodel Ensemble Forecast Algorithm

The ensemble forecast from the multimodels identified above is summarized in the following six steps:

1. PCA is performed on the six streamflows in the GRB, and the leading PCs are selected.
2. All potential predictors of the leading PCs are identified from climate diagnostics.
3. These are passed through the forecasting framework and the multimodel selection. This results in a pool of multimodels, which includes the predictor set, and the corresponding parameter set.

4. Ensemble (say, 100) forecasts of the leading PCs are generated from each model of the multimodel pool. For each ensemble, the other non-leading PCs are randomly selected (i.e., bootstrapped) from those obtained from the PCA. Thus, each ensemble forecast member consists of all PCs with the leading PCs obtained from the model forecast and the rest bootstrapped from the historic values. If ten models are selected in the multimodel pool the ensemble forecast will be a matrix of size (1000 x 6).
5. The ensemble forecast matrix of the PCs is multiplied by the Eigen vectors to back transform into the streamflow space, i.e., $Z^* = Y^* * \vec{E}$.
6. Clearly, ensembles from all the models are not equal. The model with the least GCV value should be given more weight relative to the one with a higher GCV. To this end, a vector of probabilistic weights is created based on the GCV values (the weights are normalized to sum to unity); using this weight metric, a model is selected; then an ensemble member from this model is selected at random. This is repeated numerous times (say, 100), thus, resulting in a final multimodel ensemble forecast.

Steps 2 through 6 are repeated for each lead time; thus, each lead time will have a different suite of multimodels with their own predictor and parameter sets.

3.1.6. Links to Model Averaging Literature

The typical statistical modeling approach involves identifying a single best model based on an objective criterion. This neglects model inadequacy and increases the associated risk of model inferences. To alleviate this, a combination of several candidate models, also known as a ‘model averaging’ has been proposed (Reid, 1968;

Bates and Granger, 1969; Clemen, 1989). Another approach in a similar vein is to generate ensembles from several candidate models and combine them to provide a model average probabilistic forecast. This approach has been shown to perform better than any individual model ensemble, particularly in short term and seasonal climate forecast (Hagedorn et al., 2005; Hou et al., 2001; Krishnamurti et al., 1999, 2000; Regonda et al., 2005b; Tamea et al., 2005). The candidate models are combined by weighting them, where the weights are obtained from different approaches, e.g., Regression, Bayesian framework, etc. Weighting the multimodels in a Bayesian framework is known as Bayesian Model Averaging (Raftery et al., 1997; Hoeting et al., 1999). There are several variations within this framework (e.g., Madigan and Raftery, 1994). The key message in all of these is that combining several models tends to perform better in terms of predictive skill and reliable uncertainty estimates than a single model.

The multimodel combination approach proposed in this paper is consistent with the model averaging framework and provides an attractive alternative approach for performing model averaging. The multimodels are selected based on the GCV criteria and they are combined using weights based on their GCV values as described in the previous sections.

3.1.7. Forecast Skill Evaluation

Since the framework generates an ensemble forecast, i.e., the probability density function (PDF), the skill of the forecast needs to be evaluated in probabilistic terms. One such common measure is the Ranked Probability Skill Scores (RPSS) (Wilks, 1995).

$$RPS = \sum_{i=1}^k \left[\left(\sum_{j=1}^i p_j - \sum_{j=1}^i d_j \right)^2 \right] \quad \dots 3.5$$

Essentially, it measures the accuracy of multi-category probability forecasts relative to a climatological forecast. Typically, the flows are divided into k mutually exclusive and collectively exhaustive categories for which the proportion of ensembles falling in each category constitutes the forecast probabilities (p_1, p_2, \dots, p_k). The observational vector (d_1, d_2, \dots, d_k) is obtained for each forecast, where ‘ d_k ’ equals one if the observation falls in the k^{th} category and zero otherwise.

The ranked probability skill score (RPSS) is defined as follows:

$$RPSS = 1 - \frac{RPS(\text{forecast})}{RPS(\text{climatology})} \quad \dots 3.6$$

In this research, the streamflows are divided into three categories, at the tercile boundaries, i.e., 33rd and 66th percentile of the historical observations. Values below the 33rd percentile represent ‘dry’, above 66th percentile ‘wet’, and ‘near normal’ otherwise. Of course, the climatological forecast for each of the tercile categories is 1/3.

The RPSS ranges from negative infinity to positive one. Negative RPSS values indicate the forecast accuracy to be worse than climatology, positive to be higher than climatology, zero to be equal to that of climatology, and a perfect categorical forecast yields an RPSS value of unity. In this application the RPSS is calculated for each year and the median value is reported.

3.2. Data Sets

The following datasets are used in developing the ensemble streamflow forecast framework on both Gunnison and San Juan River basins. The description of the datasets is presented below.

3.2.1. Streamflow

Streamflow locations are selected from the Hydro Climate Data Network (HCDN). This network, HCDN, was developed by USGS to analyze the climate impacts on the rivers and has more than 1000 streamflow stations across the continental USA with minimal human impact (Slack and Landwehr, 1992). For the GRB, HCDN provided six locations (Figure 2) that have continuous flow records from 1949 to 2002. The stations, described in Table 1, are situated in five of GRB's six cataloging units. Four of the six stations contribute inflows to the reservoirs of the Aspinall Unit. Spring flow, the summation of daily flows from April through July, is computed for each of the locations for further analysis.

For the SJRB, two streamflow locations, Animas River at Durango and McElmo Creek at Colorado-Utah border, are selected (Figure 4). Among all SJRB streamflow stations including HCDN listed ones, only the above-mentioned two locations satisfied the selection criteria, i.e., irrigated acreage is less than 1% of their contributing drainage area. The selected stations have continuous flow records from 1951-2003, and details are presented in Table 2. The Animas River is a part of the upper San Juan River Basin, whereas McElmo Creek is in the lower San Juan River Basin. Here too, spring flow time series is computed for the selected two locations.

3.2.2. Snow

Snow water equivalent (SWE) data is obtained from snow-course surveys conducted by the Natural Resources Conservation Service (NRCS). SWE measurements are generally taken at or about the beginning of each month and are most frequently taken at the beginning of April, which is the peak SWE in many regions. For this study, I selected stations with at least 80% of their records available from 1949-2002 for February 1st, March 1st, or April 1st. For the GRB, three, four, and six stations met the criteria for the months February, March and April, respectively. For the SJRB, five locations satisfied the same selection criteria for April month.

3.2.3. Large-scale Climate Variables

Data of ocean-atmospheric circulation variables that capture the large-scale climate forcings that drive the regional hydrology are available from the NOAA's Climate Diagnostics Center website (<http://www.cdc.noaa.gov>). These variables include Geopotential Height, Surface Air Temperature, Sea Surface Temperature (SST), Zonal Wind and Meridional Wind. These variables are provided on a 2.2deg x 2.2deg grid spanning the globe from NCEP-NCAR Re-analysis project (Kalnay et al., 1996) for the period 1949 – 2002.

Also, standard teleconnection indices such as NINO regions SSTs (NINO 1.2, NINO 3.0, NINO 3.4, and NINO 4.0), Southern Oscillation Index (SOI), Northern Atlantic Oscillation (NAO), Northern Oscillation Index (NOI), Pacific Decadal Oscillation (PDO) and Pacific Northern American Pattern (PNA) are considered.

3.2.4. Palmer Drought Severity Index

The Palmer Drought Severity Index (PDSI) is estimated based on the principle of balance between moisture supply and demand, but man-made changes are not considered in its calculation. It provides information on the severity of wet or dry conditions. The index generally ranges from -6 to +6 with negative values representing dry conditions and positive values denoting wet conditions. Data obtained from the Climate Diagnostics Center website (<http://www.cdc.noaa.gov>).

3.3. Results

The multimodel ensemble forecast framework developed in the previous section was applied to streamflow locations of the Gunnison River Basin (GRB) and San Juan River Basin (SJR). The details of the datasets used are presented, followed by results of each basin, concluding with a summary and discussion of the results.

3.3.1. Gunnison River Basin

3.3.1.1. Streamflow characteristics: Principal Component Analysis

The selected six streamflow locations exhibited spring snowmelt-dominated annual hydrograph, i.e., more than 50% of annual streamflow are from spring (April through July) flows. Further, as it discussed in the chapter 2, spring flows play a key role in various decisions. Therefore, spring flow time series is prepared for each of the six streamflow locations.

PCA was performed on the normalized spring season streamflows from the six locations. The first PC explained most of the variance (around 87%) and the remaining five PCs together explained about 13% of the variance (Figure 7a).

Clearly, the first PC (Figure 7b) is the dominant and leading ‘mode’ containing the ‘signal’, while the rest can be treated as ‘noise’. The Eigen vectors (i.e., loadings) at all the six locations (Figure 7c) corresponding to the first mode are of similar magnitude and sign suggesting that the basin is homogenous in its variability. To corroborate this, the first PC correlates strongly (correlation coefficient > 0.85) with the basin average spring flow.

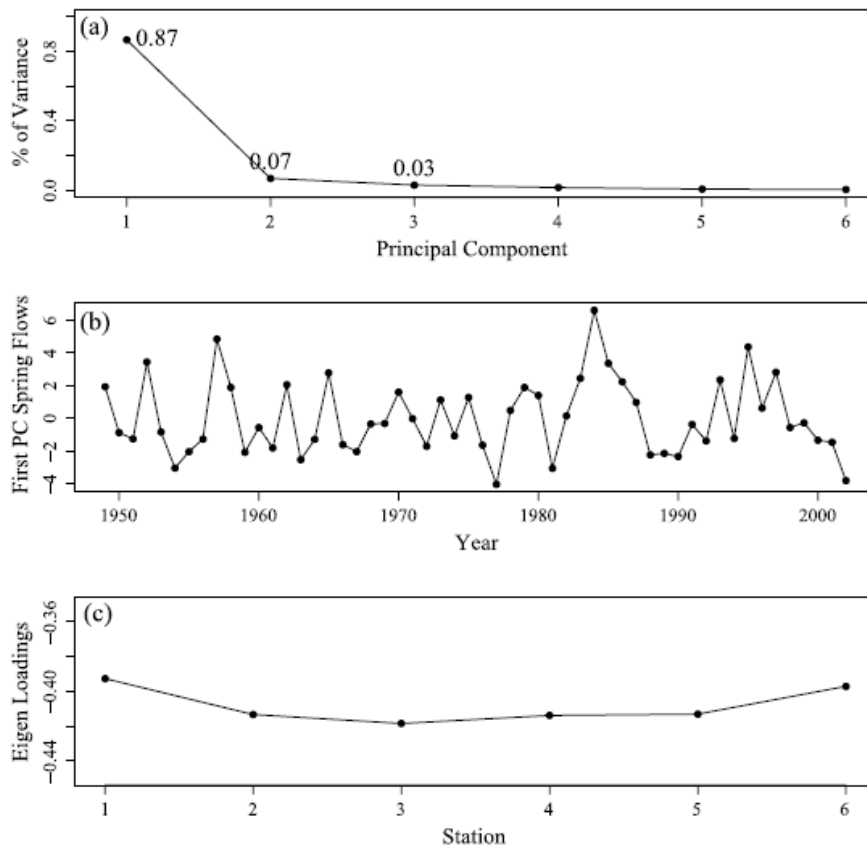


Figure 7: (a) Percentage variance explained by the six Principal Components (PCs), (b) Time series of the first PC and, (c) Eigen loadings of the first PC at the six streamflow locations.

PCA is also performed on the SWE data separately for each month (February 1st, March 1st, and April 1st). Here too, the first PC explained most of the variance in all the months. As expected, the leading PC of SWE and the leading PC of the spring

streamflows were highly correlated, with the first PC of April 1st SWE having the highest correlation (0.82) with the flow PC (Figure 8a). It is interesting to note that there are few years (e.g., 1979, 1984, 1986, 2002 shown as solid circles in Figure 8a) in which flows are not proportional to the April 1st SWE. My hypothesis is that if the preceding summer/fall is drier than normal and the following winter is wetter than normal, then a large part of the following spring runoff is absorbed by the soil and lost to the atmosphere through evaporation, thus reducing the streamflow output. To test this, the average preceding fall season Palmer Drought Severity Index (PDSI) is computed over the basin, a good surrogate for soil moisture (Dai et al., 2004), and plotted them against the residuals of the linear regression between the first PC of the streamflow and SWE (Figure 8b). The correlation between the residuals and the fall PDSI is 0.35, which is low but statistically significant. But for the years that do not follow the linear SWE-flow relationship (solid circles in Figures 8a and b) the residuals show a very strong correlation with the preceding fall PDSI (0.873, solid line in Figure 8b). This suggests the key role of the PDSI in modulating the streamflows especially during years with a drier than normal fall season followed by a wet winter and spring, and the need for it to be included in the suite of predictors.

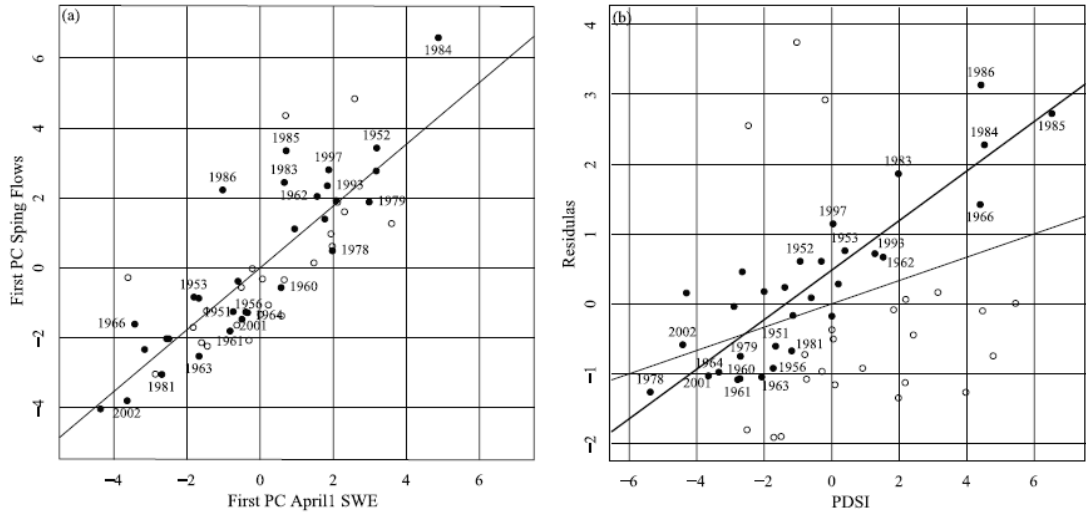


Figure 8: (a) Scatter plot of first PC of spring flow and April 1st SWE along with the best fit linear regression line, and (b) Scatter plot of residuals of the first PC of spring flow from the regression fit in (a) with the preceding fall season PDSI – the thin line is the best fit line for the scatter and the solid line is the best fit line of the filled circle points.

3.3.1.2. Climate Diagnostics - Predictor Selection

As a first step, the first PC of spring streamflow is correlated with the standard large-scale climate forcing indices of ENSO, PDO and PNA, and no relationship was found. This is consistent with the past research results for the GRB (Cayan, 1996; Clark et al., 2001; Klein, 1963; Klein and Bloom, 1987; McCabe and Legates, 1995), which suggest that climate signals (particularly ENSO and PNA) in the intermountain West tend to be weak due to the fact that the region is situated in the transition zone of the ENSO and PNA teleconnections.

The first flow PC was correlated with the preceding seasons' atmospheric and oceanic circulation variables, i.e., 700 mb geopotential heights, surface air temperature, sea surface temperature, zonal (700 mb) and meridional (700 mb) winds. Correlation maps with the November - March season are presented in Figure 9.

Negative correlations are observed between the spring flows and 700 mb heights over the western USA (Figure 9a), indicating an above average spring streamflow in the GRB with negative geopotential height anomalies in this region, and vice-versa. The negative height anomalies tend to direct the storm tracks into the basin resulting in increased SWE, and consequently, increased streamflows in the spring. The surface air temperatures are negatively correlated with the spring flows in this region (Figure 9b), consistent with Figure 9a. Correlations with zonal and meridional winds at 700mb (Figures 9c and 9d) are consistent with the 700mb geopotential heights in that winds over the southwestern US bring moisture into the GRB basin, leading to above average spring streamflows. The sea surface temperature correlation (Figure 9e) shows a weak ENSO pattern with positive correlation in the tropical Pacific and negative in the northern Pacific. The correlations in the regions described above are statistically significant. Composite maps of vector winds at 700mb corroborate the results from the correlation maps (Figure 10). In wet years (years with PC values above the 90th percentile) the average wind pattern (Figure 10a) is from the southwest direction, blowing in to the basin from the ocean bringing in moisture, and consequently, more snow and streamflow - vice-versa during dry years (Figure 10b). The sea surface temperature composites (not shown) also indicated results consistent with the correlations. These observations are qualitatively in agreement with McCabe and Legates (1995).

From the correlation maps the regions of strong correlations are identified to develop the predictors by area, averaging over these regions. The difference between the regions of positive and negative correlations is taken in order to reduce the

number of predictors and enhance the predictor signal. From Figure 8b it is observed that the land surface information during the preceding fall plays a role in the following spring melt flows. Hence, the PDSI is also included in the set of predictors. In addition, the first PC of the SWE is included. In all, the climate diagnostics suite of predictors (geopotential height anomalies, surface air temperature, winds, PDSI, SWE) were developed for the April 1st forecast and they are detailed in Table 3.

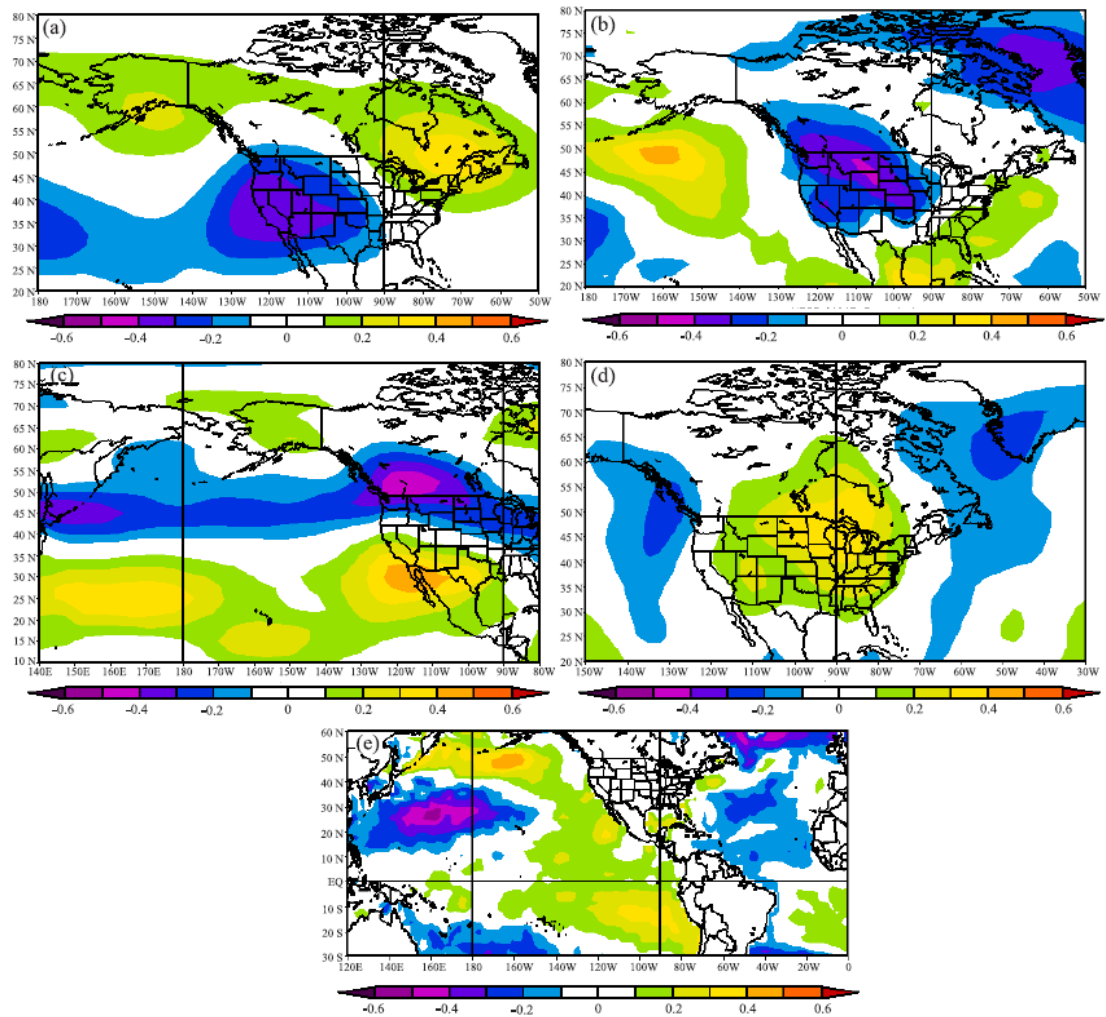


Figure 9: Correlation between the first PC of Spring flow and Nov-Mar large scale climate variables (a) Geopotential Height – 700 mb (b) Surface Air Temperature (c) Zonal wind - 700 mb (d) Meridional wind - 700 mb (e) Sea Surface Temperature. Maps were generated from NOAA’s Climate Diagnostic Center Website.

The correlation analysis is performed for all the lead times separately, e.g., for March 1st forecast, the first PC of spring flows is correlated with November-February climate variables and the predictors obtained from the maps and so on. It is found that the regions of strong correlation to be largely the same with slight differences among the lead times.

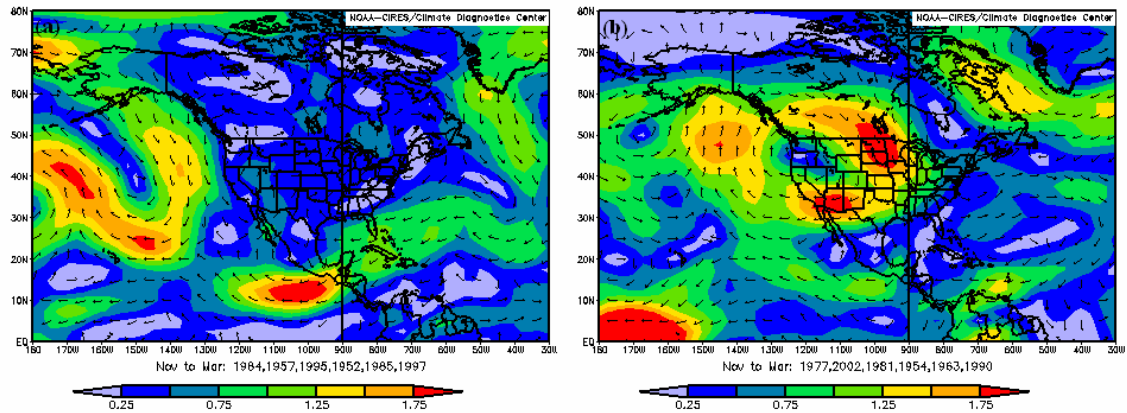


Figure 10: Composite maps of vector wind anomalies at 700 mb for (a) wet years and, (b) dry years. Maps were generated from NOAA’s Climate Diagnostic Center Website.

3.3.1.3. Multimodel Ensemble Forecast

As mentioned at the outset, spring streamflow forecasts at several lead times before the spring flow period are required by the water managers; hence, forecasts of the upcoming spring streamflows are issued on the first of every month starting December 1st through April 1st. The predictors and the first PC of spring flows are passed through the modeling framework described in the previous section. The residuals (or errors) from the model were all found to be normally distributed using a Kolmogorov-Smirnov test (Wilks, 1995). The forecasts are made in a cross-validated mode, i.e., a year is dropped from the data set, the PCA analysis is performed on the remaining data, and an ensemble forecast is issued. This is repeated for all the years.

Table 3: Suite of predictors of GRB spring streamflow for April 1st forecast.

Index Series	Climate Variable	Positively Correlated Regions		Negatively Correlated Regions	
		P1	P2	N1	N2
SAT-N1	Surface Air Temperature	-	-	Latitude: 35.0-55.0 Longitude: 235.0-265.0	-
(GPH-P1) – (GPH-N1)	Geopotential Height at 700mb	Latitude: 42.5-57.5 Longitude: 272.5-300.0	-	Latitude: 32.5-42.5 Longitude: 230.0-250.0	-
(GPH-P2) – (GPH-N1)	Geopotential Height at 700mb	-	Latitude: 55.0-62.5 Longitude: 200.0-217.5	Latitude: 32.5-42.5 Longitude: 230.0-250.0	-
(MW-P1) - (MW-N1)	Meridional Wind at 700mb	Latitude: 52.5-40.0 Longitude: 255.0-280.0	-	Latitude: 55.0-75.0 Longitude: 300.0-320.0	-
(MW-P1) – (MW-N2)	Meridional Wind at 700mb	Latitude: 52.5-40.0 Longitude: 255.0-280.0	-	-	Latitude: 57.5-42.5 Longitude: 222.5-232.5
(ZW-P1) – (ZW-N1)	Zonal Wind at 700 mb	Latitude: 35.0-25.0 Longitude: 235.0-257.5	-	Latitude: 55.0-47.5 Longitude: 235.0-255.0	-
(ZW-P2) – (ZW-N1)	Zonal Wind at 700 mb	-	Latitude: 30.0-20.0 Longitude: 145.0-185.0	Latitude: 55.0-47.5 Longitude: 235.0-255.0	-
(SST-P1) – (SST-N1)	Sea Surface Temperature	Latitude: 50.5-44.8 Longitude: 187.5-204.4	-	Latitude: 33.3-21.9 Longitude: 144.4-185.6	-
(SST-P2) – (SST-N1)	Sea Surface Temperature	-	Latitude: -8.6 - -18.1 Longitude: 247.5-275.6	Latitude: 33.3-21.9 Longitude: 144.4-185.6	-
PDSI	Palmer Drought Severity Index	Colorado Region 2 (Aug – Oct Seasonal values)			
PC1 SWE	April SWE	From the Gunnison River Basin			

Of course, for the forecasts issued on December 1st and January 1st, only the climate predictors are used (as the SWE information is not yet available). But for the

forecasts issued in subsequent months, the first PC of SWE is also included in the predictor mix.

As described in the methodology section, several models (i.e., predictor and parameter combinations) yield similar GCV values. This can be noticed in Table 4 where the first 6 models are shown for the April 1st forecast, which illustrates the difficulty in selecting a single model uniquely and underscores the need for multimodel ensemble approach. A threshold of 20% of the least GCV value is defined and all the models within this range are selected. By inspection it is found that models within this threshold tended to have GCV values clustered together as seen in Table 4. This rule of thumb seemed to work well for the application presented. But the need for a more objective criterion is recognized. The GCV based optimal values of K and p were found to be one, indicating that the relationship between the predictors and the flow is largely linear. However, the local functional estimation aspect of the method enables it to capture subtle nonlinearities between the variables that are present (Figure 11) with these parameter values.

Table 4: Multimodel combinations of GRB for April 1st forecast (presence and absence of predictors are indicated by “1” and “0”, respectively).

Number of Predictors	SAT-N1	(GPH-P1) - (GPH-N1)	(GPH-P2) - (GPH-N1)	(MW-P1) - (MW-N1)	(MW-P1) - (MW-N2)	(ZW-P1) - (ZW-N1)	(ZW-P2) - (ZW-N1)	(SST-P1) - (SST-N1)	(SST-P2) - (SST-N1)	PDSI	SWE (First PC)	GCV
1	0	0	0	0	0	0	0	0	0	0	1	2.07
2	0	0	0	0	0	0	0	0	0	1	1	2.14
2	0	0	0	1	0	0	0	0	0	0	1	2.15
2	0	0	0	0	1	0	0	0	0	0	1	2.32
3	0	0	0	1	0	0	0	0	0	1	1	2.34
3	0	0	0	0	1	0	0	0	0	1	1	2.51

The number of models selected tended to decrease from December to April. This is intuitive, in that on December 1st SWE is not available and hence the forecasts have

to be made only from climate information. Consequently, individual models have greater uncertainty, and more models qualify as candidates for the multimodel pool. However, on April 1st, SWE information is complete and it is the best predictor of the ensuing spring streamflow. Therefore, fewer models with other predictor variables are necessary to capture the streamflow dynamics and its variability. Hence, a smaller number of multimodels are selected.

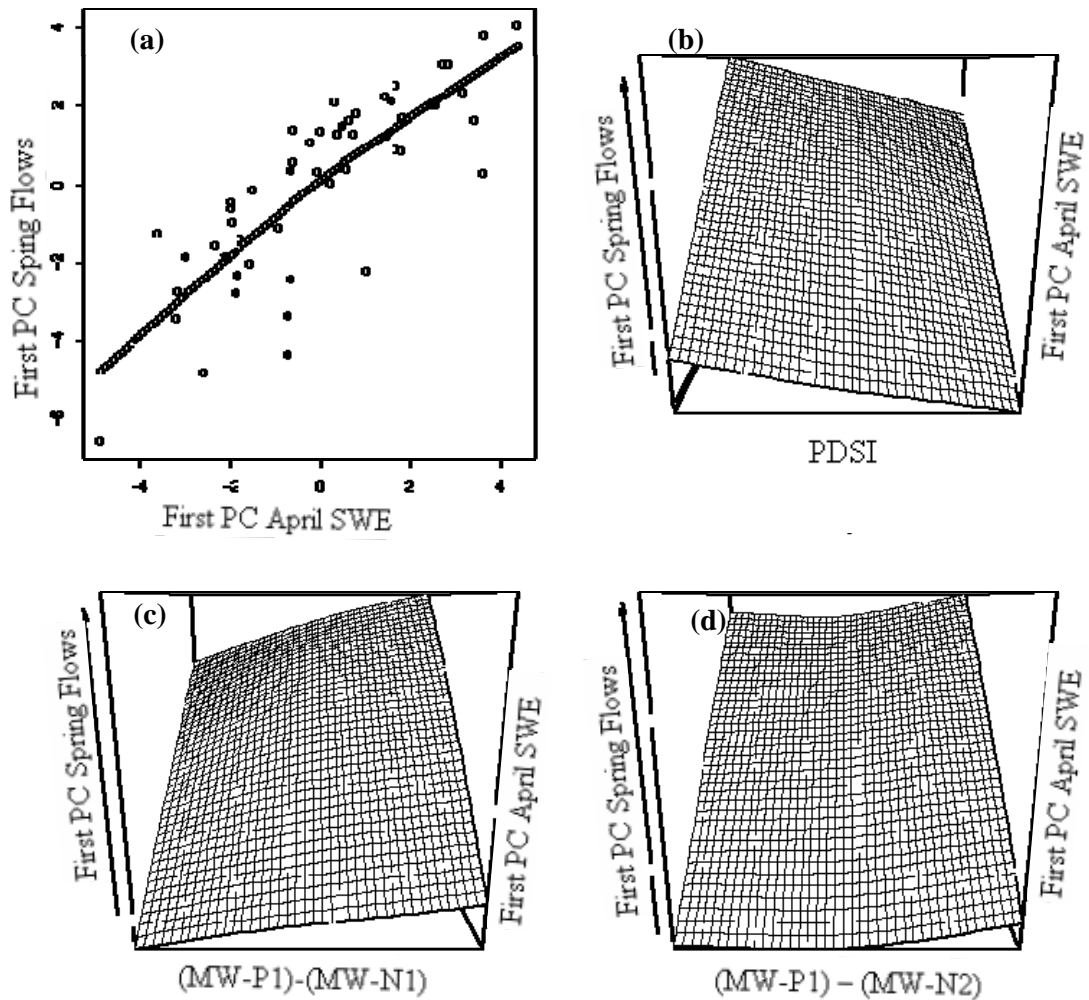


Figure 11: Using the LWP approach for $K=N$ and $p=1$, first PC flows are estimated as a function of (a) first PC SWE; (b) first PC SWE and PDSI; (c) first PC SWE and (MW-P1)-(MW-N1); and (d) first PC SWE and (MW-P1)-(MW-N2).

On the basis of criteria for selecting models for the multimodel ensemble, 15 models for the December 1st forecasts and 6 models for the April 1st forecasts are identified. Ensemble forecasts for the streamflow location, Tomichi, issued on January 1st and April 1st, are shown as boxplots in Figure 12. The box represents the interquartile range, the whiskers are the 5th and 95th percentile of the ensembles, and the horizontal line within the box is the median. The dashed horizontal lines represent the 33rd, 50th, and 66th percentiles of the historic spring streamflow data at this location, and the historic values are shown as points connected by a solid line. Three observations can be made from this figure: (i) The ensembles are shifted in the right direction of the observed streamflow in almost all years. (ii) The ensemble forecasts issued on January 1st (with only the large-scale climate information) seem to capture the observations quite well. (iii) As expected, the ensemble forecasts issued on April 1st are very good. The median RPSS for the January 1st forecast is 0.51 and the April 1st is 0.77. This indicates that skillful predictions of the spring streamflows can be made for the GRB in the middle of winter even when the snow information is absent, which is quite significant for water resources management.

In order to evaluate forecast performance for extreme flows, flows are sorted into three categories: dry years (flows less than 25th percentile of the data), wet years (flows greater than 75th percentile), and near normal (remaining) years. Boxplots of the ensemble forecasts for the wet and dry years are shown in Figures 13 and 14, respectively. It can be seen that the ensembles do quite well forecasting flow extremes even on January 1st. This is very useful to the water managers as the extreme years place undue stress on the system operations.

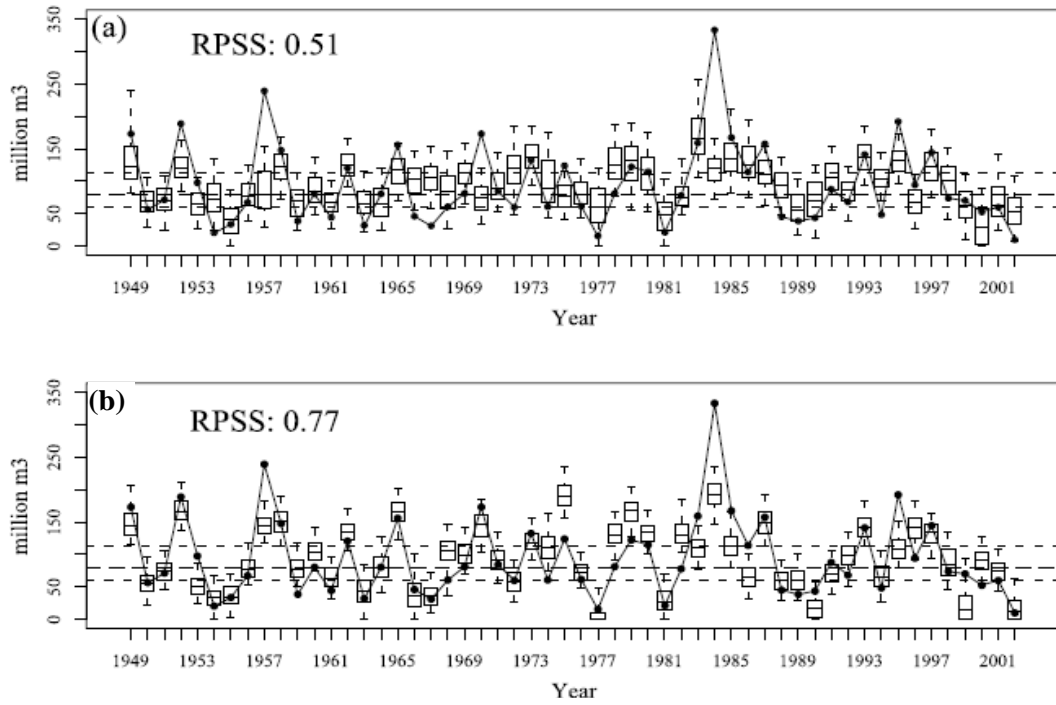


Figure 12: Boxplots of forecasted spring streamflow (million m³) at Tomichi, issued on (a) January 1st, and (b) April 1st. The dashed horizontal lines represent the 33rd, 50th and 66th percentiles of the historical flow data which are shown as points connected by solid line.

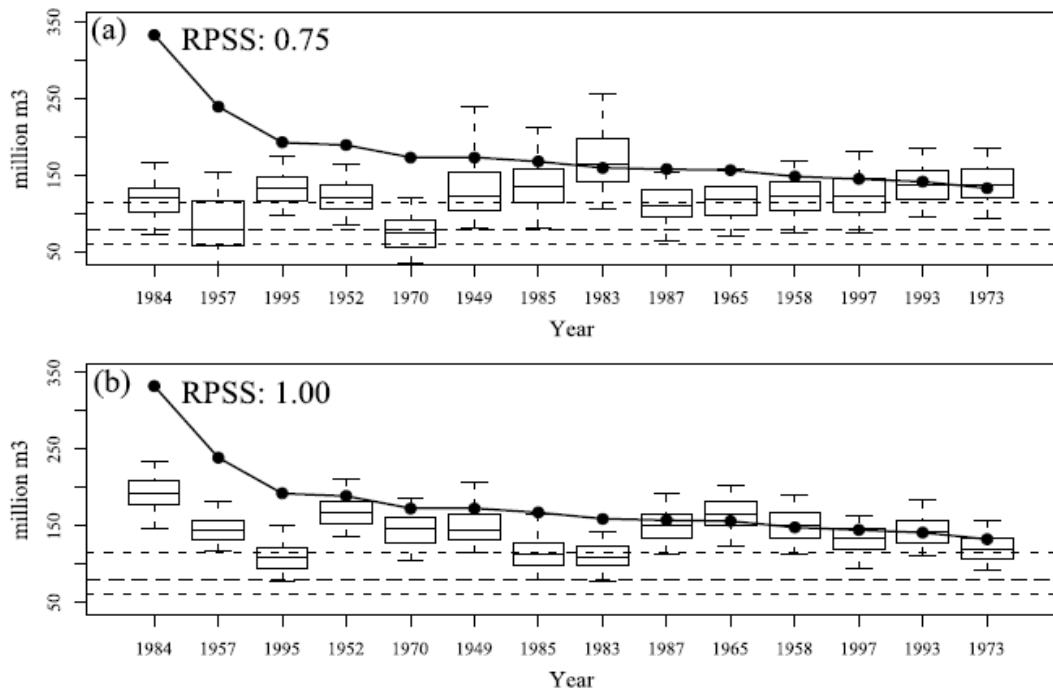


Figure 13: Same as Figure 12 but for forecast of wet years issued on (a) January 1st (b) April 1st.

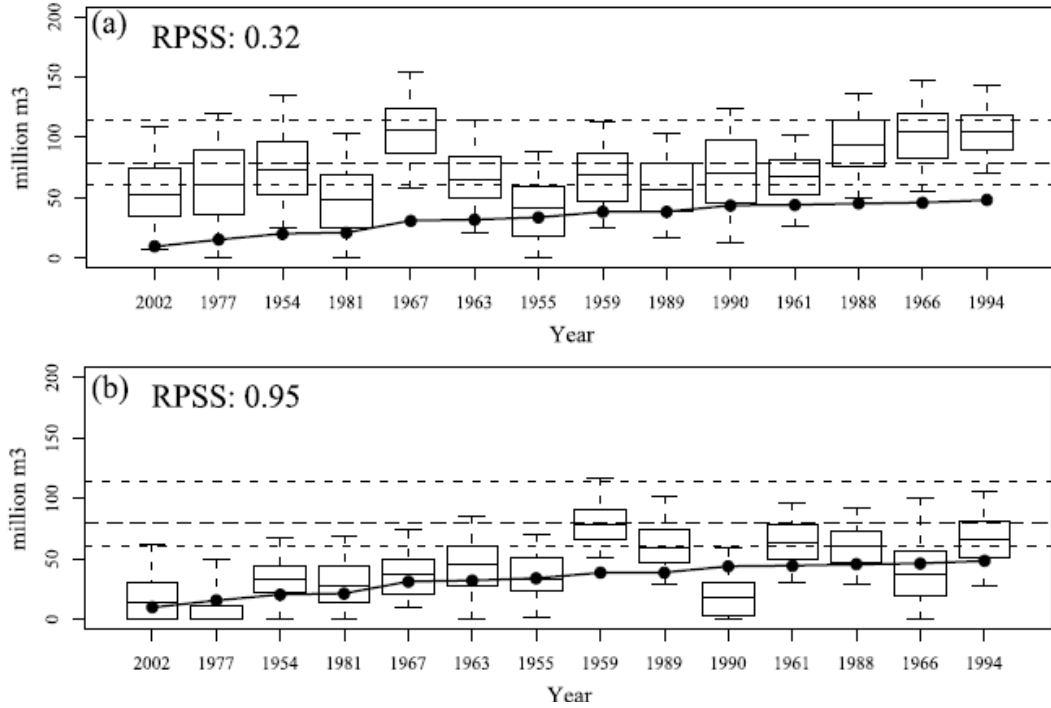


Figure 14: Boxplots of forecasted spring streamflow (million m³) at Tomichi for forecast of dry years issued on (a) January 1st, and (b) April 1st. The dashed horizontal lines represent the 33rd, 50th and 66th percentiles of the historical flow data which are shown as points connected by solid line.

Although April 1st forecast has high skill scores compared to January 1st forecast, in some years January 1st forecasts are more skillful than April 1st forecasts (e.g., 1960, 1979, 1980, 1982, 1983, 1986, 1999; Figure 12). Snow is the main predictor for April 1st forecasts, and in these years snow is not a good representative of the streamflows (Figure 8a) and selected multimodels (i.e., combination of snow, PDSI, and winds) are unable to capture the responsible physical mechanism. Hence, forecasted values are either overestimated or underestimated. In addition, there are a few years (e.g., 1984, 1990, 1995) in which April 1st forecasts are underestimated (Figure 12b). Analyzing snow on April 1st and May 1st revealed the accumulation of snow during the month of April, i.e., May 1st snow is higher than April 1st snow. This means snow on April 1st represents proportionally lower streamflows; therefore, forecasted flows corresponding to April 1st are underestimated. However, these

anomalous years and corresponding behavior are site specific. Incorporating factors such as regional processes and May 1st snow, or post processing of streamflows with respect to regional processes of a specific station may further improve the multimodel ensemble forecasts, particularly in anomalous years.

Categorical skill scores for several thresholds (5th percentile through 95th percentile) for the Brier skill score (BSS, Wilks, 1995) were also computed and similar performance of the multimodel ensembles was observed.

To test the utility of large-scale climate information, multimodel ensemble forecasts were generated at all lead times using just the large-scale climate predictors. The skills from these along with those including the SWE for forecasts issued from February 1st onwards are shown in Table 5. It can be seen that including large-scale climate information and SWE in the multimodel ensemble framework provides higher skill than just the climate predictors. Rank histograms (Hamill, 2001) of the multimodel ensembles (figure not shown) revealed a flattened (or uniform) distribution indicating that the uncertainty estimates are reliable in comparison to the single best model counterparts. As mentioned earlier, one of the advantages of the framework is to provide ensemble forecasts at all the sites capturing the spatial dependence. The average spatial correlation of the ensemble streamflow forecasts was found to be similar to that of the observations.

Table 5: Ranked Probability Skill Scores of GRB forecasts at different lead times using ‘Climate and PDSI’ predictors and using ‘Climate, PDSI and SWE’ information.

River	Climate+PDSI					Climate+PDSI+SWE		
	Dec 1 st	Jan 1 st	Feb 1 st	Mar 1 st	Apr 1 st	Feb 1 st	Mar 1 st	Apr 1 st
Taylor								
All Years	0.50	0.42	0.47	0.46	0.60	0.55	0.61	0.64
Wet Years	0.79	0.91	0.74	0.93	0.97	0.94	0.96	0.98
Dry Years	0.24	0.39	0.41	0.51	0.79	0.46	0.49	0.70
East	Dec 1 st	Jan 1 st	Feb 1 st	Mar 1 st	Apr 1 st	Feb 1 st	Mar 1 st	Apr 1 st
All Years	0.34	0.44	0.38	0.56	0.64	0.60	0.52	0.71
Wet Years	0.42	0.79	0.56	0.82	0.86	0.74	0.90	0.97
Dry Years	0.38	0.31	0.45	0.51	0.80	0.61	0.40	0.86
Tomichi	Dec 1 st	Jan 1 st	Feb 1 st	Mar 1 st	Apr 1 st	Feb 1 st	Mar 1 st	Apr 1 st
All Years	0.47	0.51	0.32	0.57	0.33	0.66	0.74	0.77
Wet Years	0.52	0.75	0.39	0.83	0.92	0.88	0.92	1.00
Dry Years	0.36	0.32	0.37	0.45	0.83	0.54	0.61	0.95
Lake Fork	Dec 1 st	Jan 1 st	Feb 1 st	Mar 1 st	Apr 1 st	Feb 1 st	Mar 1 st	Apr 1 st
All Years	0.29	0.43	0.20	0.35	0.40	0.39	0.48	0.71
Wet Years	0.07	0.46	-0.02	0.42	0.58	0.39	0.53	0.96
Dry Years	0.27	0.15	0.24	0.30	0.62	0.56	0.57	0.89
North Fork	Dec 1 st	Jan 1 st	Feb 1 st	Mar 1 st	Apr 1 st	Feb 1 st	Mar 1 st	Apr 1 st
All Years	0.36	0.46	0.40	0.56	0.63	0.46	0.45	0.78
Wet Years	0.52	0.81	0.66	0.81	0.90	0.64	0.82	0.97
Dry Years	0.21	0.21	0.38	0.42	0.82	0.50	0.33	0.65
Uncompahgre	Dec 1 st	Jan 1 st	Feb 1 st	Mar 1 st	Apr 1 st	Feb 1 st	Mar 1 st	Apr 1 st
All Years	0.43	0.40	0.33	0.35	0.33	0.61	0.66	0.66
Wet Years	0.40	0.74	0.46	0.79	0.84	0.84	0.81	0.98
Dry Years	0.21	0.30	0.27	0.30	0.63	0.45	0.62	0.88

3.3.2. San Juan River Basin

Results of multimodel ensemble application are as follows.

3.3.2.1. Streamflow characteristics - Principal Component Analysis

Two streamflow locations, Animas River at Durango and McElmo Creek at the Colorado-Utah border in the San Juan River basin, are selected (Figure 4). The Animas River is a part of the upper San Juan River Basin, which is in the San Juan

Mountains and it receives most of the annual precipitation as snow. The annual streamflows of this river are spring driven, i.e., approximately 70% of the annual streamflows is contributed by the melting of snow (Figure 5) during spring (April through July) and plays a key role in meeting various demands. The McElmo Creek is in the lower San Juan River Basin, where most of the region is plains and receives precipitation from both rain and snow. It is seen that McElmo's annual streamflows are modulated by snow in winter and by rain in the following months, thus maintaining a uniform monthly contributions to annual flows (see Figure 15). The McElmo's spring runoff contribution to the annual streamflow is small compared to the Animas River, i.e., approximately 30% of annual streamflows. Although the contribution by spring runoff is less, it is important for late fall and summer water releases. Therefore, spring streamflow time series is generated for selected two locations and is used in the multimodel ensemble forecasting.

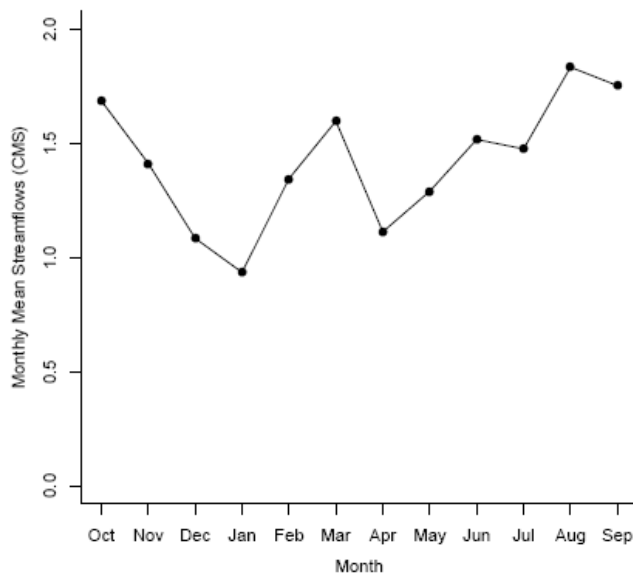


Figure 15: Annual average hydrograph of McElmo Creek at CO-UT border line.

Principal Component Analysis is applied to the normalized spring flow time series, and then PCs and corresponding percentages of variances are estimated. The first PC (Figure 16) explained 88% of the variance and is considered as leading mode and is thus treated as the signal. It also exhibited high correlations (0.94) and equal eigen loadings at both streamflow locations. Second PC, because of its less explained variance (i.e., 12%) is treated as noise. These results suggest domination of a single mechanism and similar variability at the selected streamflow locations.

PCA is also applied on the five locations of April 1st SWE. Even at these locations, first PC explained most of the variance (88%) (Figure 17a); hence it is considered as the leading PC (Figure 17b). The remaining four PCs explained 12% variance and are treated as noise, i.e., these PCs, unlike first PC, do not have any signal/information within them. High correlations (≥ 0.90) and equal eigen loadings (Figure 17c) of the leading PC at all locations suggest unique variability and climate mechanism across the basin. PCA on spring streamflows and winter SWE suggested similar results. Such results are expected because spring flows are derived from winter snow. Corroborating further, the first PC of spring flows and April 1st SWE are highly (i.e., 0.79) correlated (Figure 18). Although there is a strong linear relation between SWE and spring flows, the relation is not found to be valid during some years. Preceding season's drier/wetter conditions are expected as potential cause for the scatter in the linear relation. The significant correlation (i.e., 0.4) among PDSI (i.e., surrogate for soil conditions) and residuals of linear regression between SWE and spring flows explains the influence of soil conditions for the deviation in the behavior.

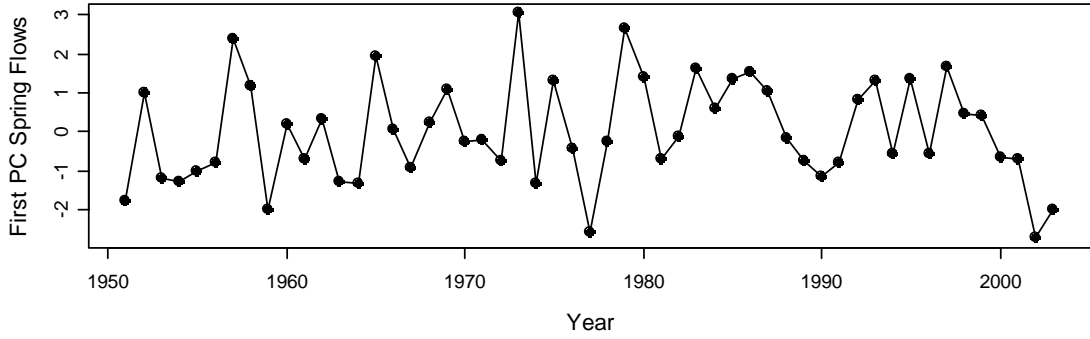


Figure 16: Time series of the first PC of spring streamflows of SJRB.

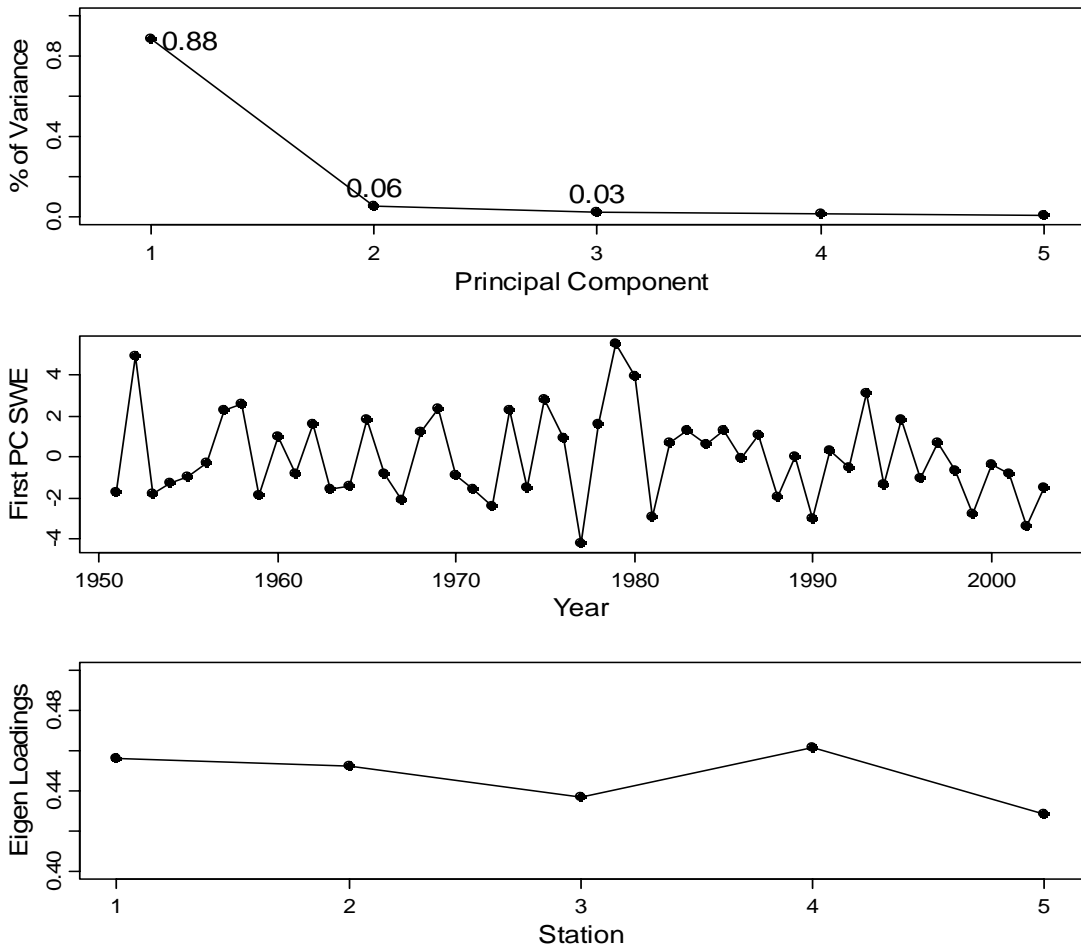


Figure 17: (a) Percentage variance explained by the five Principal Components (PCs), (b) Time series of the first PC and, (c) Eigen loadings of the first PC at the five SWE locations.

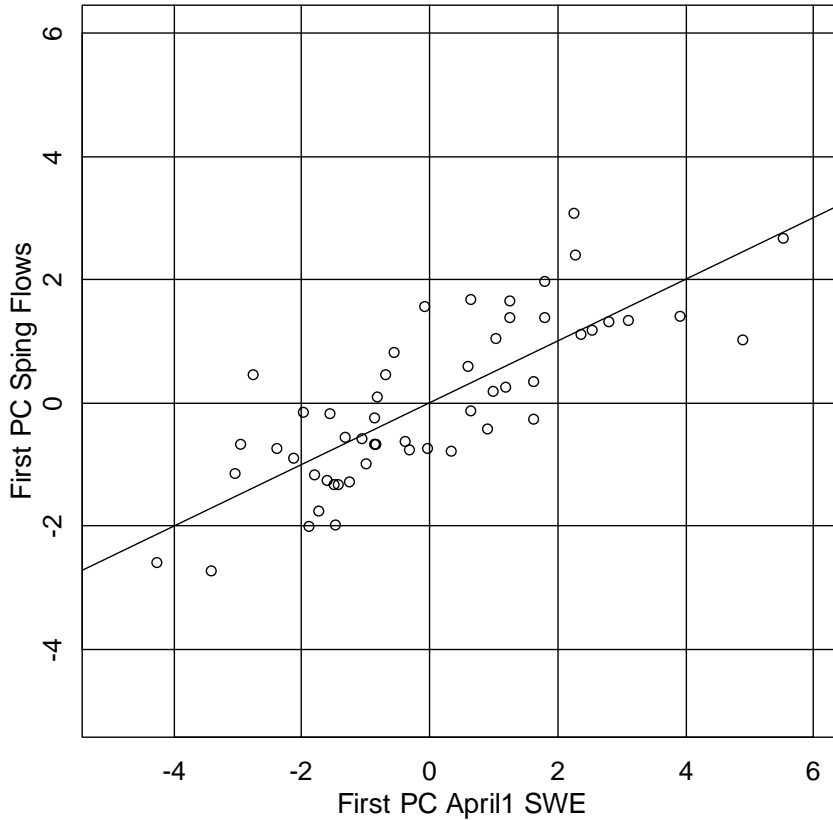


Figure 18: Scatter plot of first PC of, spring flow and April 1st SWE along with the best fit linear regression line.

3.3.2.2. Climate Diagnostics-Predictor selection

The first flow PC is correlated to various teleconnection indices for different months of winter, i.e., October through March. The teleconnection indices include NINO region Sea Surface Temperatures (SST) anomalies, Southern Oscillation Index (SOI), Pacific Decadal Oscillation (PDO), Pacific Northern American pattern (PNA), Northern Atlantic Oscillation (NAO), and Northern Oscillation Index (NOI). Few of these indices exhibited significant correlations in some winter months (Table 6). This is unlike teleconnection patterns of the GRB streamflows; The SJRB's expansion into Southwestern US, in which strong links of teleconnections exist, enhanced the teleconnections link when compared to the GRB.

Table 6: Teleconnection indices that are significantly correlated and corresponding seasons with their correlations are mentioned.

Teleconnection Index	For January 1 st forecast	For April 1 st forecast
NINO 1.2	October - December: 0.29	October - March: 0.31
NINO 3.0	NA	March: 0.28
NINO 3.4	NA	March: 0.28
NINO 4.0	NA	NA
Southern Oscillation Index (SOI)	November: -0.32	January-February: -0.32
Northern Atlantic Oscillation (NAO)	October - December: 0.38	October - March: 0.37
Northern Oscillation Index (NOI)	NA	January - February: -0.45
Pacific Decadal Oscillation (PDO)	NA	March: 0.33
Pacific Northern American Pattern (PNA)	December: -0.34	March: -0.40

The first flow PC is also correlated to large-scale ocean-atmospheric circulation variables (mentioned in the ‘GRB results’ section) over two different seasons, November-December and November-March. Correlation patterns of November-March season are presented in Figure 19. For both GRB and SJRB, similar correlation features (Figures 8 and 19) are identified revealing similar large-scale climate drivers responsible for streamflow variability. This is further supported by similar composite maps of both basins (Figures 9 and 20). In addition to common features, SJRB streamflows are influenced by the elements of the Atlantic Ocean. These are exhibited in terms of first flow PC strong correlations with Atlantic sea surface temperatures (Figure 19e) and Atlantic Ocean related standard indices such as NAO and NIO (Table 6).

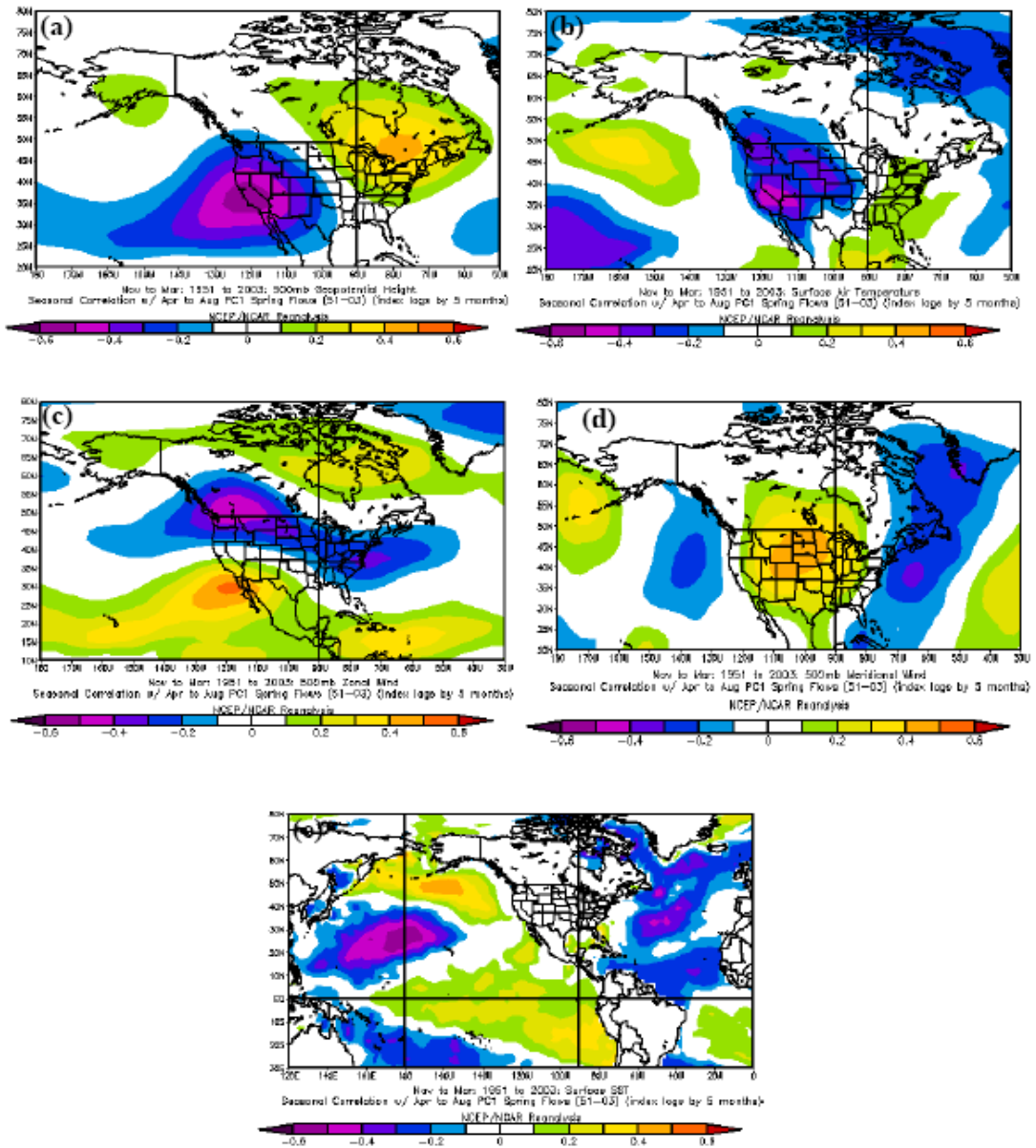


Figure 19: Correlation between the first PC of Spring flow and Nov-Mar large scale climate variables (a) Geopotential Height – 500 mb (b) Surface Air Temperature (c) Zonal wind - 500 mb (d) Meridional wind - 500 mb (e) Sea Surface Temperature. Maps were generated from NOAA’s Climate Diagnostic Center Website.

From these strongly correlated regions, potential predictors are prepared by averaging the climate variables information over the region. Similar correlation patterns are observed for November-December season as well and a different set of predictors are generated from corresponding strongly correlated regions of the season.

Similar to the previous section, a new predictor set with the difference between the regions of positive and negative correlations is prepared. April 1st forecast includes the first PC of SWE in addition to large-scale climate variables, PDSI and other teleconnection indices, which are potential predictors for January 1st forecast.

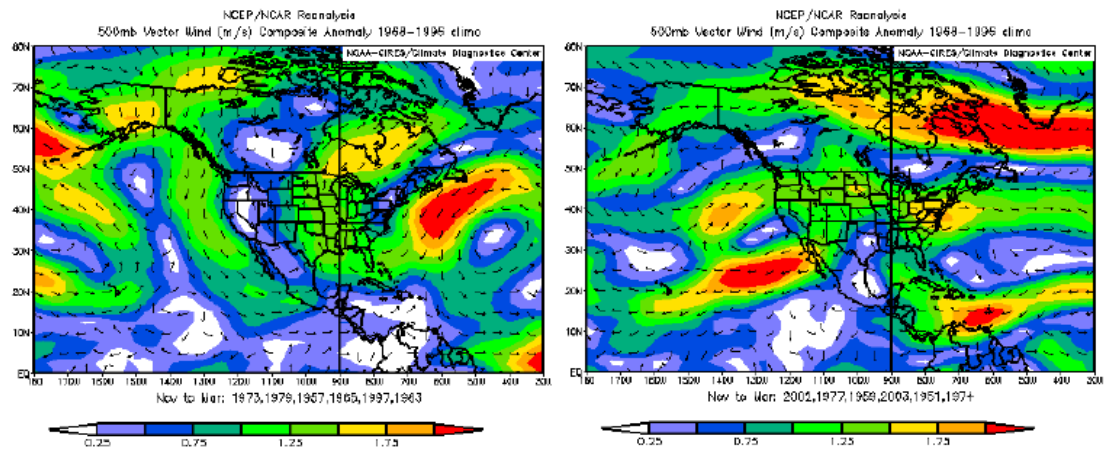


Figure 20: Composite maps of vector wind anomalies at 500 mb for (a) wet years and, (b) dry years. Maps were generated from NOAA’s Climate Diagnostic Center Website.

3.3.2.3. Multimodel Ensemble Forecast

Similar to the spring streamflow forecasts of the GRB, the selected predictors and first flow PC are passed through multimodel selection algorithm, and an ensemble forecast of spring streamflows is made for all years in the cross validated mode from each of the multimodels. The forecasts are issued at two different lead times, on January 1st and April 1st. The January 1st forecast predictor set consists of only climate information (as the SWE information is not available at that time of the year) (Table 7) whereas April 1st forecast comprises of both climate and SWE information (Table 8).

Table 7: Suite of predictors of SJRB spring streamflow for January 1st forecast.

Index Series	Climate Variable	Positively Correlated Regions		Negatively Correlated Regions	
		P1	P2	N1	N2
SAT-N1	Surface Air Temperature	-	-	Latitude: 32.5-52.5 Longitude: 235.0-257.5	-
(GPH-P1) – (GPH-N1)	Geopotential Height at 700mb	Latitude: 32.5-45.0 Longitude: 280.0-295.5	-	Latitude: 30.0-52.5 Longitude: 235.5-260.0	-
(GPH-P2) – (GPH-N1)	Geopotential Height at 700mb	-	Latitude: 40.0-52.5 Longitude: 202.5-220.0	Latitude: 30.0-52.5 Longitude: 235.5-260.0	-
(MW-P1) - (MW-N1)	Meridional Wind at 700mb	Latitude: 32.5-50.0 Longitude: 260.0-280.0	-	Latitude: 30.0-57.5 Longitude: 220.0-240.0	-
(MW-P1) – (MW-N2)	Meridional Wind at 700mb	Latitude: 32.5-50.0 Longitude: 260.0-280.0	-	-	Latitude: 40.0-70.0 Longitude: 290.0-320.0
(ZW-P1) – (ZW-N1)	Zonal Wind at 700 mb	Latitude: 27.5-37.5 Longitude: 240.0-267.5	-	Latitude: 47.5-60.0 Longitude: 239.0-254.0	-
(ZW-P2) – (ZW-N1)	Zonal Wind at 700 mb	-	Latitude: 15.0-35.0 Longitude: 267.5-300.0	Latitude: 47.5-60.0 Longitude: 239.0-254.0	-
(SST-P1) – (SST-N1)	Sea Surface Temperature	Latitude: 42.5-51.0 Longitude: 187.5-210.0	-	Latitude: 12.5-37.5 Longitude: 140.0-190.0	-
(SST-P2) – (SST-N1)	Sea Surface Temperature	-	Latitude: -5.0 - -27.5 Longitude: 255.5-285.0	Latitude: 12.5-37.5 Longitude: 140.0-190.0	-
(SST-P2) – (SST-N2)	Sea Surface Temperature	-	Latitude: -5.0 - -27.5 Longitude: 255.5-285.0	-	Latitude: 7.5-25.0 Longitude: 305.0-342.5
PDSI-CO-2	Palmer Drought Severity Index	Colorado Region 2 (Aug – Oct Seasonal values)			
PDSI-NM-1	Palmer Drought Severity Index	New Mexico Region 1 (Aug – Oct Seasonal values)			

Table 8: Suite of predictors of SJRB spring streamflow for April 1st forecast.

Index Series	Climate Variable	Positively Correlated Regions		Negatively Correlated Regions	
		P1	P2	N1	N2
SAT-N1	Surface Air Temperature	-	-	Latitude: 35.0-52.5 Longitude: 237.5-262.5	-
(GPH-P1) – (GPH-N1)	Geopotential Height at 700mb	Latitude: 42.5- 55.0 Longitude: 267.5-295.0	-	Latitude: 27.5-45.0 Longitude: 225.0-250.0	-
(MW-P1) - (MW-N1)	Meridional Wind at 700mb	Latitude: 37.5- 50.0 Longitude: 247.5-272.5	-	Latitude: 35.0- 47.5 Longitude: 215.0-230.0	-
(MW-P1) – (MW-N2)	Meridional Wind at 700mb	Latitude: 37.5- 50.0 Longitude: 247.5-272.5	-	-	Latitude: 35.0- 70.0 Longitude: 290.0-315.0
(ZW-P1) – (ZW-N1)	Zonal Wind at 700 mb	Latitude: 25.0- 32.5 Longitude: 227.5-250.0	-	Latitude: 42.5- 57.5 Longitude: 230.0-260.0	-
(ZW-P1) – (ZW-N2)	Zonal Wind at 700 mb	Latitude: 25.0- 32.5 Longitude: 227.5-250.0	-	-	Latitude: 35.0- 40.0 Longitude: 280.0-295.0
(SST-P1) – (SST-N1)	Sea Surface Temperature	Latitude: 45.0- 51.0 Longitude: 190.0-210.0	-	Latitude: 14.0- 36.0 Longitude: 145.0-201.0	-
(SST-P2) – (SST-N1)	Sea Surface Temperature	-	Latitude: -8.0 - -22.0 Longitude: 255.0-280.0	Latitude: 14.0- 36.0 Longitude: 145.0-201.0	-
(SST-P2) – (SST-N2)	Sea Surface Temperature	-	Latitude: -8.0 - -22.0 Longitude: 255.0-280.0	-	Latitude: 26.0- 44.0 Longitude: 300.0-328.0
PDSI	Palmer Drought Severity Index	Colorado Region 2 (Aug – Oct Seasonal values)			
PC1 SWE	April 1 st SWE	From the SJRB			

Following the same rule of thumb that is applied in the GRB, multimodels that are within 20% of the least GCV are selected. The January 1st forecast selected 21 models (Table 9) whereas April 1st forecast selected 11 models (Table 10). The decrease in

Table 9: Multimodel combinations of SJRB for January 1st forecast (presence and absence of predictors are indicated by “1” and “0”, respectively).

Number of Predictors	SAT	GPH-I	GPH-II	MW-I	MW-II	ZW-I	ZW-II	SST-I	SST-II	SST-III	PDSI-CO	PDSI-NM	NINO1.2	NAO	PNA	SOI	GCV	GCV RATIO
2	0	0	0	0	0	0	1	0	1	0	0	0	0	0	0	0	1.04	1.00
2	0	0	0	1	0	0	0	0	1	0	0	0	0	0	0	0	1.05	1.01
2	0	0	0	0	1	0	0	0	1	0	0	0	0	0	0	0	1.09	1.05
2	0	1	0	0	0	0	0	0	1	0	0	0	0	0	0	0	1.10	1.06
2	0	0	1	0	0	0	0	0	1	0	0	0	0	0	0	0	1.12	1.07
3	0	0	0	0	0	0	1	0	1	0	1	0	0	0	0	0	1.12	1.08
2	0	0	0	0	0	0	1	0	0	1	0	0	0	0	0	0	1.12	1.08
2	0	0	0	1	0	0	0	0	0	1	0	0	0	0	0	0	1.13	1.08
3	0	0	0	0	1	0	0	0	1	0	0	0	0	0	1	0	1.13	1.08
2	0	0	1	0	0	0	0	0	0	1	0	0	0	0	0	0	1.14	1.10
2	0	1	0	0	0	0	0	0	0	1	0	0	0	0	0	0	1.16	1.11
3	0	0	0	0	1	0	0	0	1	0	1	0	0	0	0	0	1.17	1.13
3	0	0	0	0	0	0	1	0	0	1	1	0	0	0	0	0	1.18	1.14
3	0	0	0	1	0	0	0	0	1	0	1	0	0	0	0	0	1.19	1.14
3	0	0	1	0	0	0	0	0	1	0	0	0	0	1	0	0	1.21	1.16
3	0	1	0	0	0	0	0	0	1	0	1	0	0	0	0	0	1.21	1.16
3	0	0	0	1	0	0	0	0	1	0	0	1	0	0	0	0	1.22	1.17
2	1	0	0	0	0	0	0	0	1	0	0	0	0	0	0	0	1.23	1.18
3	0	0	0	1	0	0	0	0	0	1	1	0	0	0	0	0	1.24	1.19
1	0	0	0	0	1	0	0	0	0	0	0	0	0	0	0	0	1.25	1.20
3	0	0	1	0	0	0	0	0	1	0	1	0	0	0	0	0	1.25	1.20

Table 10: Multimodel combinations of SJRB for April 1st forecast (presence and absence of predictors are indicated by “1” and “0”, respectively).

Number of Predictors	SAT	GPH	MW-I	MW-II	ZW-I	ZW-II	SST-I	SST-III	SST-III	PDSI-CO	PDSI-NM	NINO 1.2	NINO 3.0	NINO 3.4	NAO	NOI	PDO	PNA	SOI	PC1-SWE	GCV	GCV RATIO	
2	0	0	0	0	0	0	0	0	0	0	0	0	0	0	0	0	0	0	1	0	1	0.68	1.00
3	0	0	0	0	0	0	0	0	0	1	0	0	1	0	0	0	0	0	0	0	1	0.75	1.09
2	0	0	0	0	0	0	0	0	0	1	0	0	0	0	0	0	0	0	0	0	1	0.75	1.10
3	0	0	0	0	0	0	0	0	0	1	0	0	0	1	0	0	0	0	0	0	1	0.77	1.13
3	0	0	0	0	0	0	0	0	0	1	0	0	0	0	0	0	0	1	0	0	1	0.78	1.13
2	0	0	0	0	0	0	0	0	0	0	0	0	1	0	0	0	0	0	0	0	1	0.78	1.15
1	0	0	0	0	0	0	0	0	0	0	0	0	0	0	0	0	0	0	0	0	1	0.78	1.15
2	0	0	0	0	0	0	0	0	0	0	0	0	0	0	0	0	0	1	0	0	1	0.80	1.17
3	0	0	0	0	0	0	0	0	0	1	0	1	0	0	0	0	0	0	0	0	1	0.80	1.17
2	0	0	0	0	0	0	0	0	0	0	0	0	0	1	0	0	0	0	0	0	1	0.81	1.18
2	0	0	0	0	0	0	0	0	0	0	0	1	0	0	0	0	0	0	0	0	1	0.82	1.19

number of multimodels is similar to that seen in the GRB. On the January 1st forecast, each of the potential predictors (and models as well) provide information on future spring streamflow, whereas on the April 1st forecast, only SWE explains most of the spring streamflows dynamics and variability. Hence, fewer multimodels are selected for April 1st forecast compared to the January 1st forecast. In all models, the GCV based optimal values of K and p are found to be one, indicating that the relationship between the predictors and flows is linear on a broader scale. However, local function aspect of the method enables to capture subtle nonlinearities between variables, if any.

Ensemble forecasts for both streamflow locations, issued on January 1st and April 1st, are shown as box plots in Figures 21 and 22. The notation of box plots is same as explained in the results section of the GRB. The following observations are made: (1) Ensembles of both lead times are shifted in the right direction for almost all years. (2) The January 1st issued ensemble forecasts captured observations quite well even in the absence of snow pack. (3) The April 1st issued ensemble forecast is quite good compared to the January 1st forecast. These observations suggest good skill of the multimodel ensemble forecast framework and provide valuable information starting from the middle of winter. Forecast performance is also evaluated in extreme years, by categorizing flows into three categories: dry years (flows less than 25th percentile of data), wet years (flows greater than 25th percentile of data), and near normal (remaining) years. Box plots of the wet and dry years for both locations are shown in Figures 23, 24, 25, and 26. These plots suggest better performance of streamflow forecasts for both wet and dry years. Although forecasts do not capture actual

observations in terms of magnitude, the range of forecasts potentially suggests the extreme conditions in almost all years. Better skills are depicted by April 1st forecasts when compared to January 1st forecast (Table 11). These skillful observations of extreme conditions (wet/dry), especially on January 1st (3-months lead time), provide useful information for water managers and help them take better decisions to reduce the stress on water resources.

3.3.3. Comparison between multimodel ensemble and current framework

Multimodel ensemble forecasts are compared with the Colorado Basin River Forecast Center's (CBRFC) forecasts, which are currently used by the U.S. Bureau of Reclamation (BOR) for the operations of reservoirs in the Gunnison basin. The CBRFC's April to July volume forecasts at four reservoirs (i.e., Taylor Park, Blue Mesa, Morrow Point and Crystal – detailed in Chapter 5) of the Gunnison basin are considered for the comparison. The seasonal (April to July) volume forecasts are adjusted reservoir inflows, and closely approximate natural or unimpaired flows into a reservoir. The actual reservoir inflows are available for a period of 28 years from 1978-2005 and were obtained from the BOR (P. Davidson, personal communication, 2005). The archive of CBRFC forecasts (one single value, i.e., most probable forecast, for each year) for a period of 15 years spanning 1991-2005 was provided by the CBRFC (CBRFC scientists, personal communication, 2005). The multimodel ensemble forecast framework was applied to actual reservoir inflows, and then cross validated ensemble of reservoir inflows were forecasted on January 1st and April 1st (detailed in Chapter 5). These forecasts were compared with the CBRFC archive forecasts for the overlapping period, 1991-2005. Boxplots of ensemble inflow

forecasts for Blue Mesa reservoir are developed, and compared with the actual reservoir inflows (blue solid circle) and most probable CBRFC forecast (red solid circle) (Figure 27). These plots, similar to streamflow forecasts of the GRB and SJRB, suggest good skill of the multimodel ensemble forecast framework starting from early winter (e.g., shifting ensemble of forecasts in the right direction, capturing observations fairly well). The methods' performance is quantified by estimating the correlation coefficient between actual inflows, median of ensemble of inflow forecasts and most probable CBRFC's forecast. The correlation coefficient values are tabulated in Table 12. High correlation values suggest good performance of multimodel ensemble forecast and CBRFC forecast on January 1st and April 1st, respectively. On April 1st, both forecasts exhibited good performance (i.e., correlation coefficient 0.7~0.8) with a little difference in their performance, whereas on January 1st the difference in the forecast performance is a bit higher, i.e., multimodel ensemble forecast (correlation coefficient 0.5~0.7) performed better than CBRFC forecast (correlation coefficient 0.3~0.5).

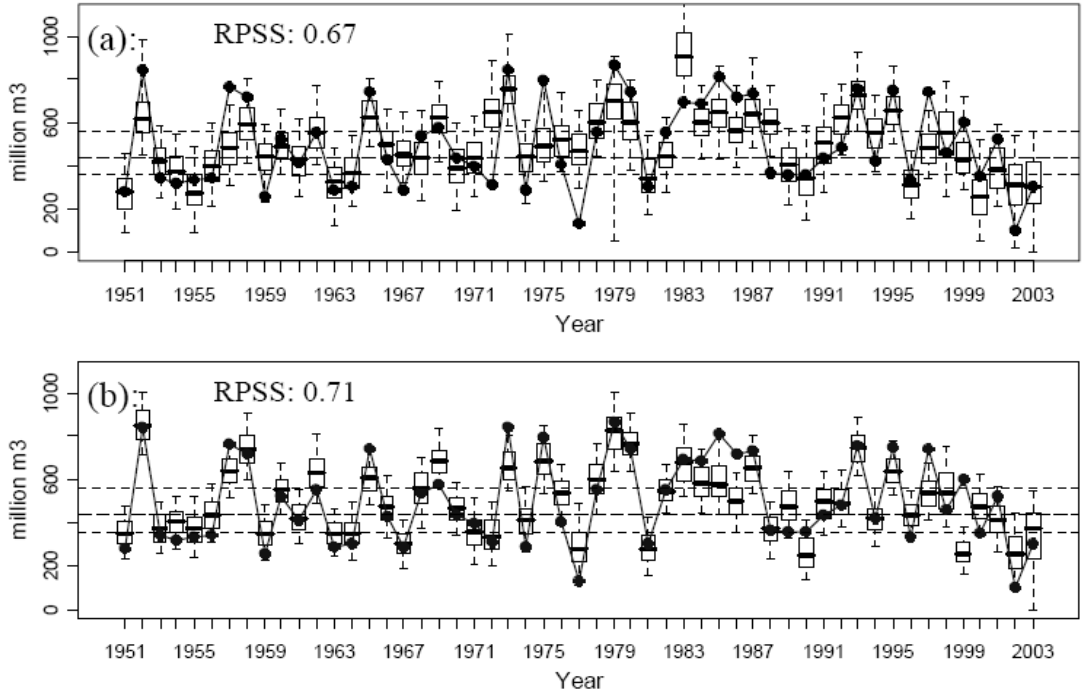


Figure 21: Boxplots of forecasted spring streamflow (million m³) for Animas River at Durango issued on (a) January 1st, and (b) April 1st. The dashed horizontal lines represent the 33rd, 50th and 66th percentiles of the historical flow data which are shown as points connected by solid line.

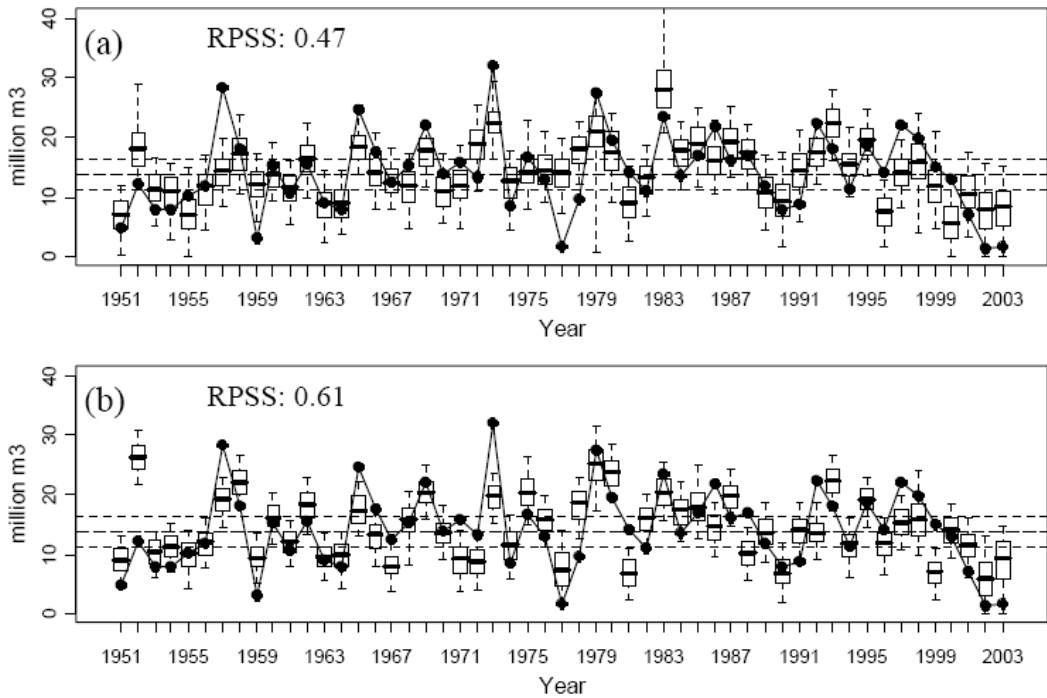


Figure 22: Same as Figure 21 but for forecasts of all years for McElmo Creek at CO-UT state borderline issued on (a) January 1st and (b) April 1st.

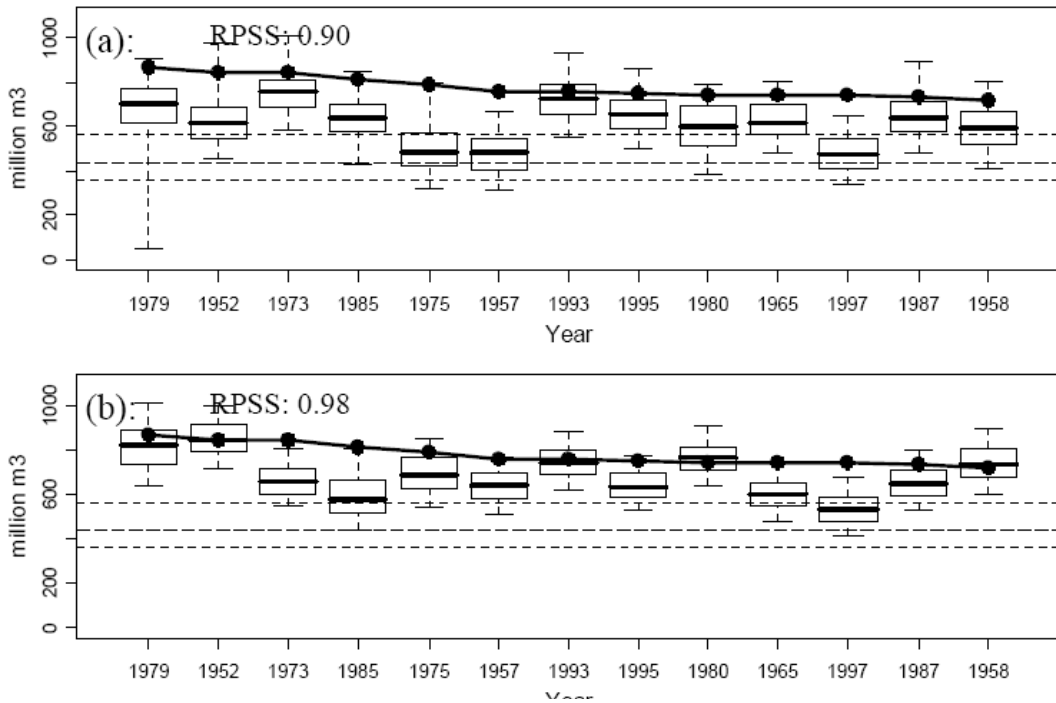


Figure 23: Boxplots of forecasted spring streamflow (million m³) for Animas River at Durango for forecast of wet years issued on (a) January 1st, and (b) April 1st. The dashed horizontal lines represent the 33rd, 50th and 66th percentiles of the historical flow data which are shown as points connected by solid line.

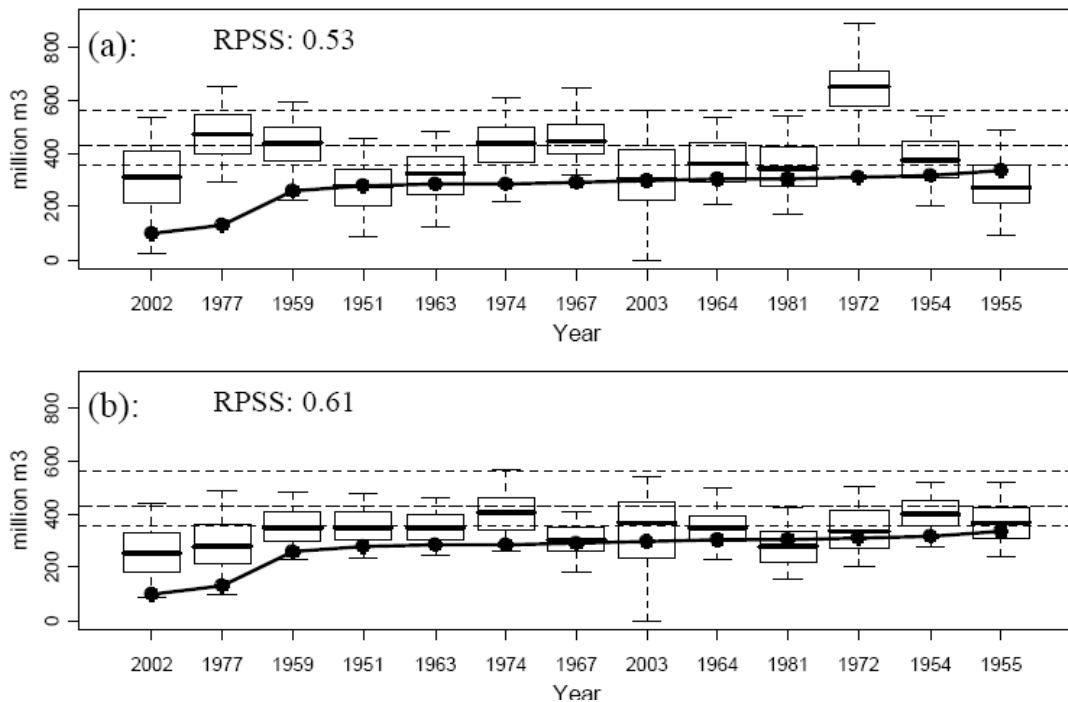


Figure 24: Same as Figure 23 but for forecasts of dry years for Animas River at Durango issued on (a) January 1st and (b) April 1st.

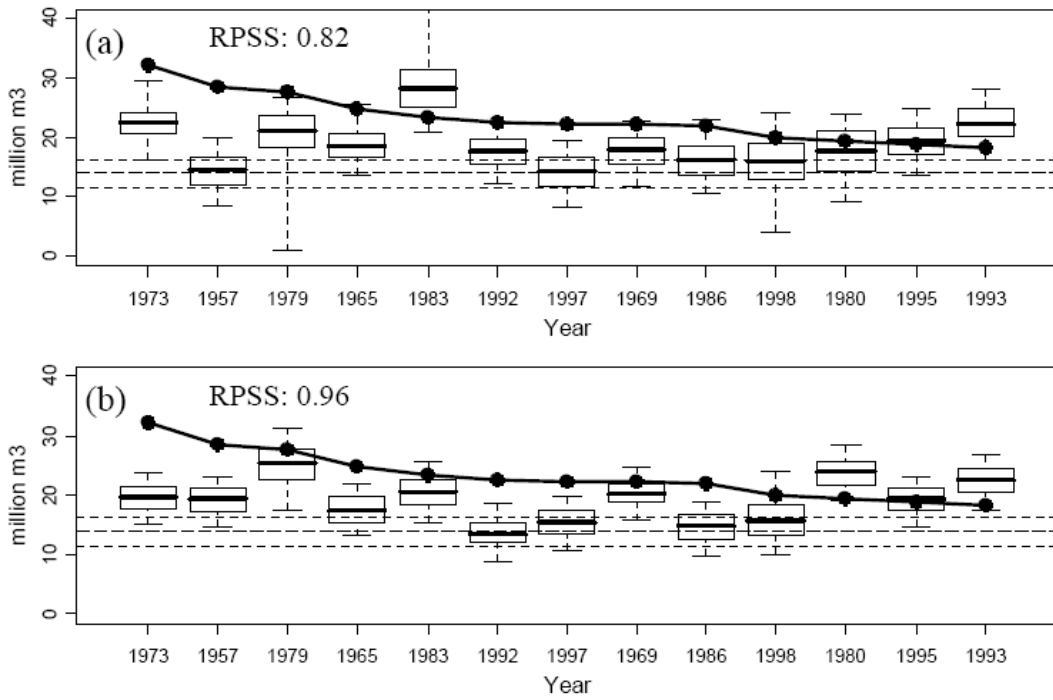


Figure 25: Boxplots of forecasted spring streamflow (million m3) for McElmo Creek at CO-UT state borderline for forecast of wet years issued on (a) January 1st, and (b) April 1st. The dashed horizontal lines represent the 33rd, 50th and 66th percentiles of the historical flow data which are shown as points connected by solid line.

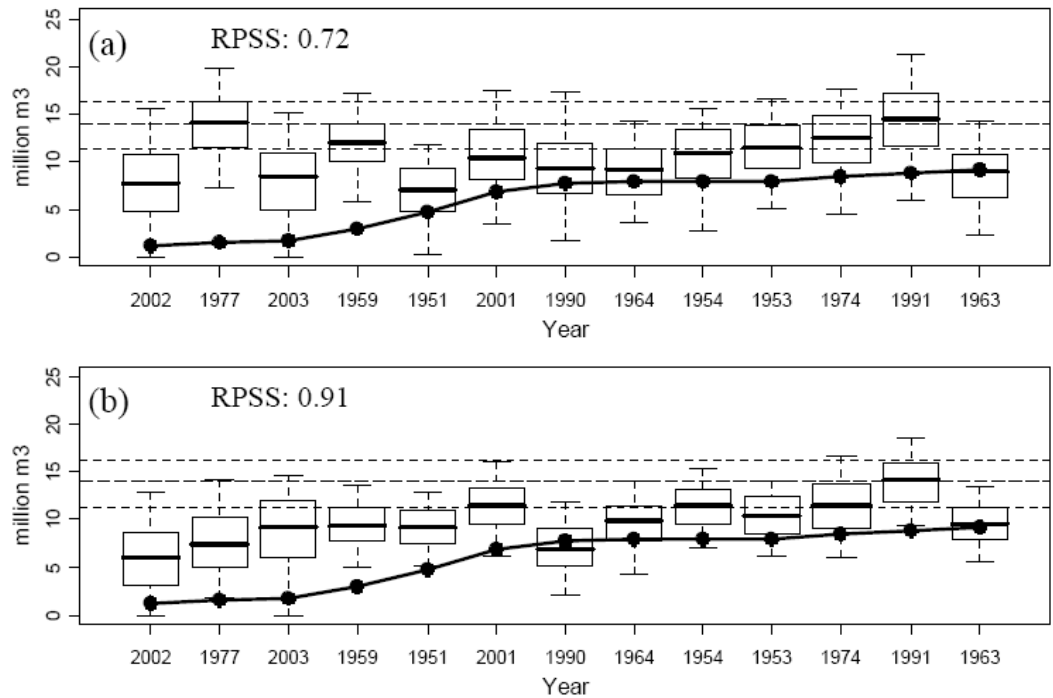


Figure 26: Same as Figure 25 but for forecasts of dry years for McElmo Creek at CO-UT state borderline issued on (a) January 1st and (b) April 1st.

Table 11: Ranked Probability Skill Scores of SJRB forecasts at different lead times using ‘Climate and PDSI’ predictors and using ‘Climate, PDSI and SWE’ information.

River	Animas River at Durango		McElmo Creek near CO- UT Border Line	
	Climate + PDSI	Climate + PDSI + SWE	Climate + PDSI	Climate + PDSI + SWE
	Jan 1 st	Apr 1 st	Jan 1 st	Apr 1 st
All Years	0.67	0.71	0.47	0.61
Wet Years	0.90	0.98	0.82	0.96
Dry Years	0.53	0.61	0.72	0.91

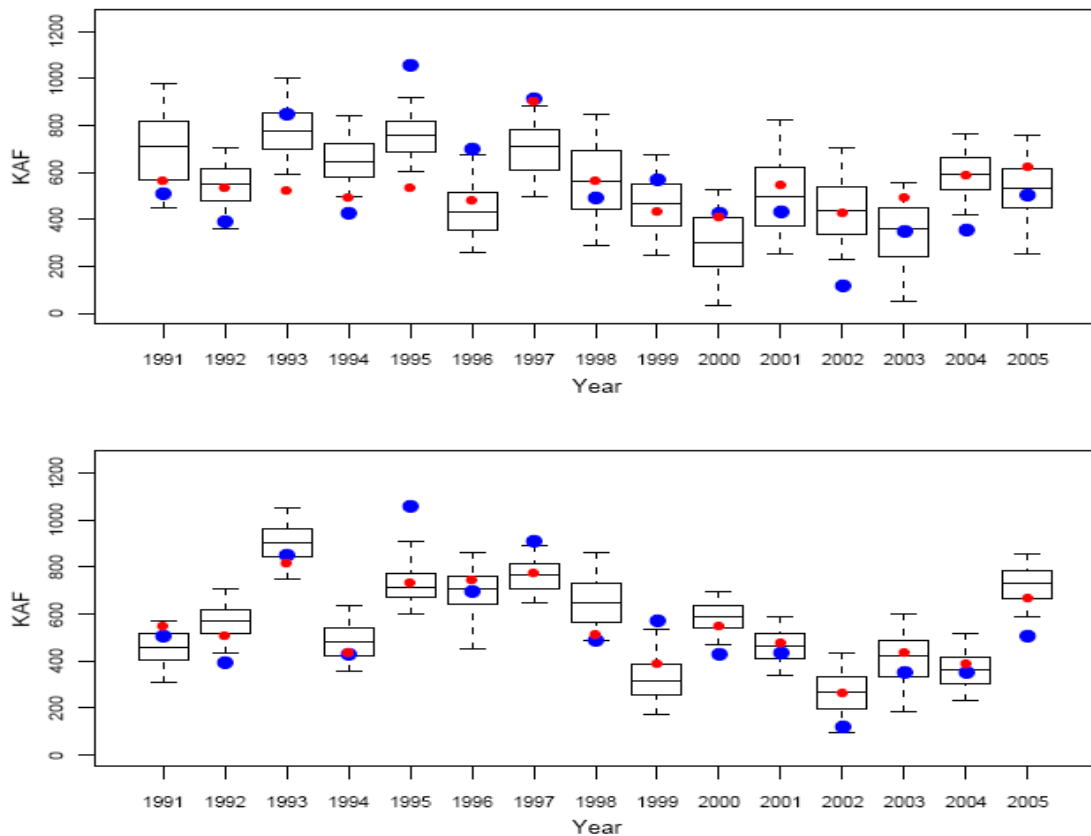


Figure 27: Comparison between multimodel ensemble streamflow forecast with CBRFC most probable forecast, for Blue Mesa reservoir inflows (a) January 1st forecast; (b) April 1st forecast. Boxplots corresponds to multimodel ensemble forecast; blue and red circles correspond to actual and most probable CBRFC forecast.

Table 12: Correlation coefficients among actual observations, median of multimodel ensemble forecast and CBRFC's most probable forecast for two different lead times.

Lead Time Reservoir	Jan 1 st Forecast		April 1 st Forecast	
	Multimodel forecast	CBRFC forecast	Multimodel forecast	CBRFC forecast
Taylor Park	0.554	0.357	0.660	0.832
Blue Mesa	0.625	0.446	0.749	0.862
Morrow Point	0.693	0.338	0.744	0.792
Crystal	0.700	0.505	0.726	0.848

3.4. Summary and Discussions

A multimodel ensemble framework to forecast streamflows at several locations simultaneously is presented. The framework has four main steps. (1) Principal Component Analysis is performed on the spatial streamflows to identify the dominant modes of variability. (2) Large scale ocean-atmospheric predictors are identified for the dominant modes. (3) Objective criterion, Generalized Cross Validation (GCV) is used to select a suite of candidate models. (4) Ensembles of forecast of the dominant modes and consequently the spatial flows are issued from the candidate models. The forecast model is based on the LWP approach that is data driven. Application of this framework to the GRB showed skilful long lead forecasts. Furthermore, the multimodel ensemble forecast including large-scale climate features and SWE rendered better performance in terms of skill and reliability of uncertainty estimates than the single best model counterpart or a model with only the SWE information.

Also, an interesting land-surface effect on the streamflows is observed: when the fall season is dry and following winter is wet, then the spring streamflows tend to be relatively lower compared to what would be expected from a wet winter. Therefore, the soil moisture information of the preceding fall was included as a potential

predictor, which improved the forecasts. This is corroborated by the presence of PDSI in several of the leading candidate models (see Table 4, 9, and 10).

Other factors such as vegetation feedbacks on the spring melt (e.g., Wang et al., 2005) together with soil moisture effects (i.e., quantified by the PDSI), snow pack ripening, spring (daily) wind patterns, air temperature, relative humidity, melt patterns in association with topography and shading factors (Lundquist and Flint, 2005), and cloud cover need to be investigated to better understand the streamflow mechanism and incorporated in the framework to potentially improve the forecast skill. Objective methods for selecting the multimodels, combining their ensembles and dealing with multi-collinearity of the predictors are some of the aspects of the modeling approach that need detailed investigation. Other nonlinear time series approaches that reconstruct the dynamics of the underlying process from observations for prediction (see e.g., Porporato and Ridolfi, 1997, 2001; Regonda et al., 2005b; Sivakumar et al. 2002; Tamea et al., 2005) also offer interesting alternatives for consideration, although, they require a large number of data observations.

Having a skillful forecast of the upcoming spring flows during early winter when the snow information is incomplete is of significant importance to water managers in their planning and operation. In this regard, a decision support model of the GRB is driven with ensemble of streamflow forecasts and resulted ensemble of decision variables is evaluated. This is presented in the chapter 5.

CHAPTER 4

A NEW METHOD TO PRODUCE CATEGORICAL STREAMFLOW FORECASTS

Often water managers require categorical streamflow forecast. That is, they would like to know the probability of streamflow in a defined category. This information can be obtained from the ensembles as described in the Chapter 3. Alternatively, a simpler approach based on logistic regression can be devised to obtain the categorical forecasts directly. In this chapter, a new framework for multi-site categorical forecast is developed and applied to streamflows in the Gunnison River Basin (GRB). This is a complementary approach to the multimodel ensemble forecast framework described earlier.

4.1. Introduction

Streamflow forecasts are provided in two forms according to the water manger's need - categorical (probabilities of wet or dry conditions) and volume (monthly or seasonal streamflows) flow forecasts. A categorical streamflow forecast provides the probability of occurrence of a particular event, e.g., the chance of having higher streamflow. A volume flow forecast provides the amount of streamflows e.g., on daily, monthly, or seasonal time scales.

Two approaches are used to forecast streamflow: physical- and statistical- models. In physical models, a hydrologic model is run using station data up to the start of the forecast to estimate the basin conditions (e.g., snowpack, soil moisture), and is then run into the future, with an “ensemble” of weather/climate forecasts, to produce

ensemble forecasts of streamflow (e.g., Day, 1985; Clark and Hay, 2004). The ensemble of weather/climate forecasts comprise a finite number of individual realizations of precipitation and temperature over the next several weeks or several seasons, which, when used as input to the hydrologic model, produce the same number of future realizations of streamflow. Categorical forecasts can be produced by counting the number of individual ensemble members that are above a pre-defined threshold. Statistical models on the other hand use empirical relations to forecast streamflow (Garen, 1992). For example, snow water equivalent on April 1st may be used in a regression model to predict streamflow averaged over the months April through September. Uncertainty in the statistical models can be estimated easily (e.g., using the standard deviation of the regression residuals), and ensemble forecasts can be produced by sampling from the distribution of regression residuals (Grantz et al., 2005; Regonda et al., 2006). Now, as with the physical models, categorical probabilities from the regression models can be computed from ensemble forecasts. Also, there are statistical methods (e.g., discriminant analysis) that directly estimate categorical forecasts for specific thresholds but require strong distributional assumptions, which when not satisfied, often the case with real data sets, require indirect resampling of errors.

Piechota et al. (1998) developed a categorical forecast framework based on linear discriminant analysis (LDA). This approach has two main steps. First, probability density functions (PDFs) of a given predictor (e.g., the Southern Oscillation Index) were estimated for three subsets of streamflow data (below-normal, normal, and above normal), and the categorical forecast was estimated using Bayes rule

$$\Pr(Q_i | X) = \frac{p_i f_i(x)}{\sum_{i=1}^{k=3} p_i f_i(x)} \quad \dots 4.1$$

Here $\Pr(Q_i | X)$ is the probability of streamflow (Q) in the i -th category, given the predictor X ; p_i is the prior probability of the i -th category (i.e., the fraction of observations in the i -th category); and $f_i(x)$ is the probability of the predictor variable computed using data from only the i -th category. Piechota et al. (1998) estimated the PDFs in equation 4.1 using non-parametric kernel density estimation (Lall, 1995). This first step is hence very similar to contingency table analysis (e.g., estimating the joint probability of X and Q for different categories of X and Q), except the probability of X , $f_i(x)$, is allowed to vary within each of the k categories of Q . The second step in the Piechota et al. (1998) method is extension to multiple predictor variables. Multiple variables (X_1, \dots, X_n) were included by assigning weights to each potential predictor variable, hence

$$\Pr(Q_i | X_1, \dots, X_n) = \sum_{j=1}^n w_j \Pr(Q_i | X_j), \quad 0 \leq w_j \leq 1, \quad \sum_{j=1}^n w_j = 1 \quad \dots 4.2$$

in which w_i are the weights assigned to each predictor variable. The weights were determined by minimizing the error in historical forecasts.

The Piechota et al. (1998) approach is attractive in that it provides a direct method to produce categorical streamflow forecasts. However, the method is somewhat cumbersome in that it requires both kernel density methods for estimating the PDF for each forecast category for use in equation 4.1, as well as optimization methods for

identifying the weights for use in equation 4.2. Together equations 4.1 and 4.2 are similar to logistic regression

$$\Pr(Q_i | X_1, \dots, X_n) = \frac{1}{1 + \exp(\beta_0 + \sum_{j=1}^n \beta_j X_j)} \quad \dots(4.3)$$

where $(\beta_0, \dots, \beta_n)$ are regression coefficients obtained by a maximum likelihood procedure. Logistic regression offers potential improvements over LDA as it fits a function throughout the data and hence does not rely on the likely noisy ratio of probabilities in the LDA approach. Further, logistic regression is included in many statistical software packages.

Apart from the Piechota et al. (1998) studies, almost all of the current methods used to generate categorical streamflow forecasts are somewhat indirect. The purpose of this study is two-fold. First, develop a simple and direct method to produce categorical streamflow forecasts at multiple locations. Second, compare the direct forecasting methods against indirect ensemble-based methods. The main intention is that new method to be complementary to the multimodel ensemble forecasting technique that is developed in Regonda et al. (2006) and, also an attractive alternative to the methods of Piechota et al. (1998).

The proposed framework and its application to the six key streamflow locations (Figure 2) in the GRB are described in the following sections. These locations are along the main reservoir system in the basin, and also points of release of water that satisfy various basin needs (e.g., agriculture, municipal, and transbasin diversions).

4.2. Methodology

The proposed integrated framework has the following three components: (i) Use Principal Component Analysis (PCA) to identify the leading modes of spatial variability in regional streamflow – these modes are also known as the leading principal components (PCs); (ii) Assess relationships between the leading streamflow PCs and global ocean and atmospheric variables to identify potential predictors; and (iii) Use logistic regression to issue categorical streamflow forecasts. Results from Regonda et al. (2006) are used for components (i) and (ii), while the logistic regression framework is developed in this study. Categorical forecasts are evaluated using the Brier skill score.

This method was applied to six streamflow locations in the GRB and, categorical spring streamflow forecasts were issued on the 1st of each month from December (i.e., 4 month lead-time) through April 1st in a cross-validated mode, in which all data from a given year is dropped from the forecasting framework while predicting in that year. The methodology along with the data and the application is described below.

4.2.1. Data

The daily discharges at the six streamflow locations for the period 1949-2004 were obtained from the U.S. Geological Survey (USGS) [<http://water.usgs.gov/>]. As expected, the streamflows exhibited a snow driven annual hydrograph (Figure 3), which has spring snow melt (April – July) resulting in the major contribution (greater than 70 percent) of annual flows. Hence, spring seasonal flows (averaged flow during April – July) are considered in this analysis, and developed spring streamflow time series for each of the six locations.

Snow Water Equivalent (SWE) data were obtained from Natural Resource Conservation Service (NRCS). The SWE measurements are taken around the beginning of each month, and records of February, March and April are considered, respectively, at 10, 14, and 14 locations in the basin.

Monthly global ocean and atmospheric variables such as Sea Surface Temperatures, Geopotential Height, Zonal Wind, and Meridional Wind, and Palmer Drought Severity Index (an index of soil moisture) were obtained from the Climate Diagnostic Center website (<http://www.cdc.noaa.gov>).

4.2.2. Forecast Method

4.2.2.1. Step 1: Principal Component Analysis (PCA)

PCA decomposes the space-time multivariate data set (time series of streamflows at six locations of the GRB) into orthogonal space (eigen vectors) and time (principal components) patterns using eigen-decomposition (see e.g., Von Storch and Zwiers, 1999). The space-time patterns are ordered according to the percentage of data variance explained (i.e., the first space-time pattern explains most of the data variance), and the leading PCs, corresponding to the space-time patterns that explain most of the data variance, are selected.

PCA on the spring streamflows at the six locations of the GRB resulted in the first PC explaining 87 percent of the variance, and the remaining five explained 13 percent of the variance. Clearly, the first PC is the leading mode and furthermore, it had uniform Eigen loadings (not shown) and high correlation (≥ 0.8) with all the six streamflows. This indicates that the leading PC is a robust indicator of basin-wide streamflow variability.

4.2.2.2. Step 2: Predictor Selection

Since the leading PC captures most of the data variance of the spring streamflows, predictors are searched by finding the correlation of the leading PC with large-scale ocean and atmospheric variables across several regions of the world, from preceding seasons. The regions with strong correlations are identified, and predictors are created by averaging the value of the variables from these regions. This is done for each lead time. For example, January 1st forecast considers the large scale ocean-atmospheric variables of November-December season, and similarly April 1st forecast considers the November-March season, etc. In addition, the first PC of the monthly SWE and the average Palmer Drought Index (PDSI) from the GRB region of the antecedent fall were also added to the suite of predictors. The variability of SWE in the basin is quite homogeneous, as can be seen by the fact that the first PC of SWE captures over 70% of the variance in all the months (i.e., 73%, 70%, and 70% variances are explained by February 1st, March 1st, and April 1st SWEs, respectively) furthermore, the first PC of SWE is highly correlated (correlation coefficient > 0.70) with the first PC of the spring streamflows (i.e., 0.72, 0.76, and 0.84 respectively for February 1st, March 1st, and April 1st SWEs) – hence, the first PC of SWE is a good predictor. The PDSI was included because drier conditions in the antecedent fall lead to an increased infiltration in the following spring when the snow starts to melt, and thus, reducing the spring streamflows. The details on the diagnostics and selection of the predictors are provided in the ‘GRB results’ section.

From the suite of predictors identified from the climate diagnostics, Regonda et al. (2006) developed several regression models for the first streamflow PC using a

nonparametric local polynomial framework, for each lead time. Each of the regression models consists of a different subset of predictors, and is used to issue ensemble forecasts of the first PC. Since many models have similar skill, it is difficult to identify a single ‘best’ model. Consequently, Regonda et al. (2006) combines predictions from multiple regression models to obtain multimodel ensemble forecast of the first streamflow PC, and subsequently back-transforms the multimodel ensemble forecast to all the six locations in the basin, simultaneously. Categorical forecasts are then issued from the multimodel ensemble forecast.

In this study the goal is to develop and demonstrate the utility of a logistic regression based framework for categorical forecasting. For simplicity at each lead time the ‘best’ predictor set identified by Regonda et al. (2006) (i.e., predictors of the model with the lowest error) is used to produce ensemble streamflow forecasts and the corresponding categorical probabilities. That is, the multimodel forecasts are not used. The same combination of predictors from the single best local polynomial model is then used as explanatory variables in the logistic regression model to estimate categorical forecast probabilities directly. These predictor sets are described in Table 13 for different lead times. A more formal approach would be to identify the ‘best’ subset of predictors using the logistic regression.

4.2.2.3. Step 3: Categorical Forecast Framework - Logistic Regression

As described earlier, the goal of this study is to develop a framework that issues categorical forecasts of streamflows. To this end, probabilities corresponding to events of different threshold values need to be estimated. This consists of the following steps:

- (i) A threshold value, say the 20th percentile, is chosen for the first PC.
- (ii) The first PC time series is reduced to a binary (1 if the PC value exceeds the threshold, 0 otherwise) series.
- (iii) Logistic regression is employed (Hosmer and Lemeshow, 1989) to obtain the threshold probabilities. This method was outlined in the Introduction but is repeated here for completeness:

$$P_{\text{logit}} = \Pr(Q_i | X_1, \dots, X_n) = \frac{1}{1 + \exp(\beta_0 + \beta_1 X_1 + \beta_2 X_2 + \dots + \beta_n X_n)} \quad \dots 4.4$$

where P_{logit} is the probability of the event of interest (e.g., PC value exceeding the 20th percentile) and $(\beta_1, \beta_2, \dots, \beta_n)$ are regression coefficients for each of the predictor variables (X_1, X_2, \dots, X_n) . Correspondingly, the probability of non-exceedance of the threshold value is $(1 - P_{\text{logit}})$. The regression coefficients are obtained via maximum likelihood estimation procedure (for details see, Hosmer and Lemeshow, 1989). The library ‘glm’ in the free software R (<http://www.r-project.org>) is used.

- (iv) Typically, PCA tends to change the distribution of the original variables to normal distribution. Thus, if the distribution of the original variables is non-normal then this transformation can lead to incorrect categorical probabilities. Kolmogorov-Smirnov (KS) test is performed on spring season streamflows at each location to test the normality of the distribution. In addition, the distributional difference between the first PC and each of the streamflows is also tested. All the spring flows, except Taylor River, were found to be normally distributed also, the distribution of all the seasonal streamflows were found to be as that of the first PC, at 95% confidence level. These tests

suggest that the PC analysis retained the distributional properties of the original data consequently, the rank probability as well. Furthermore, the first PC was found to be highly positively correlated with the streamflows in the basin and explains 87% of the variance. These diagnostics indicate that one can translate the probabilistic forecast of the PC directly to the streamflows at all the six locations. Thus, the P_{logit} value obtained from equation 4.4 (step iii, above) for a given threshold (say the 20th percentile of the PC value) is interpreted as the probabilistic forecast of same threshold (i.e., 20th percentile) exceedance of the streamflows.

- (v) Steps (i) through (iv) are repeated for several thresholds.

This framework is applied in a cross-validated mode to obtain the probabilistic streamflow forecasts for all the years at the six locations for different lead times.

An alternative approach would be to fit logistic regression models to each individual streamflow gage in the GRB. The PCA step in Regonda et al. (2006) has important advantages, as it preserves the spatial correlation structure over the basin when forecasts of the PC are disaggregated to individual stream gages. In the logistic regression model developed in this paper, the probability for the PC is distributed uniformly over the basin, hence the capabilities for spatial disaggregation in the original Regonda et al. (2006) method are lost. Nevertheless, use of the PC has other advantages, as it filters the data and reduces noise in the predictand variable. Moreover, use of the PC for logistic regression provides scope to compare the logistic regression approach with the original Regonda et al. (2006) method.

Table 13: Best predictor set for the Logistic Regression at different lead times.

Forecast Date	# of Predictors	Predictor 1	Predictor 2
December 1 st	1	SST ^{Dec1}	-NA-
January 1 st	2	ZW ^{Jan1}	PDSI
February 1 st	1	SWE ^{Feb1}	-NA-
March 1 st	2	SWE ^{Mar1}	SST ^{Mar1}
April 1 st	1	SWE ^{Apr1}	-NA-

SST^{Dec1} is the averaged Sea Surface Temperature anomalies difference between (14.3° N-41.0° N – 71.2° W-39.4° W) and (42.9° N-52.4° N – 176.2° E-150.0° W) for December 1st; between (21.9° N-42.9° N – 60.0° W-30.0° W) and (23.8° S-10.5° S – 110.6° W-78.8° W) is SST^{Mar1} for March 1st. ZW^{Jan1} is the averaged zonal wind difference between (50.0° N-60.0° N – 125.0° W-100.0° W) and (60.0° N-65.0° N – 155.0° W-142.5° W) for January 1st. PDSI is August -October Palmer Drought Severity Index of preceding year averaged over climate division 2 (which includes the GRB) of Colorado; SWE^{Feb1} corresponds to the first PC of snow water equivalent in the basin on February 1st – similarly, SWE^{Mar1} and SWE^{Apr1}.

4.2.3. Forecast Evaluation

The performance of the categorical probabilistic forecasts issued from the logistic regression framework is evaluated using the Brier Skill Score (BSS). This is a widely used measure to verify categorical probabilistic forecasts (Wilks, 1995). The BSS is computed for each threshold and is defined as (Wilks, 1995):

$$BSS = 1 - \frac{BS_{\text{forecast}}}{BS_{\text{clim}}} \quad \dots 4.5$$

where BS_{forecast} and BS_{clim} are the Brier Score (BS) corresponding to the logistic regression (or best model ensemble) forecast and climatology, respectively. The BS is the mean squared difference of forecasted probabilities and observations (equation 4.6) and is defined as

$$BS = \frac{\sum_{i=1}^N (p_i - o_i)^2}{N} \quad \dots 4.6$$

where p_i refers to the forecast probabilities for a given threshold value (i.e., either estimated from equation 4.4 or from the ‘best model’ ensemble); o_i refers to the outcomes; o_i is one if the observed flow exceeds the threshold volumes, and zero otherwise; N is number of forecasts, in this case the number of years. Replacing p_i with climatological probability in equation 4.6 results in the BS_{clim} – for example, the climatological probability of 20th percentile exceedance will be 0.8. The BSS values range from negative infinity to 1; negative values of BSS indicate forecast performance worse than climatology, and positive values indicate forecast performance better than climatology. A BSS of “0” implies that the forecast accuracy is the same as that for climatological forecasts. In contrast, a BSS of 1 can only occur for perfect forecasts.

4.3. Results

Skill score, i.e., the cross-validated BSS are estimated for the categorical streamflow forecasts issued from the logistic regression framework developed in this paper and also from the ‘best model’ ensemble of Regonda et al. (2006), at all the six locations and at different lead times. Figure 28 displays the BSS values for the forecasts issued on January 1st and April 1st. It can be seen that the BSS values from both the approaches are greater than climatology – suggesting skillful long-lead forecasts. Forecasts issued on April 1st show better performance relative to those issued on January 1st. This increase in performance with a decrease in lead time is to be expected; on April 1st almost all of the seasonal snow is present on the ground in the basin thus, providing accurate information of the resulting streamflow from the melt. Lower forecast performance is observed at higher threshold values at both lead

times. This is because of fewer (rare) events, which results in fewer data points making the logistic regression unstable (Bradley et al, 2003; Clark and Slater, 2006). The skill from both methods is comparable. However, the logistic regression framework can directly provide the categorical forecast at less computation cost which makes it quite attractive.

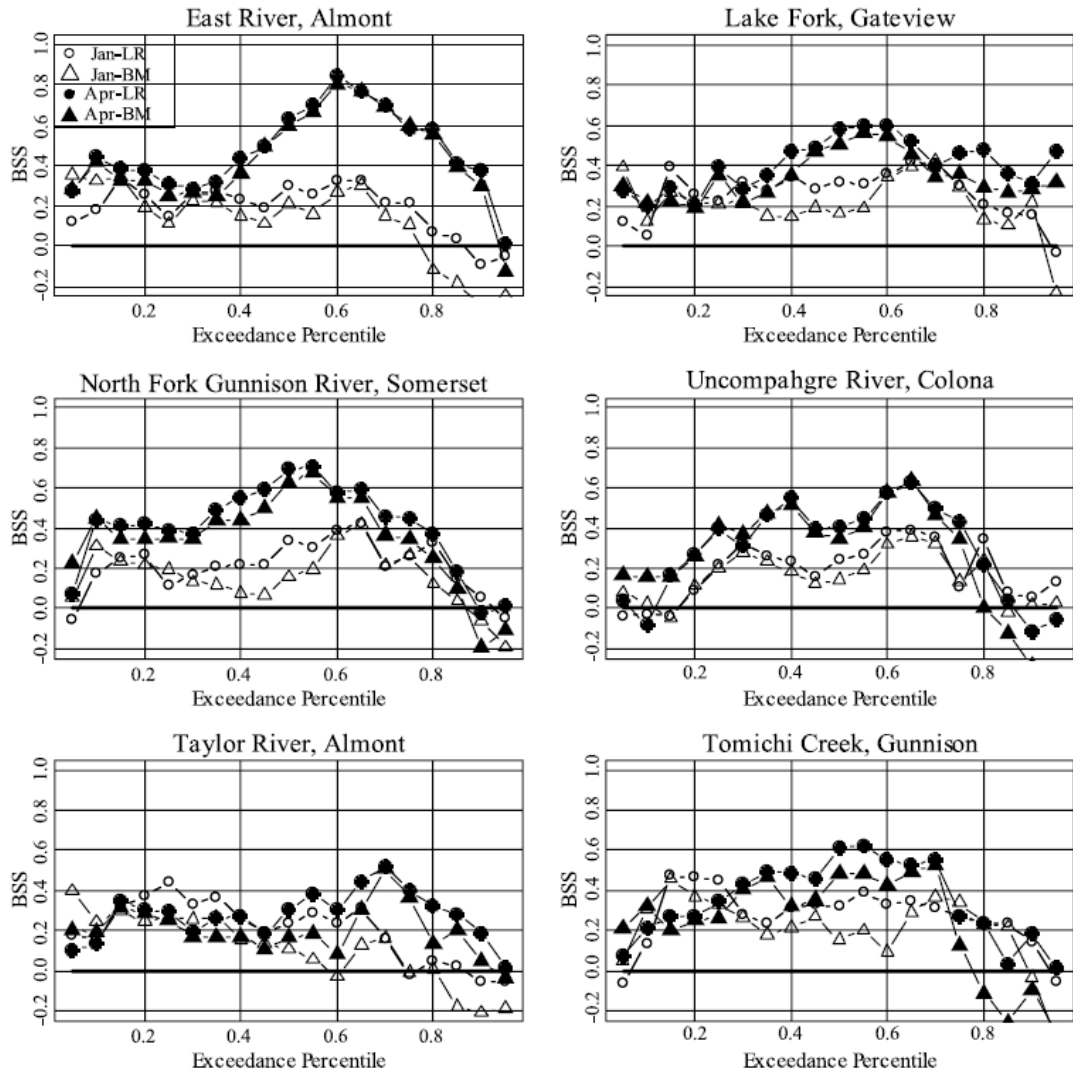


Figure 28: BSS of forecasts from the logistic regression (LR) framework (circles) and the “best model” (BM) ensemble of Regonda et al. [2006] (triangles), issued on 1 January (open circles and open triangles) and 1 April (solid circles and solid triangles) at the six locations in the GRB. Exceedance percentiles and BSS are plotted on x and y axes, respectively.

4.4. Summary

The developed framework is a simple and direct method to produce probabilistic categorical streamflow forecasts. In this, the categorical forecasts of the leading mode (or principal component) of the spatial streamflow at different thresholds is estimated via logistic regression. Large-scale climate features are used to obtain the predictors, and used in the logistic regression. These categorical forecasts are then uniformly transferred to the corresponding categorical forecast of streamflows at all the locations. The framework was applied to categorical forecasts of the April-June (spring) streamflows in the GRB at several month lead times starting from December 1st. The forecasts exhibited significant skill even at long lead times. Furthermore, the skills were comparable or better in some cases to those obtained from a ‘best model’ nonparametric regression based forecasts of Regonda et al. (2006). Also skill scores from the multimodel ensemble forecasts of Regonda et al. (2006) are estimated and comparable results were observed. Both these approaches are complimentary and serve different purposes – the logistic regression method will be useful if a quick categorical forecast is required, while the ensemble approach can provide the entire probability density function of the streamflows that can be used to drive decision support models.

The framework developed in this research is flexible and simple to implement. It works very well if the leading mode captures most of the data variance, and has uniform Eigen loadings and high correlations with all the basin streamflows – such as the case in the application to the GRB is demonstrated. If there are more than one leading PC that capture a significant part of the spatial variance, then this framework

can be applied to all the significant leading PCs and the estimated categorical forecasts from each of the PCs optimally combined following Rajagopalan et al. (2002). Other potential improvements could include optimally combining categorical forecasts from multimodels and also using the nonparametric logistic regression (Loader, 1999) method.

CHAPTER 5

DECISION SUPPORT SYSTEM FOR GUNNISON RIVER BASIN

FORECASTS

This chapter develops an experimental decision support system (DSS) for the water resources management of the Gunnison River Basin (GRB). The DSS consists of a RiverWare model of the GRB along with multimodel ensemble forecast framework. The streamflow forecast framework, described in Chapter 3 generates an ensemble of streamflows which drive the solution of the model. The result is an ensemble of outputs that can be represented as a probability distribution function conditioned on the forecast for modeled various decision variables.

5.1. Introduction

In Chapters 3 and 4, I have accomplished improved forecasts of spring runoff volume starting from early winter, in the absence of snow information, especially the January 1st forecast which gives a four month lead time. Similar good skills in forecasted decision variables at the four month lead time would provide significant information to water managers and assist in their planning operations. To evaluate this kind of benefits in conjunction with streamflow forecasts, the DSS model is run with January 1st and April 1st streamflow forecasts, and the skills of forecasted decision variables are evaluated. Compared to April 1st forecasts, streamflows of January 1st forecasts have less skill, but use only climate information and forecast at longer lead time (i.e., four months). Although the DSS model with April 1st forecasts is expected to perform better than January 1st forecasts, improvements in the

forecasted decision variables due to climate information will have its own significant implications from water management perspective. The key aim of this study is to investigate the transferability of the skills in the streamflow forecasts to the water resources decision variables. A background on the water issues and management policies are first presented to provide good understanding of basin features and operational policies that are incorporated into the DSS model. Then, the DSS and its development are described, followed by the evaluation method and the results.

5.2. Water Issues and Management Policies

Water issues in the GRB are a microcosm of those in the state of Colorado and the entire Colorado River Basin. Water managers and policy makers of the region pay much attention to the following issues: trans-basin diversions; interstate obligations, including the Colorado Compact and the potential for the upper basin states to fully develop their compact allotments; changes in water allocation and uses; salinity control and other water quality problems; and ecosystem sustainability efforts, including releases for the endangered fish recovery programs, stream and lake protection, and the Black Canyon National Park (BCNP) preservation (Ray, 2004). In addition to the above issues, water in the GRB is mainly utilized for irrigation, municipal and industrial demands, hydropower generation, and in preservation of endangered fish habitat.

To meet the different and often conflicting water demands efficiently under varying hydrologic conditions (described in the Chapter 1), water development projects have been constructed and management policies have been formulated. Among them, reservoir management plays a key role in dampening the effects of

year-to-year variability of stream inflows and providing reliable water supplies for various purposes in accordance with policies.

The U.S Bureau of Reclamation (BOR) operates the reservoirs according to a set of rules that are developed to meet the basin objectives. They forecast operations using a 24-month projection that is updated frequently by incorporating the available inflow forecasts along with basin water users' interests. In this basin, agriculture is the primary consumer of water; it uses most of the spring runoff as summer releases. However, another major concern of the water managers is to find the releases of spring and summer flows from the reservoirs that can also satisfy the needs of ecosystem sustainability efforts and maximize the hydropower generation.

In this study, I develop a DSS of the GRB in which physical and structural basin features are integrated with operational policies, and then use this DSS to analyze the efficacy of the operations with the benefits of improved streamflow forecasts.

5.3. The RiverWare Model

In the GRB, operational planning of water resources is carried out with RiverWare, a generalized river basin modeling tool (Zagona et al., 2001) that is widely used in the river basins of the western US, owing to its versatility and ability to interface with other models. Its' applications – long-term planning to short-term operations on the Colorado River, daily operations at Hoover Dam, forecasting and water supply assessment on Yakima River, water accounting in the Truckee River basin, optimized daily scheduling operations of reservoirs at TVA – suggest RiverWare flexibility with variety of application in diverse set of hydrologic basins (e.g., Zagona et al., 2001; Magee and Goranflo, 2002; Wheeler, et al., 2002). In

addition, RiverWare has the ability to model reservoir operations in an optimal manner on different time scales (e.g., 1 hour, 1 day, 1 month) (e.g., Eschenbach et al., 2001; Emmert, 2005; Zagona et al., 2006).

RiverWare provides a construction kit in which the physical water system and structural components (i.e., rivers, reservoirs, diversion canals, water consumers, power generators, etc.) of the basin are represented by objects. The objects contain the data and the physical process algorithms for the components. The basin operational policies are embodied into rules written in the RiverWare policy language. The rules, collectively known as a rule set, approximate the real-time decisions made by water managers. Streamflows, along with the operational criteria, drive this model; results are values of the decision variables (e.g., storage levels and releases for fish, hydropower generation, recreation, reserved water rights, etc.). RiverWare has a “point and click” user interface and includes various visualization features. It has three different solution approaches: (i) pure simulation, in which user supplies inputs such as reservoir storage, pool elevation, and releases, and the simulation solves for the unknowns (solves an exactly specified problem); (ii) rulebased simulation, in which logical operational rules drive the simulation; and (iii) optimization, in which the system is globally optimized according to operational constraints and objectives provided by the user.

For operational forecasting, the BOR uses a combination of rulebased simulation and pure simulation, doing if-then scenarios to meet the operational policy requirements. In this work, I use rulebased simulation, implementing the operational policies into logic that can be applied consistently in the numerous model runs.

This work uses a RiverWare model of the GRB (Figure 29) developed by the BOR for the 24-Month Study. I developed a rule set that describes the operating policies as specified by the BOR (P. Davidson, personal communication, 2005). Whereas the 24-Month Study model is a monthly model that forecasts operations for two years, this study uses a model that forecasts for only one year. Details about the model follow.

The model includes the three reservoirs (Blue Mesa, Morrow Point, and Crystal) of the Aspinall Unit, and Taylor Park reservoir. Of these, Taylor Park is a storage reservoir and the other three are power reservoirs – capable of generating hydropower. Reservoir objects are represented as triangle-shaped icons, and are capable of modeling the physical processes of the reservoir, (e.g., mass balance, evaporation, hydropower). Data pertaining to operational policies (e.g., fish releases, guide curves, demand schedules) reside on ‘data objects’, symbolized as rectangular-shaped icons. Reach objects perform the river reach simulation including routing water from one reservoir to another, accounting for local inflows, diversions, and return flows. The Water User object (represented by an icon with a tap symbol) models water demands and consumptive use, as well as the generation of return flows. Here I provide only a limited description of the RiverWare objects; the RiverWare manual (<http://cadswes.colorado.edu>) gives detailed information on the functioning of these objects.

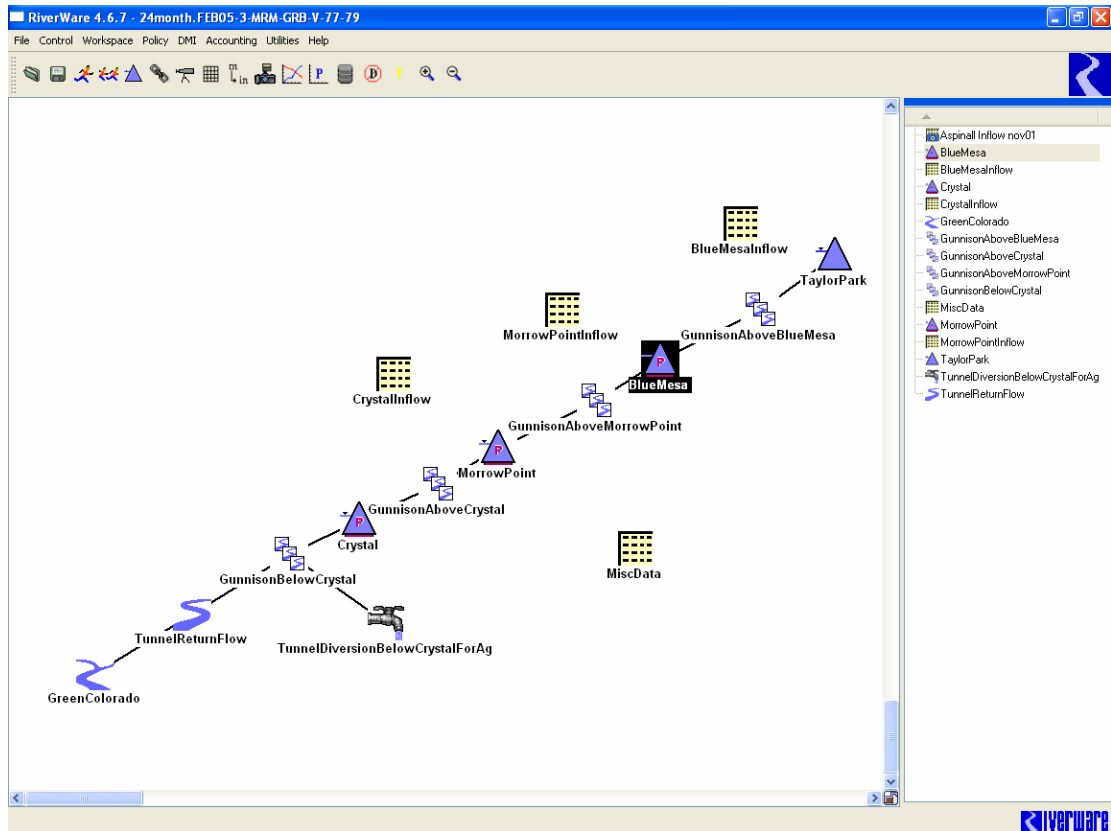


Figure 29: RiverWare workspace showing 24-month study model of the Gunnison River Basin.

The operational policies are expressed in logical rules, that have an *if-then* logical structure. The *if* part of the logic examines the values of variables such as inflows, storages, demands, and current date; the *then* clause sets values of decision variables in the model according to the state of the system. The prioritized rules form a rule set.

The main goals of the rule set (or policies) in the GRB model are to provide sufficient water for irrigation demands, fish releases, hydropower and, importantly, to avoid spilling. Water releases to meet downstream demands and fish releases are implemented at the downstream end of the Aspinall unit, i.e., as releases from Crystal reservoir. However, firm and non-firm hydropower is generated by all three of the reservoirs' power plants and spill must be avoided on all of them. In rules, March

through September is considered the irrigation season, whereas October through February of the following year is treated as winter season. Part of the irrigation season, April through July, is known as the filling period, during which time reservoir releases are managed to allow the reservoirs to fill by the end of July.

5.3.1. Taylor Park Reservoir Operations

Taylor Park is mainly a storage reservoir and does not generate hydropower. The reservoir's inflows/outflows are small in magnitude compared to Blue Mesa's inflows/outflows. The releases are made in compliance with the following rules. (1) At any time, reservoir elevation is neither allowed to go below its suggested lower elevation (9270 feet) nor allowed to exceed its' maximum elevation (9328 feet). (2) Reservoir releases meet downstream demands in accordance with the season. (3) In April, i.e., during the filling period, the elevations are not allowed to exceed 9305 feet in order to protect fish.

5.3.2. Blue Mesa Reservoir Operations

Blue Mesa Reservoir with its large storage capacity plays a key role in many operations of the *Aspinall Unit*. Although Blue Mesa is the upstream reservoir, its operating criteria address the flow requirements downstream of Crystal because Morrow Point and Crystal are not large enough to have significant operating flexibility. Thus, its releases are controlled mainly to meet downstream fish flows all year and irrigation releases in summer. Since hydropower is also a primary objective of the *Aspinall Unit*, Blue Mesa's releases are intended to maximize hydropower generation and avoid spilling both at Blue Mesa itself and at the two downstream

reservoirs. “No spill” is one of the chief goals of the water management, meaning putting the release through turbines instead of the spillway, so as not to lose the opportunity to generate hydropower, thus improving the effective use of water.

To meet these requirements, the following rules are developed. (1) The minimum releases during the irrigation season are the summation of diversion requirements at the Gunnison tunnel and 300 cfs required for fish downstream of the tunnel diversion. (2) Maximum releases are to generate more hydropower and are constrained to avoid non-utilization of water (i.e., spilling or controlled bypassing of water) at any of the reservoirs of the Aspinall Unit. (3) The storage target from April through the end of July (known as the filling period) is to fill the reservoir to 7516.4 feet (3 feet below spillway). (4) From mid-October through mid-November, the reservoir releases are reduced to minimize down stream river flows for spawning of fish. (5) Throughout the winter, reservoir releases, hence downstream river levels should remain relatively constant in order to protect the fish eggs. If a change is warranted then it is to be as consistent as possible; for instance, if an increase in streamflows is needed, it should be such that the increased flows persist during the winter months through the spring runoff months. Decreases should be later in summer going into fall and winter. (6) The water elevation should not exceed 7490 feet by the end of December – this eliminates icing problems and protects fish eggs from dying. (7) At any time, water levels in the reservoir should not drop below the active capacity. (8) In meeting the above requirements, the releases are estimated accounting for intervening flows at Morrow Point and Crystal reservoirs.

5.3.3. Morrow Point Reservoir and Crystal Reservoir Operations

Although both reservoirs are power generation reservoirs, they have small storage capacities. Unlike Blue Mesa which has large storage and power generation capacity, these reservoirs have a single main purpose of generating maximum hydropower. In this regard, the following rules are developed. (1) At all times of year, to the extent possible, reservoir elevations are maintained at the maximum elevation in order to maintain head for hydropower generation. (2) Spills are avoided, but since there is not much storage flexibility, this is accomplished by modifying releases from upstream reservoirs.

The above rule set with its sequence of execution is presented in Figure 30. The methodology for driving the model with streamflow forecasts and the results are presented in the following sections.

5.4. Methodology

5.4.1. Multimodel Ensemble Forecast Framework

In the DSS, the GRB model is run in *rulebased simulation* mode, driven by an ensemble of streamflow scenarios from the multimodel ensemble forecast framework. The results of the model runs (one run for each forecast trace) are an ensemble of values of various decision variables.

The multimodel ensemble forecast method described in the Chapter 3 issues spring snowmelt runoff volume forecasts at various lead times. However, the DSS model requires monthly streamflows as it operates on a monthly time scale. Hence,

Taylor Park Reservoir

1. Solve Taylor Park releases for all months meeting following rules.
2. At any time, reservoir elevation is neither allowed to go below its suggested lower elevation (9270 feet) nor is allowed to exceed its' maximum elevation (9328 feet).
3. In April, i.e., during filling period, water elevations are not allowed to go beyond 9305 feet in order to protect fish.

Blue Mesa Reservoir

4. Estimate demands, i.e., tunnel diversion releases + fish releases – intervening flows at MP and CR.
5. During irrigation season (March – September), reservoir releases are made such that (a) mainly it allows reservoir filling during filling period, i.e., fills reservoir by end of July; and (b) downstream demands are satisfied, and more hydropower is generated, avoiding spilling at the same time.
6. For winter season (October – February), compute demands and available water for each month of winter starting from current month to end of winter, and then estimate reservoir outflows so as to (a) maintain minimum fish releases during October and November, (b) bring BM elevation down to 7490 feet or lower by end of December; and (c) maintain consistency in river levels throughout rest of the winter.

Morrow Point Reservoir

7. Estimate releases as per rule curve, which maintains reservoir at its maximum elevation.
8. If reservoir spills, then modify Blue Mesa Reservoir releases, which is the only controllable source of reservoir inflows.

Crystal Reservoir

9. Similar to Morrow Point Reservoir, reservoir outflows are calculated as per rule curve to maintaining reservoir at its full capacity.
10. In case of spilling, reservoir releases from both Blue Mesa and Morrow Point are modified to avoid/reduce spill.

Additionally, at any time, reservoir releases at all the above locations are within the threshold of designed values such as minimum and maximum releases and maintaining elevation greater than inactive capacity.

Figure 30: Rules for operations of the reservoirs in the Gunnison River Basin.

the forecasted spring streamflows volumes have to be disaggregated into monthly flows. A simple disaggregation algorithm is proposed as follows.

1. For a given seasonal streamflow forecast, identify K historical years that have seasonal streamflow volumes similar to this forecast flow (i.e., K nearest

neighbors). K is chosen by the heuristic approach, i.e., square root of observations (Lall and Sharma, 1996) and has been found to work quite well.

2. The K-nearest neighbors are weighted with highest weight assigned to the nearest neighbor (volume that matches most closely) and least to the farthest.
3. Based on these weights one of the years is selected (Lall and Sharma, 1996).
4. The monthly distribution of the volume in this selected year is applied to the forecast flow, thus obtaining disaggregated monthly flows corresponding to the seasonal volume forecast.

The decision model forecasts operations for an entire year, so inflows for the remaining months of the year must be forecast as well. After the monthly disaggregation described above, the flow forecast framework adds the non-spring monthly flows of the resampled year to the forecast, thus forming a streamflow scenario for the entire year. For the April 1st forecast, the DSS runs from April through March of the following year. In this case, the non-spring monthly flows of the resampled year and the flows of January through March of the following year is selected, in conjunction with the disaggregated monthly flows.

5.4.2. Test Case

The DSS model requires as inputs the accumulated intervening monthly streamflows at each of the four reservoirs and the monthly demands, for twelve months. Also, the model needs initial conditions, i.e., storage at the initial time of the run at each of the reservoirs. These inputs, along with the rule set, drive the DSS model simulation for the subsequent 12 months, solving for all decision variables to meet the objectives (e.g., irrigation demands, fish flows, recreational releases,

reservoir outflows, storage levels, hydropower, etc.). Each model run uses a 12-month streamflow trace as input and results in a 12-month trace of each of the decision variables.

The DSS ensemble streamflow forecast framework generates an ensemble of forecasts for each year of the (1978-2004) period – separately for the January 1st and April 1st forecasts. When run through the model, this results in an ensemble of forecasted decision variables. The model is then run with the observed streamflows to obtain ‘simulated observed’ values of the decision variables. The forecast skills are computed against these ‘simulated observed’ values. The skill scores, RPSS (defined and described in the Chapter 3), are computed for the six key decision variables (i.e., inflows, outflows, storage, power, spill, demands). Unlike two downstream reservoirs, i.e., Morrow Point and Crystal, inflows at first two upstream reservoirs (i.e., Taylor Park and Blue Mesa) are not treated as decision variables; because inflows at first two upstream reservoirs are direct streamflows into reservoir, whereas inflows at two downstream reservoirs are sum of direct streamflows into that reservoir and outflows from the upstream reservoirs, which is a decision variable. In Blue Mesa reservoir inflows, contribution of Taylor Park outflows is small compared to direct streamflows into Blue Mesa reservoir. Three equal categories are used for the RPSS computation. The skills are computed for the spring (April-July) and winter (September-December) seasons. For example, spring season storage skill provides information about reliability/risk in maintaining the required storage at the end of spring season which has important implications to water releases of the following seasons.

The RPSS estimation of the decision variables differs from the method that described in Chapter 3, especially in climatological probabilities of the decision variables. The method is as follows. (1) The DSS is first run with the historical flows obtaining the values of the decision variables for each month and consequently, season. From this, the threshold boundaries i.e., the 33rd and 66th percentiles, of the decision variables are obtained. (2) For each year, the DSS is run with climatological streamflows – all the historical streamflows excluding the flow in the year under consideration, i.e., cross-validated model. This results in “climatological” ensembles of decision variables for each year and proportion of ensembles in each category was estimated – obtaining the climatological probabilities for each year. (3) Lastly, the DSS is driven with the streamflow forecast ensembles to obtain the forecast categorical probabilities for each year. These probability estimates are used in the RPSS computation. For each decision variable, the RPSS is calculated for each year and the median value is reported. In order to evaluate the forecast performance for extreme hydrologic conditions, decision variables are sorted into two categories – wet years (flow values greater than 75th percentile) and dry years (flow values less than 25th percentile) – and the median value of RPSS of corresponding years is reported.

To investigate the benefit of streamflow forecasts that were made with and without snow information, the DSS model is run separately for the January 1st and April 1st streamflow forecasts. The ‘simulated observed’ decision variables vary between these two runs because reservoir initial conditions differ, i.e., reservoir conditions in December of the previous year act as initial conditions for January 1st DSS run, whereas conditions in March are for April 1st DSS run. The skills in the

decision variables are calculated for two different DSS runs, at four reservoirs, and are described below.

5.5. Results

The twelve monthly streamflows forming a flow scenario are used to drive a model simulation, resulting in values for the various decision variables obtained for each year at two lead times (January 1st and April 1st).

5.5.1. Data

In this study, accumulated intervening streamflows and storage at four reservoirs, and demands are used. The data was obtained from the BOR for the period 1979-2004 (P. Davidson, personal communication, 2005).

5.5.2. Streamflow Characteristics

Intervening streamflows at the four reservoir locations are the inflow points of the model. Annual hydrographs of these locations suggest spring snow melt flows (Figure 31). Ensemble forecast of spring runoff volume at the four locations are generated using the multimodel ensemble approach described in Chapter 3. The first (leading) principal component (PC) explains almost all of the data variance (93%) and its Eigen loadings are of the same sign and magnitude (Figure 32). The first PC was found to be highly correlated (0.99) with the first PC of the six streamflow locations of the GRB used in Chapter 3. As a result, the predictors identified in Chapter 3 (Table 4) can be used for the four streamflow locations here. As expected, the ensemble of spring flow forecasts exhibit good skills at April 1st and January 1st forecast lead times – which can be seen in the Ranked Probability Skill Scores (RPSS) (Figure 33,

Table 14). The RPSS scores are based on a three equi-probability flow categories defined at the tercile boundaries. The climatological probability of each category is 1/3. The description of this skill score and the equations for computation are detailed in Chapter 3 (equations 3.5 and 3.6).

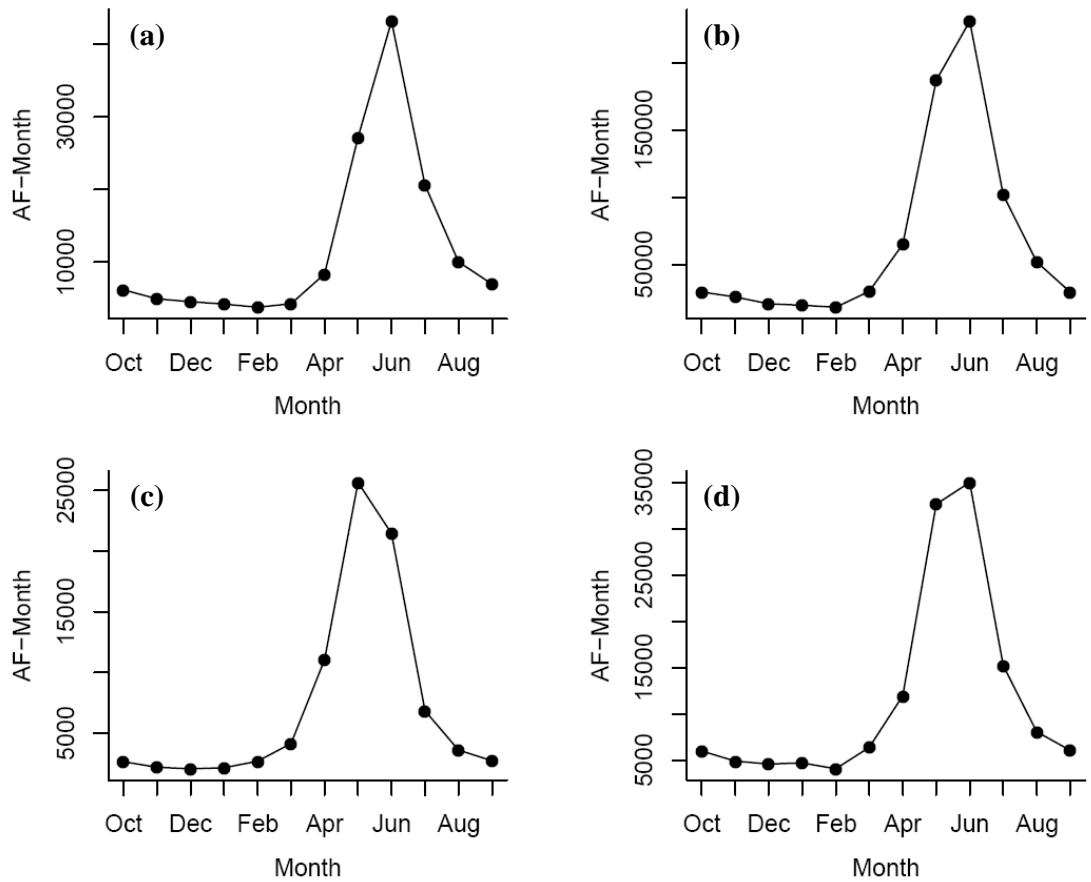


Figure 31: Annual average hydrograph of four reservoir locations of the Gunnison Decision Support System (a) Taylor Park Reservoir, (b) Blue Mesa Reservoir, (c) Morrow Point Reservoir, and (d) Crystal Reservoir.

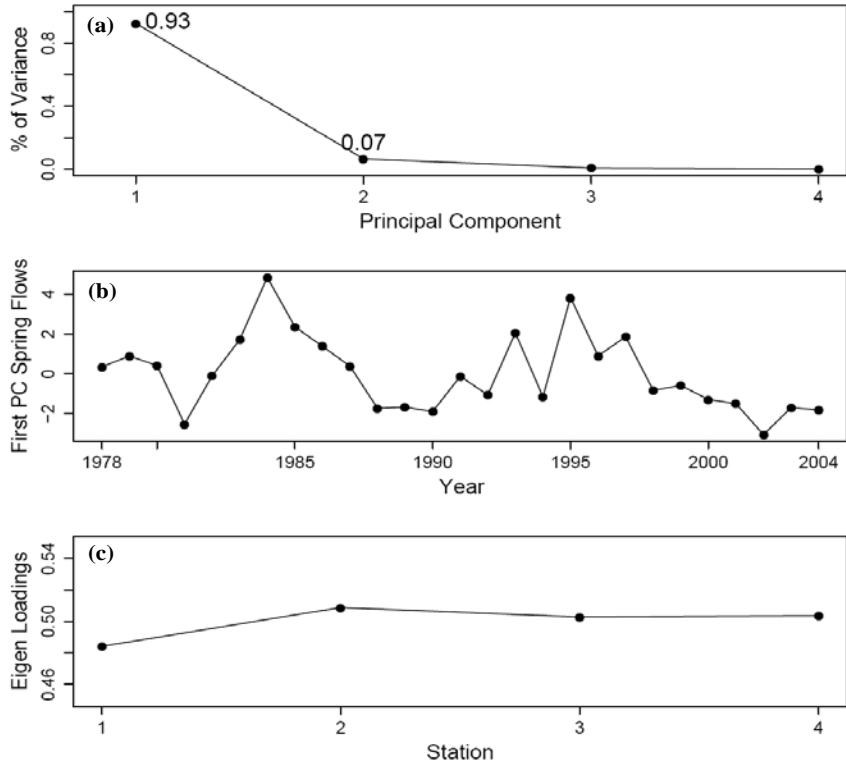


Figure 32: (a) Percentage variance explained by the four principal components (PCs), (b) time series of the first PC, and (c) eigen loadings of the first PC at the four reservoir locations.

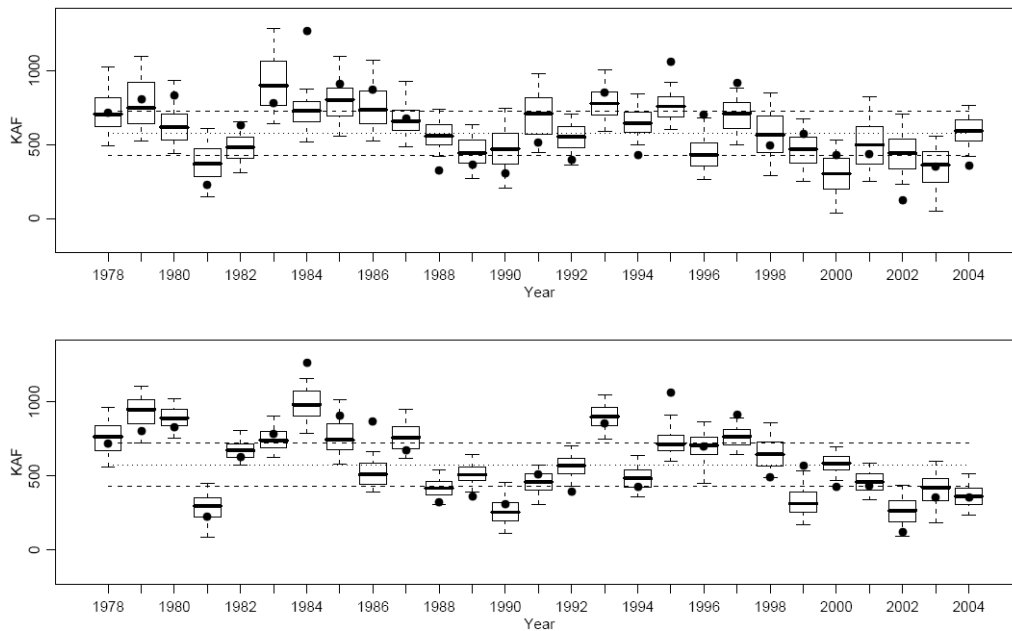


Figure 33: Box plots of spring streamflow (KAF) at Blue Mesa Reservoir issued on (a) January 1st and (b) April 1st. The dashed horizontal lines represent the 33rd, 50th, and 66th percentiles of the historical flow data, which are shown as solid circles.

Table 14: Ranked Probability Skill Scores of Spring Streamflows Forecasts at Different Lead Times Using Climate and PDSI Predictors and Using Climate, PDSI, and SWE information.

Reservoir	Climate + PDSI (January 1 st)	Climate + PDSI + SWE (April 1 st)
Taylor Park		
All Years	0.44	0.62
Wet Years	0.74	0.87
Dry Years	-0.18	0.55
Blue Mesa		
All Years	0.53	0.71
Wet Years	0.65	0.86
Dry Years	0.44	0.91
Morrow Point		
All Years	0.47	0.80
Wet Years	0.95	0.96
Dry Years	0.47	0.89
Crystal		
All Years	0.49	0.83
Wet Years	0.94	0.97
Dry Years	0.44	0.91

The disaggregation method described in the previous section was applied to obtain the ensembles of forecasted spring monthly flows and also the non-spring monthly flows. Boxplots of basic distributional statistics (mean, standard deviation, skew, minimum and maximum flow, and lag-1 monthly correlation) of the forecasts for each month are generated and then compared with the historical values. These are shown in Figure 34 for the Blue Mesa reservoir inflows for the January 1st (left column) and April 1st forecasts (right column). It is seen that the statistics are generally well captured (i.e., historical value is within the box) but more so for the high flow spring season. The standard deviation is slightly under-simulated by the disaggregation method. This is expected, as the disaggregation approach is too simple and does not explicitly model these statistics. Nonparametric methods such as those

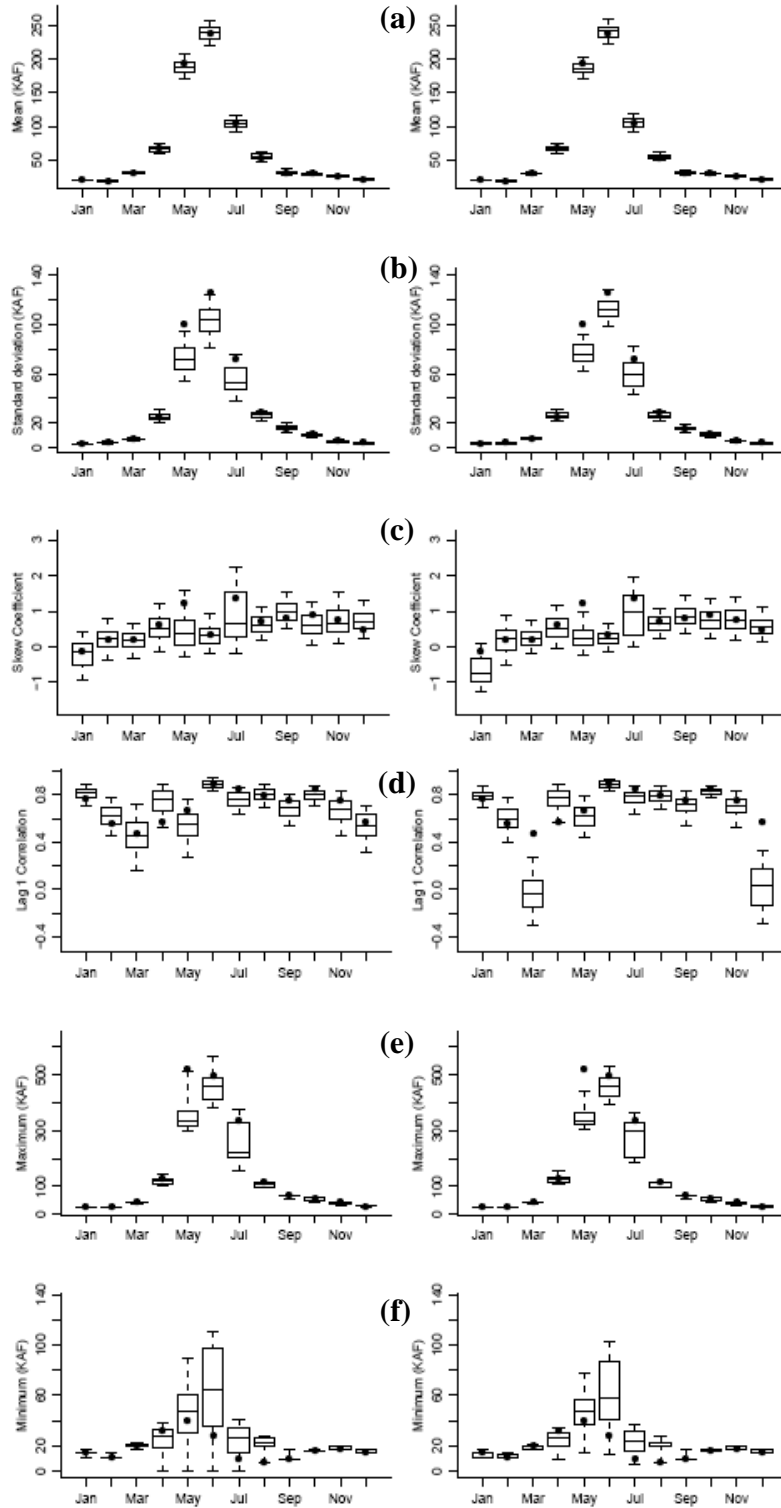


Figure 34: Boxplot of statistics for Blue Mesa Reservoir (a) mean, (b) standard deviation, (c) skew coefficient, (d) lag-1 correlation coefficient, (e) maximum flow and, (f) minimum flow. Left and right columns correspond to January 1st and April 1st forecasts.

developed by Prairie et al. (2006b) would help address these. Qualitatively, similar results were obtained for other reservoirs inflows (figures are not shown).

Biases were estimated for the ensembles of disaggregated streamflows for all months of forecasts issued on January 1st and April 1st. These were within 5% of the observed median and not systematic. Also, reliability of disaggregated monthly flows was verified by performing Kolmogorov-Smirnov (KS) test. The estimated high p-values imply the reliability of ensembles of disaggregated flows derived from both January 1st and April 1st forecasts. These results indicate that the disaggregation methodology was performing reasonably well.

5.5.3. Decision Variables

5.5.3.1. Taylor Park Reservoir

The RPSS of the inflow, outflow and storage at this reservoir are shown in Figure 35. Recall that Taylor Park reservoir is primarily for storage – hence, only two decision variables. The reservoir rule set allows most of the inflows to go through as outflows if the reservoir elevation does not go below the specified value. Typically, reservoir inflows satisfy this elevation criterion at the first time step and subsequently, the inflows are released as outflows. Reservoir outflows are equal to inflows for both forecasted and climatological streamflows in almost all years. Therefore, both inflows and outflows exhibited approximately similar skill score in most of the months and in two seasons (Figure 35). Substantial skill scores are observed in all the variables for the spring season, more so for the April 1st forecasts – suggesting that the ensemble streamflow forecasts provide useful information for decision making. The skills in the following winter are lower as the flow ensembles

during this season are not based on large scale climate and are so far in the future that they are not skillful. In winter, typically streamflows are low in magnitude and maintain reservoir at lower elevations. Both forecasted and climatological streamflows are able to maintain the reservoir at a lower elevation during several months other than spring season. Therefore ‘undefined’ skill score values are observed for reservoir storage in non-spring months, e.g., winter storage skill (Figure 35b).

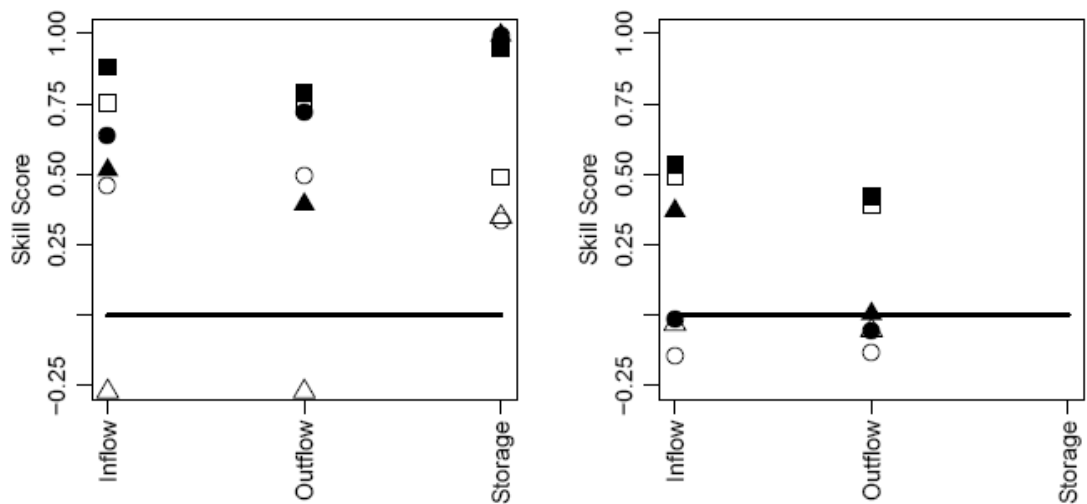


Figure 35: Ranked Probability Skill Scores of decision variables of Taylor Park correspond to (a) spring (April through July) season and (b) winter (September through December) season. Circles, rectangles, and triangles represent all years, wet years, and dry year.

5.5.3.2. Blue Mesa Reservoir

Skill scores of six decision variables for each month and for the two seasons (spring and winter) are computed (Figures 36 and 37). The following observations can be made from these figures: (1) positive skill scores are observed in all the decision variables, for most of the months and for both the seasons. Also, for few months other than spring season, negative skill scores are seen e.g., skill score of

storage and demands in few months of winter season; (2) Skills during the spring months are much higher than during other (e.g., Figures 37a and 37b); (3) in spring, skill scores of all decision variables are approximately equal to the skill of inflows whereas in winter, decision variables' skill is higher than skill of inflows (inflows into this reservoir is sum of forecasted intervening flows and the DSS derived Taylor Park outflows); (4) increased skills are observed for decision variables with April 1st streamflow forecasts compared to January 1st, more so during dry years. Overall, these observations highlight the utility of ensemble streamflow forecasts in providing skilful long lead forecasts of the decision variables, which can be of immense use in water resources management and planning decisions.

Skills in the hydropower generation (Figure 37), which has a nonlinear relation with release and water elevation, are also high. This is quite significant as hydropower generation is one of the main objectives of the GRB water resources system.

Typically, the reservoir spills during spring due to large quantity of inflows, while in all other months spill is zero. Both the January 1st and April 1st forecasts of the spring runoff approximate the actual streamflows magnitudes better than climatology and hence exhibit high skill scores. During other months neither forecasted nor climatological nor actual streamflows result in spills, so the skills are undefined [Figures 36 and 37b]. Similar observations are made from high storage skills during spring months, except in June, in which undefined skill scores are observed, because all streamflow scenarios were able to maintain the reservoir at its full capacity as per the rule set (Figure 36). (See rule 3 of Blue Mesa Reservoir.) Positive skill scores of

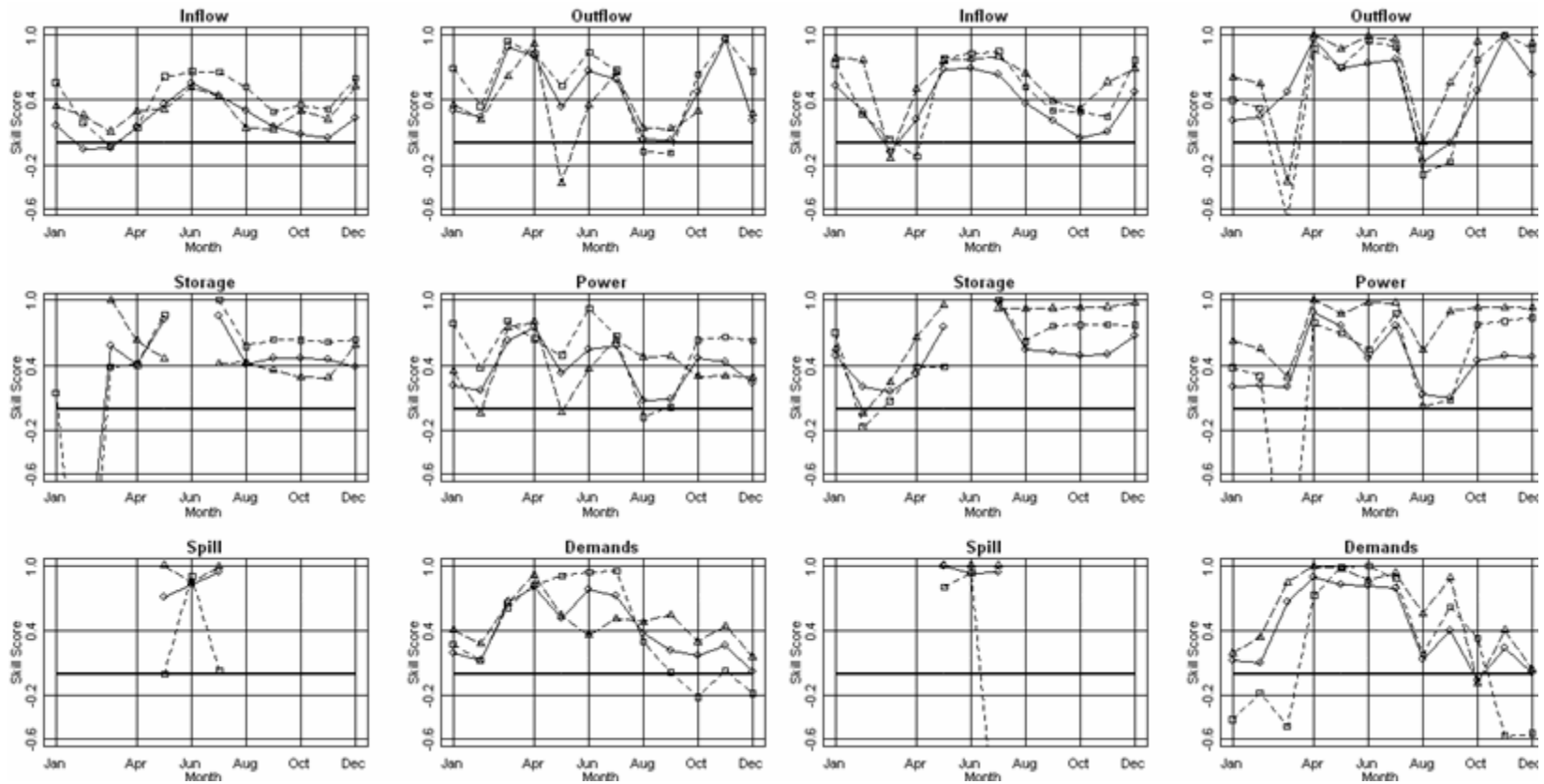


Figure 36: Ranked Probability Skill Scores of decision variables of Blue Mesa Reservoir for all months. First two left and last two right columns refer January 1st and April 1st issued forecasts respectively. Circles, rectangles, and triangles represent all years, wet years, and dry years respectively.

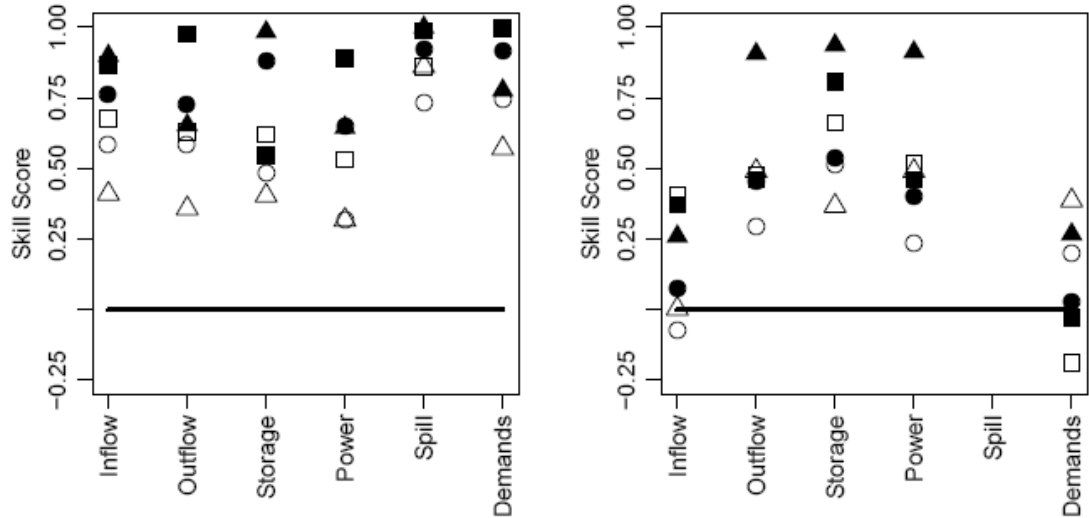


Figure 37: RPSS of decision variables of Blue Mesa Reservoir correspond to (a) spring (April through July) season and (b) winter (September through December) season. Circles, rectangles, and triangles represent all years, wet years, and dry year.

demand indicate the ability of forecasted streamflows to meet the ‘simulated observed’ demands as compared to the climatological streamflows.

To illustrate the performance of the forecasts in the extreme years, probability density functions (PDFs) of the ensembles of decision variables are shown for a representative dry year, 1981, and a wet year of 1985 (Figures 38 and 39). It can be seen that the PDF of the decision variables are shifted to the left of the climatological PDF in the dry year (Figure 38) and to the right in the wet year (Figure 39) – more so for the April 1st forecasts. Furthermore, the forecast PDF capture the ‘simulated observed’ values (shown as solid vertical lines) quite well. This has significant implications for water management. For example, if a lower storage is predicted well in advance, management strategies can be adopted to mitigate the impact of low streamflows ahead of time. Also, forecasts provide valuable information in making more revenue in terms of power generation; for the wet year 1985, January 1st forecasts suggested hydropower of 225 MW which approximates ‘simulated

observed' hydropower, i.e., 250 MW, whereas expected hydropower from climatological forecasts is, 162 MW, far below than 'simulated observed' (Figure 39).

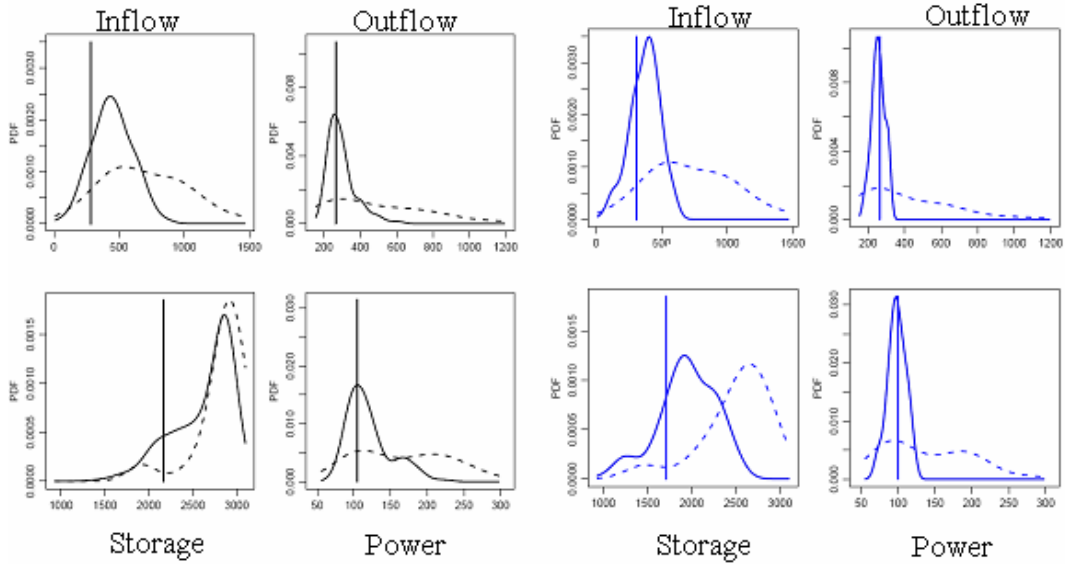


Figure 38: Probability Density Function (PDF) of decision variables of Blue Mesa Reservoir for year 1981 (dry year). Decision variables derived from forecasted and climatological streamflows are indicated with solid lines and dashed lines respectively. Solid vertical lines correspond to decision variables derived from actual streamflows. Black and blue lines correspond to the DSS that run on January 1st and April 1st respectively.

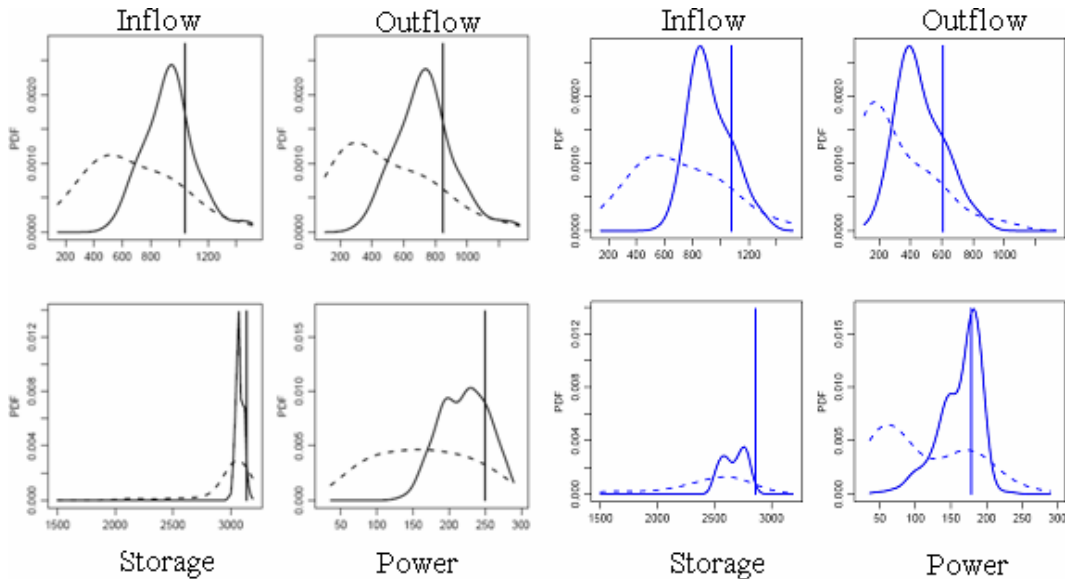


Figure 39: Same as Figure 38, but for year 1985 (wet year).

Similar significant skills and observations were made for Morrow Point reservoir (Figure 40) and Crystal reservoirs (Figure 41).

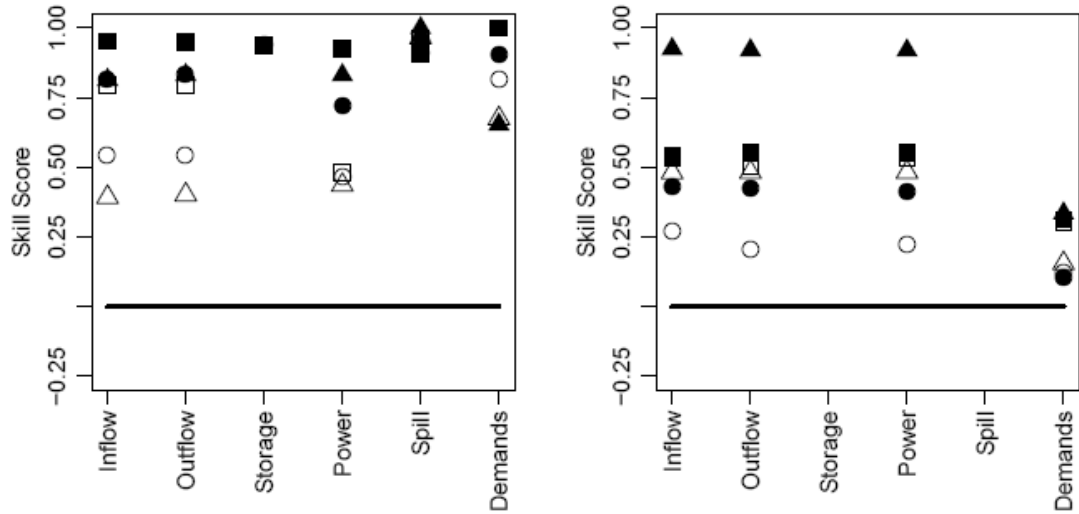


Figure 40: RPSS of decision variables of Morrow Point Reservoir correspond to (a) spring (April through July) season and (b) winter (September through December) season. Circles, rectangles, and triangles represent all years, wet years, and dry year.

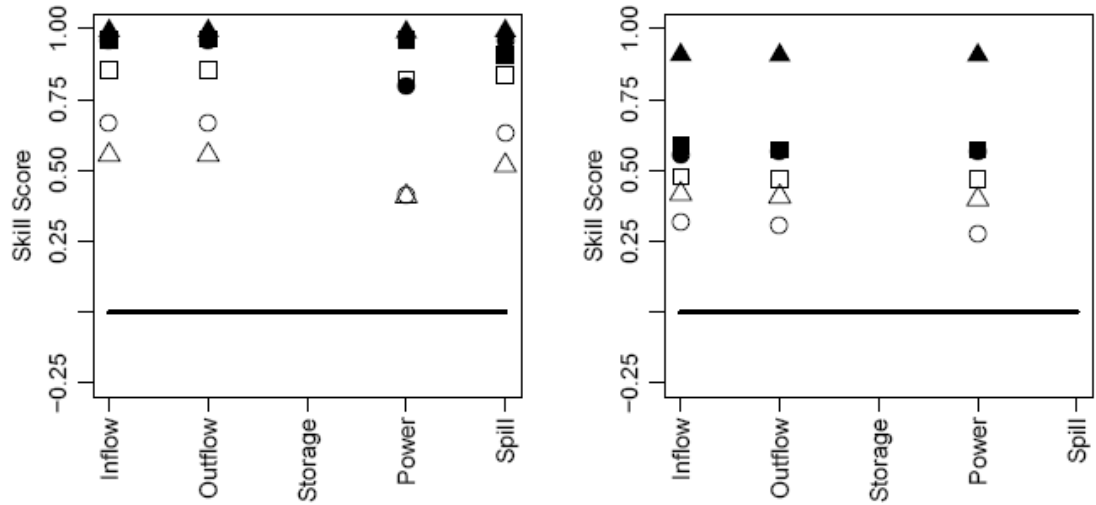


Figure 41: Same as Figure 40, but for Crystal Reservoir.

5.6. Summary and Discussion

In this chapter, the ensemble streamflow forecast method was integrated with the GRB model to form a DSS to generate ensembles of decision variables. The skills in the streamflow forecasts identified in the Chapter 3 seem to transfer quite well to the decision variables, as seen by their skilful forecasts.

Positive skill score of decision variables highlights the influence of forecasted streamflows compared to the climatological streamflows in driving the model. The better performance of decision variables especially with January 1st forecasts, which uses only climate information, provides four month lead time allowing water managers to modify/make better decisions in spring season. The lower performance of streamflow forecasts is not linearly transformed onto decision variables, i.e., in several months, a few decision variables derived from both January 1st and April 1st forecasts exhibited approximately similar performance (Figure 36). Also, the nonlinear transferability skill is observed between streamflow forecasts and decision variables, i.e., negative skill of streamflow forecasts resulted in positive skill of decision variables, and vice versa. However, there are few variables which are not influenced by skill in streamflows, for example, filling the Blue Mesa reservoir by July end, maintaining reservoir elevation at its maximum in Morrow Point and Crystal reservoirs. All three different streamflow scenarios (i.e., actual, forecasted, climatological) met the above criteria resulting the same value of decision variable, and consequently undefined skill scores. This suggests ‘carry over storage’ influence and less influence of streamflow magnitudes on the decision variables.

There have been few attempts at evaluating the streamflow forecast skills in a decision making context. Hamlet et al. (2002) shown the influence of long-lead streamflow forecast in terms of better management of releases and increased power production on the Columbia River Basin. Grantz et al. (2006) investigated the streamflow forecast skill on a simplistic decision framework on the Truckee and Carson River basins but not a full fledged realistic DSS. In this regard, the research presented in this chapter makes a unique and significant contribution. Significant long lead skills in the decision variables offers great promise for improved water management planning and decision making – especially in the GRB which is water stressed. The approach can be easily transferred to other basins and thus, it is a generalized framework.

As mentioned, this is a first step at developing an integrated streamflow forecast-to-DSS framework and further developments are required. Nonparametric disaggregation methods (Prairie et al., 2006b) need to be used for better representation of the monthly streamflows. Although, most of the key decision rules have been included in the development of the DSS, other operational rules need to be included in the DSS to make it more realistic. Further evaluation of the approach with actual decisions that were made would provide realistic insights. Also, driving the DSS model under optimization mode and evaluating skill scores in monetary terms provides information on the value that added to the economy.

CHAPTER 6

A NEW FRAMEWORK TO SIMULATE STREAMFLOW SCENARIOS ON LONG TIME SCALES

In this chapter, a novel approach is developed to simulate streamflow scenarios on long time scales (decadal or longer) combining the observational and paleo reconstructed streamflows. This approach provides the ability to generate a richer variety of drought and flood scenarios than those in the observational record. Such variety will be of great use to water managers for long-term planning and development of basin water resources.

6.1. Introduction

Long-term planning and development of water resources require information on plausible hydrologic variability, especially on extreme wet and drought conditions. Traditionally, stochastic time series models are fit to observational data which are then used to generate synthetic streamflow scenarios that retain the statistical properties of the observed flows. Several methods using parametric and more recently, nonparametric methods, have been developed over the years, for single site (Bras and Iturbe, 1985; Salas, 1985) and multi-site basin-wide (Valencia and Schaake, 1973; Salas, 1985; Santos and Salas, 1982, Tarboton et al., 1998; Koutosyiannis, 2001; Sharma and O'Neil, 2002; Prairie et al., 2006b) streamflow simulation. The main drawback of this approach is that, long sequences of wet or dry years beyond those in the observed data are rarely or not at all simulated, thereby, offering very limited flow variability. Past (paleo) reconstruction of streamflows

using tree rings provide flow variability over several centuries before the observational record. These reconstructions have been performed widely on the western US river basins, more so recently, after the long severe drought during 2000-2005 (Woodhouse et al., 2006). For example, paleo streamflow reconstructions at Lees Ferry gauge on the Colorado River (Cook et al., 2004) reveal a fairly regular occurrence of droughts of five years or longer, yet during the observational period (1900-2005) there has been only one occurrence of such an event – suggesting to the contrary that long droughts are rare event. Also, Stockton and Jacoby (1976) reconstructed annual streamflows at Lees Ferry on the Colorado River for the period of 1520-1961, and observed persistent below average and above average flow conditions in the late decades of 16th century and in the early decades of 20th century, respectively. The late 16th century flows were much drier than the recent dry spell. Such knowledge of hydrologic variability might have resulted in a different Colorado River Compact, which was developed with limited hydrologic information and during the wetter conditions of the early 20th century, unlike the current compact which over appropriated the water in the basin. With increased water demands and the propensity of severe sustained droughts in the Upper Colorado River Basin (UCRB) (Woodhouse et al., 2006), water resources management, planning and development becomes extremely challenging.

Clearly, limited historical observations are not capable of providing a detailed understanding of the hydrologic variability in the basin, and longer paleo reconstructions have to be used. This leads to the question - how to combine paleo reconstructions with observational data to generate streamflow scenarios? In this

chapter, a new and novel framework is developed and applied to data from the Gunnison River Basin (GRB). A brief description of paleo streamflow reconstructions is provided followed by the description of the proposed methodology and the results of application.

6.2. Paleo streamflow reconstructions

For streamflows reconstruction, tree ring sites are carefully selected where the same hydroclimate processes, mainly precipitation and evapotranspiration control both processes, i.e., variability in streamflows and variations in the tree ring widths (Meko et al., 1995). Tree ring based climate reconstructions are attractive because, trees put on annual rings with the outer corresponding to the current year and the innermost to the earliest, thus, providing a clear chronology. Furthermore, they are best suited for reconstruction of integrated variables such as streamflows as the tree growth is a result of integration of climatological, physiological and biological factors (Meko et al., 1995). In the UCRB, a set of 62 locations were identified meeting the above criteria and considered as potential proxy indicators of hydrologic conditions (Woodhouse et al., 2006). At each site, fifteen or more trees are typically sampled from which tree ring cores were obtained, cross dated and measured using standard dendrochronological techniques (Stokes and Smiley, 1968; Swetnam et al., 1985). Measured series are standardized and combined into a single site tree ring index (Cook et al., 1990). These indices are also corrected for geometric bias and ‘whitened’ to remove the serial correlation which is partly attributed to biological factors (Fritts, 1976). Thus, developed tree ring indices are related to the corresponding observational streamflow during the overlapping period. Typically,

linear regression is fitted on the contemporary overlapping period to describe the streamflows based on the tree ring index. The fitted regression is then used to estimate (i.e. reconstruct) streamflows during the pre-observational period based on the tree ring index – there are several variations to this basic methodology (see Woodhouse et al., 2006 and references therein).

Since the reconstructed streamflows during the pre-observational period are based on the fitted regression model, the variance of the reconstructions is substantially smaller than that of the observational record. Furthermore, the reconstructions can vary quite a bit depending on the reconstruction method selected – this was seen in the reconstruction of the Lees Ferry streamflows from different methods (Stockton and Jacoby, 1976; Hidalgo et al., 2000; Woodhouse et al., 2006). But all the reconstructions agree on the ‘wet’ or ‘dry’ state of the system. Given this, the water managers are discomforted at using the magnitude of streamflows from these reconstructions for planning studies, but would use the ‘state’ information (i.e., wet or dry). This motivates the need for a model that uses the ‘state’ information from the paleo reconstructions and the magnitude from the observational record for simulating streamflow scenarios, which is described below.

6.3. Proposed Approach

The proposed approach has two main components. (1) Generating the state of the system (i.e., wet or dry). (2) Conditionally generating a streamflow magnitude from the observed data. This can be thought of as simulating from the conditional probability density function (PDF)

$$f(X_t / S_t, S_{t-1}, X_{t-1})$$

where X_t is the current flow, S_t is the current state, X_{t-1} is the previous flow, and S_{t-1} is the previous state.

The approach proceeds as follows:

1. A threshold value is selected to define the state (wet or dry) of the system. Typically, annual mean or median of the observed flows is chosen as the threshold.
2. The paleo streamflow time series is reduced to a binary (1 if the streamflows exceeds the threshold, 0 otherwise) series.

Suppose a streamflow scenario of 30 years is desired,

3. A consecutive block of 30 years is selected from the binary series of the paleo record. This is also known as ‘block bootstrap’ (Vogel and Shallcross, 1996).
4. For each year, ‘t’, K number of historical years that are closest to the current ‘feature vector’ consisting of the current state (S_t), previous state (S_{t-1}) and previous flow (X_{t-1}) are selected.
5. The selected K-nearest years are weighted, with maximum weight to the nearest year and minimum to the farthest.
6. From the weights, which is a probability metric, one of the years is resampled. The streamflow corresponding to the selected year becomes the simulated flow value for year ‘t’.

Steps 4 through 6 are repeated for all the 30-years; thus, it results a streamflow scenario.

Steps 4 through 6 are the standard K-NN time series resampling developed by Lall and Sharma (1996) and subsequently, used for multivariate weather generation by Rajagopalan and Lall (1999) and Yates et al., (2003) and others.

If longer length of flow sequence is desired (say 90 years) then several shorter blocks are bootstrapped (e.g., 3 blocks of 30 years) and joined to obtain a sequence of system state of the desired length. This enables a richer variety of as opposed to a single block of 90 years. The flow magnitudes are simulated using the above described K-nearest neighbor resampling approach.

6.4. Application

The above methodology was applied to the annual streamflows of the GRB. The Gunnison River near Grand Junction, Colorado, is selected for this study as streamflows at this location represent the total flows of the GRB and furthermore, paleo reconstruction streamflows were also available at this site. The paleo reconstructed streamflows are for the 429 year period of 1569-1997, obtained from the National Climate Data Center, NOAA (C. Woodhouse, personal communication, 2006). Natural streamflow were provided by the U.S. Bureau of Reclamation for a period of 98 years spanning 1906-2003 (J. Prairie, personal communication, 2006). The time series of the paleo and natural streamflows are shown in Figure 42. A close correspondence (correlation coefficient of 0.87) can be seen between the two data sets during the recent overlap period.

Five hundred simulations each of 98 years long were simulated from the framework described in the previous section. Similar number of simulations were generated from a lag-1 K-Nearest Neighbor time series resampling approach

(henceforth referred to as KNN1) based on the only natural flow data, for comparison. Essentially, this uses steps 4 through 6 but the feature vector is only the flow from the previous year. This was successfully developed and applied to data from Weber River near Oakley, Utah, by Lall and Sharma (1996). A suite of distributional and drought statistics were computed for each simulation and presented as boxplots along with the statistics of the observed data. The results are described below.

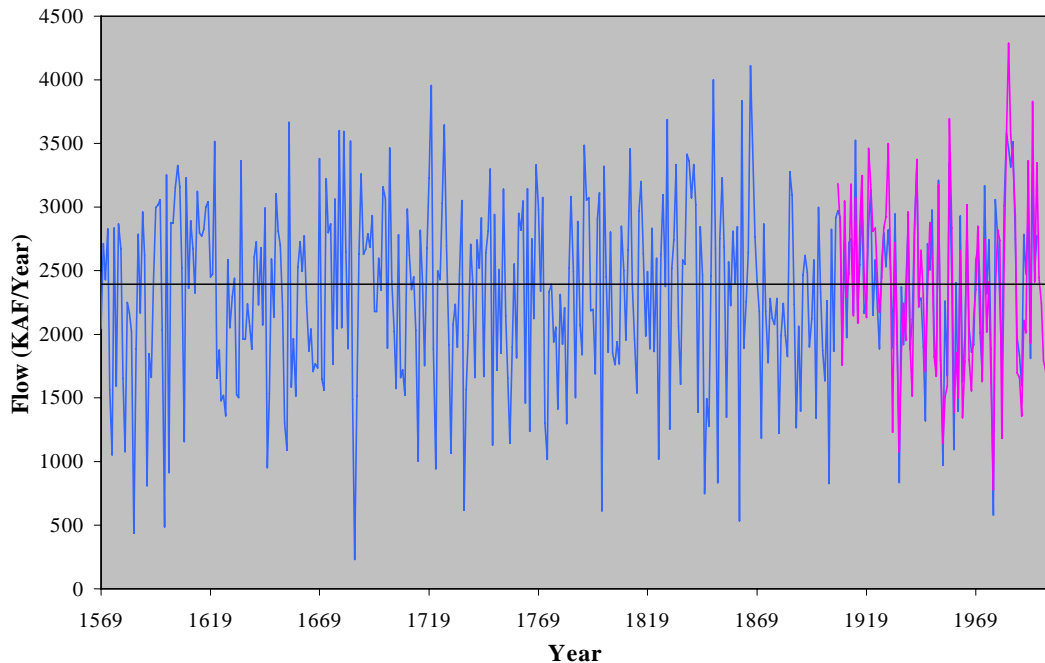


Figure 42: Time series of Paleo reconstructed streamflows (blue line) and natural streamflow estimates (red line) are shown. Mean of the natural streamflow estimates is plotted with thick solid line.

6.5. Results

6.5.1. Performance Statistics

Distributional (mean, standard deviation, skew, minimum and maximum flow, and lag-1 monthly correlation), drought (longest drought, maximum drought) and

surplus (longest surplus and maximum surplus) statistics are calculated for each simulation of the ensemble. The Longest Drought (LD) is the maximum number of consecutive years in which flows are below a threshold values; the Maximum Drought (MD) is the maximum amount of water during a drought, vice versa for the surplus statistics – Largest Surplus (LS) and Maximum Surplus (MS). Probability density functions (PDF) of the streamflow magnitudes from the simulations are also computed. The ensembles of statistics are presented as boxplots, along with the corresponding statistics from the paleo reconstructed streamflows (solid circles) and natural streamflow (solid triangles).

Further, system risk (reliability) is assessed by a sequent peak algorithm, which provides the storage required for various levels of firm yield.

As expected the simulations from KNN1 capture all the basic statistics very well. The simulations from the proposed method showed slight over simulation of the mean and variance (Figures 43a and b). This is because the paleo reconstructions are on average wetter than the observational period – as can be seen from the information in Table 15. The PDFs are also shifted slightly to the right (i.e., wetter) relative to the observed record (Figure 44). The other statistics are reasonably well captured.

Table 15: Probabilities of wet and dry conditions for paleo reconstructed streamflows and natural streamflow estimates. Wet years, if flow is greater than mean of natural flows, and vice versa for dry years.

	Paleo reconstructed streamflows (1569-1997)		Natural Flows (1906-2003)	
	Number of Years	Probability	Number of Years	Probability
Wet Years	221	0.52	47	0.48
Dry Years	208	0.48	51	0.52

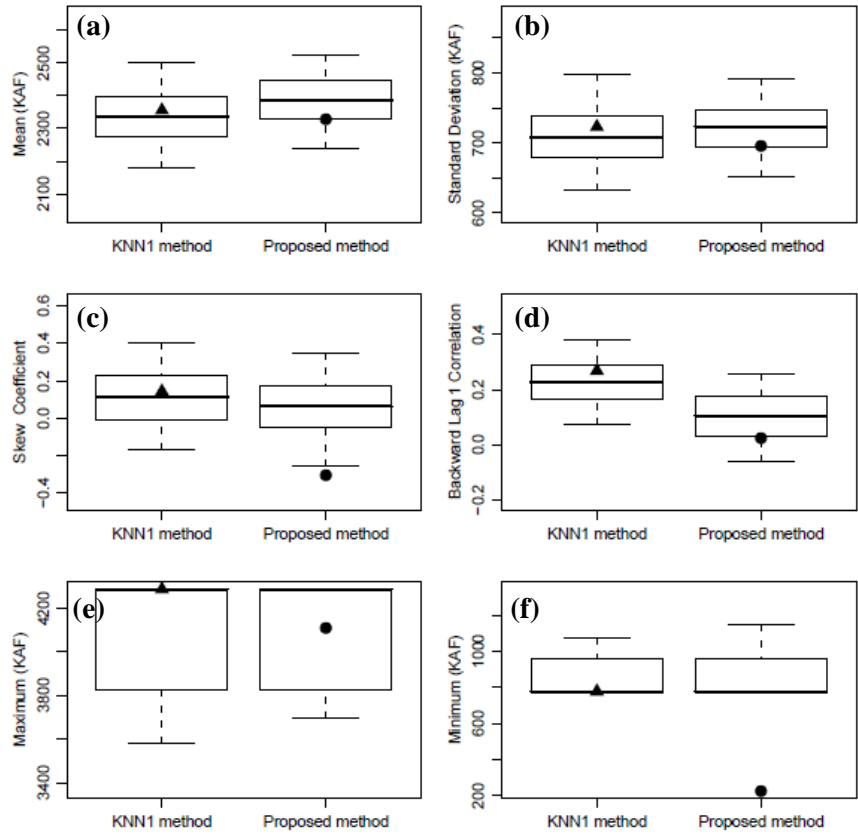


Figure 43: Boxplots of statistics of streamflow scenarios derived from KNN1 (left column) and proposed methods (right column). Solid triangles and solid circles correspond to the statistics computed for natural streamflow estimates and paleo reconstructed streamflows, respectively. Statistics are (a) mean, (b) standard deviation, (c) skew, (d) lag-1 correlation coefficient, (e) maximum, and (f) minimum.

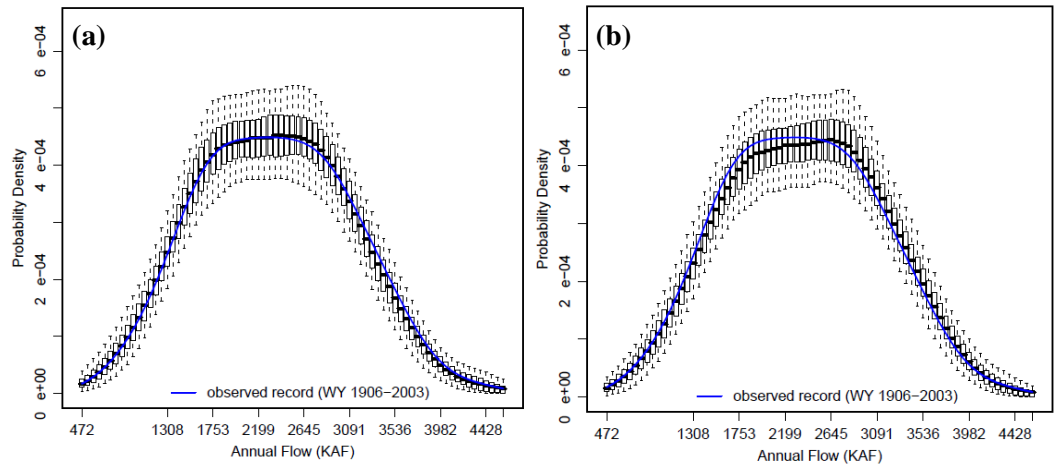


Figure 44: Probability Density Function of annual streamflows generated from (a) traditional KNN method, and (b) KNN conditioned on paleo streamflows. Blue line corresponds to the natural streamflow estimates.

Boxplots of average drought and surplus statistics are shown in Figure 45. Paleo reconstructed streamflows shown slightly higher average LS values (solid circles) whereas, natural streamflows exhibited high average LD values (solid triangles). The KNN1 simulations overestimated the average LD statistics and slightly underestimated average LS statistics (Figure 45a), because natural streamflows exhibited more dry events (Table 15). While the simulations using the paleo reconstructions captured both statistics well but underestimated average LD statistics (Figure 45b). However, both methods captured average drought and surplus volume (i.e., MD and MS) of water (Figures 45c and 45d). The drought and surplus statistics are based on a threshold of mean annual natural flows. As such they vary significantly depending on the threshold. A better approach to demonstrate this would be by a storage-yield curve obtained from the sequent peak algorithm.

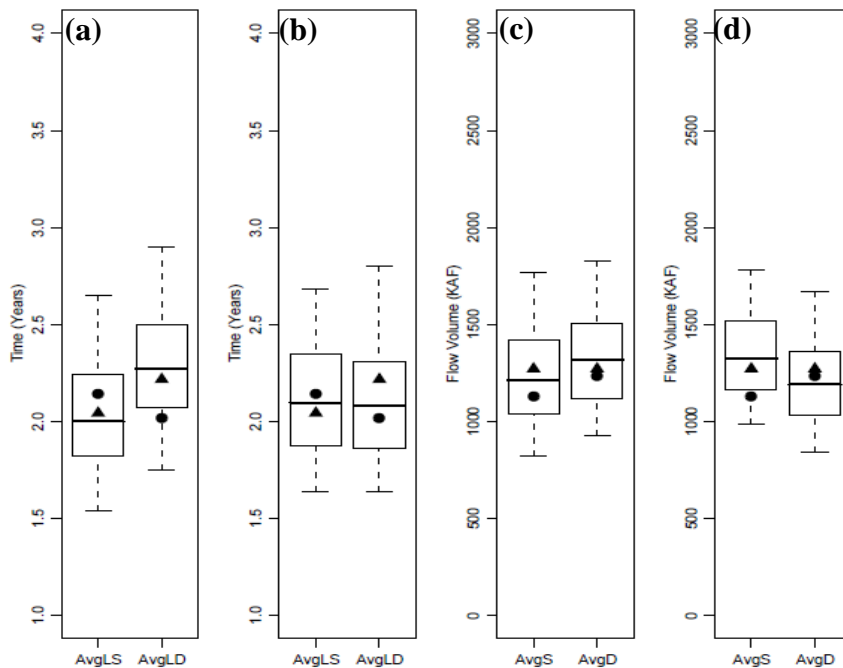


Figure 45: Boxplots of drought statistics (a) KNN1 – LS and LD, (b) proposed method – LS and LD, (c) KNN1 – MS and MD, and (d) proposed method – MS and MD.

6.5.2. Sequent Peak Algorithm

The sequent peak algorithm determines the storage required for a desired yield for a given flow sequence (Viessman and Welty, 1985). It solves a water balance equation and calculates the storage required at each time step; the maximum of the storage values is the required storage for the desired yield to be met at all times with the particular flow sequence. The storage values are obtained for all the flow scenarios and for several yield values. The same is repeated on the natural flow sequence. They are then displayed as boxplots (Figure 46). The sequent peak algorithm is mathematically described as follows.

$$K_t = R_t - Q_t + K_{t-1} \text{ if positive} \\ = 0 \text{ otherwise}$$

K_t is the required storage capacity

R_t is the release

Q_t is the inflow

Where,

At lower yields, simulations from both KNN1 and the proposed approach, suggest a small storage. However, as the yield increases, KNN1 simulations indicate the need for higher storage (Figure 46a) than those from including paleo reconstructions (Figure 46b). This is consistent with earlier results in that, the KNN1 based on the natural flow, which has lower average flows, would require larger storage. While the paleo reconstructions had on an average wetter conditions (Table 15) and therefore, consistent with lower storage requirements.

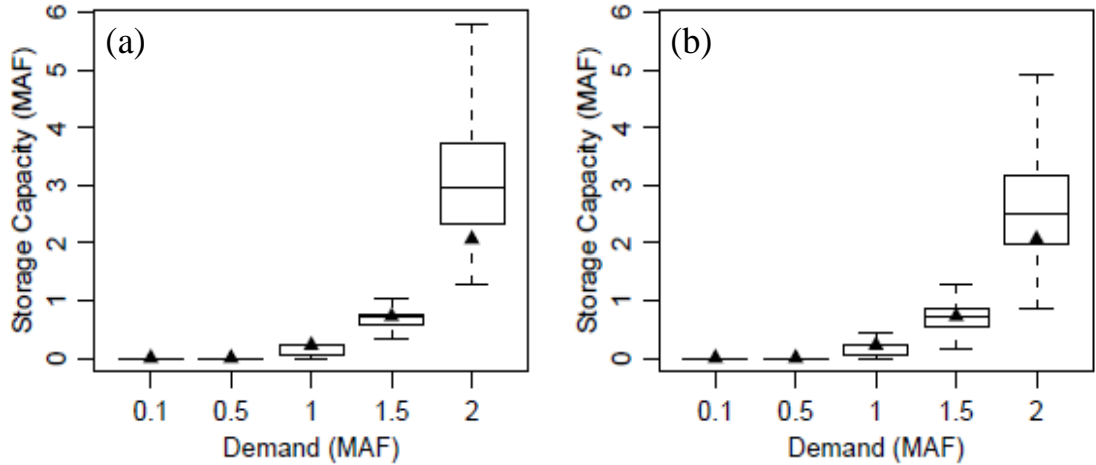


Figure 46: Boxplot of Yield-Storage of simulations from (a) Traditional KNN approach (b) KNN conditioned on paleo streamflows approach.

The Cumulative Distribution Function (CDF) of the storage values at a given yield along with the existing storage information can provide a rough estimate of the risk of not meeting the yield requirements – e.g., at an yield of 2500 KAF, if 33,686 KAF is the existing storage, then the CDF of the storage derived from KNN1 and proposed approach would suggest a risk of about 0.55 and 0.30, respectively (Figure 47).

The sequent peak approach meets all of the yield and therefore, the risk estimates tend to be very conservative. For estimates of system reliability and risk of various components of the management in the basin, the flow scenarios have to be input through a decision support model.

6.6. Summary

A new and novel approach was presented, in which the strong aspects (i.e., the state representation) of paleo reconstructed flows and the observational flows (i.e., magnitude) are combined. In this approach, blocks of paleo reconstructed flows are

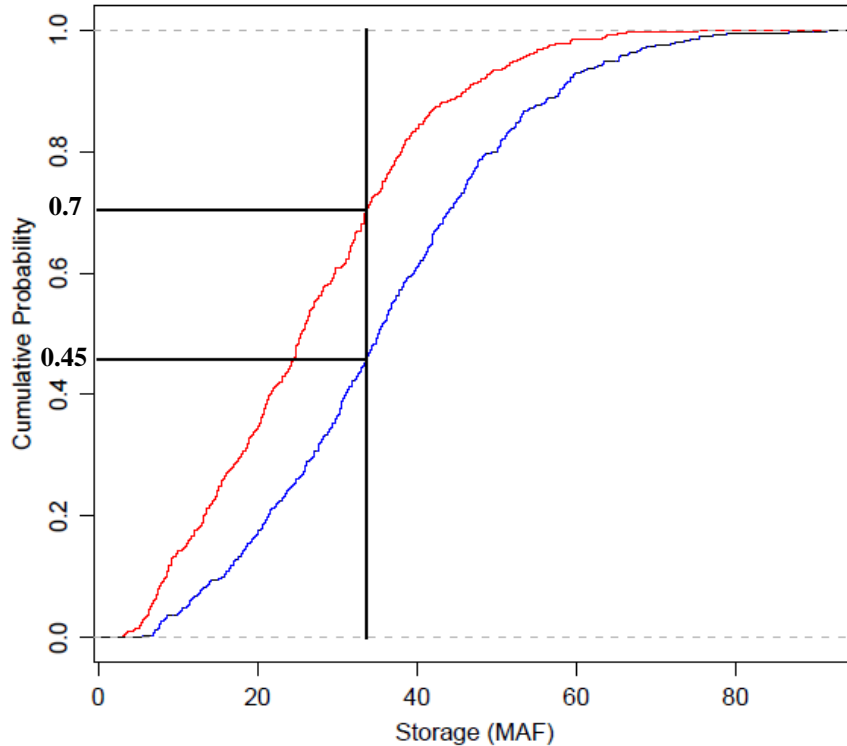


Figure 47: The CDF of the storage values, derived from KNN1 (blue line) and proposed methods (red line), conditioned on yield of 2500 KAF. The vertical line corresponds to the storage value derived from natural streamflows.

bootstrapped and the state information (i.e., wet or dry) of each year in the block is selected. The flow magnitudes are then generated from the observational data keeping the year to year (i.e., lag-1) correlation. This combined approach has the ability to generate a rich variety of streamflow scenarios and more importantly sequences of wet and dry conditions which are key to water resources system operation. The paleo reconstructions were wetter than average compared to the observational record. As a result, the combined approach generated wetter sequences on average.

This approach is nonparametric, simple and robust. However, it has a few drawbacks that can be improved – listed below.

(1) If longer lengths of scenarios are required, e.g., 90 years, then blocks of 90 years have to be resampled from the paleo record. This would greatly reduce the variety of the sequence.

(2) Flow magnitudes are generated by bootstrapping the observational record, so no new flows can be generated.

The first can be addressed by a non-homogeneous Markov Chain model (Rajagopalan et al., 1996). In this, the state sequence is modeled as a lag-1 Markov Chain whose transition probabilities vary each year. The transition probabilities are nonparametrically estimated for each year using a Kernel estimator (Lall et al., 1996; Rajagopalan et al., 1996). The simulation now involves using the transition probabilities to generate the state of the system (wet or dry) rather than using the actual state information of the paleo data. This enables the generation of a much richer variety of state sequences addressing the drawback in (1). For generating magnitudes of flows not seen, traditional parametric methods can be used (Salas, 1985) or a local polynomial based modification of the KNN1 (Prairie et al., 2006a) can be used. Nonetheless, the approach developed in this chapter provides a firm start point.

CHAPTER 7

SUMMARY AND CONCLUSIONS

7.1. Summary

This research developed an integrated climate diagnostics-to-decision support system framework and applied to the Gunnison River Basin (GRB). It has two major components. (1) Development of a statistical ensemble streamflow forecasting framework. (2) Development of a decision support system and evaluation of skills in decision variables. In addition, a novel approach to simulate streamflow scenarios on long time scales (decadal or longer) combining the observational and paleo reconstructed streamflows, was developed. The presented research demonstrates the utility of ensemble streamflow forecasts in a realistic decision making context, and this makes a unique and major contribution. This generalized framework can be easily transferred to other basins.

Conclusions on the each major component of the research are presented below followed by suggestions for future extensions.

7.2. Conclusions

7.2.1. Multimodel ensemble forecast framework

The framework has four main steps. (1) Principal Component Analysis is performed on the spatial streamflows to identify the dominant modes of variability. (2) Large scale ocean-atmospheric predictors are identified for the dominant modes. (3) Objective criterion, Generalized Cross Validation (GCV) is used to select a suite

of candidate models. (4) Ensembles of forecast of the dominant modes and consequently the spatial flows are issued from the candidate models. The forecast model is based on the locally weighted polynomial approach that is data driven. Application of this framework to the GRB showed skilful long lead forecasts. Furthermore, the multimodel ensemble forecast including large-scale climate features and Snow water equivalent (SWE) rendered better performance in terms of skill and reliability of uncertainty estimates than the single best model counterpart or a model with only the SWE information.

Also, an interesting land-surface effect on the streamflows is observed: when the fall season is dry and following winter is wet, then the spring streamflows tend to be relatively lower compared to what would be expected from a wet winter. Therefore, the soil moisture information of the preceding fall was included as a potential predictor, which improved the forecasts. This is corroborated by the presence of Palmer Drought Severity Index (PDSI) in several of the leading candidate models.

Having a skillful forecast of the upcoming spring flows during early winter when the snow information is incomplete is of significant importance to water managers in their planning and operation. In this regard, a decision support model of the GRB is driven with ensemble of streamflow forecasts and resulted ensemble of decision variables is evaluated.

7.2.2. Categorical Streamflow Forecast Framework

The developed framework is a simple and direct method to produce probabilistic categorical streamflow forecasts. In this, the categorical forecasts of the leading mode (or principal component) of the spatial streamflow at different thresholds is estimated

via logistic regression. Large-scale climate features are used to obtain the predictors, and used in the logistic regression. These categorical forecasts are then uniformly transferred to the corresponding categorical forecast of streamflows at all the locations. The framework was applied to categorical forecasts of the April-June (spring) streamflows in the GRB at several month lead times starting from December 1st. The forecasts exhibited significant skill even at long lead times. Furthermore, the skills were comparable or better in some cases to those obtained from a ‘best model’ nonparametric regression based forecasts of multimodel ensemble forecast framework. Also skill scores from the multimodel ensemble forecasts are estimated and comparable results were observed. Both these approaches are complimentary and serve different purposes – the logistic regression method will be useful if a quick categorical forecast is required, while the ensemble approach can provide the entire probability density function of the streamflows that can be used to drive decision support models.

The framework developed in this research is flexible and simple to implement. It works very well if the leading mode captures most of the data variance, and has uniform Eigen loadings and high correlations with all the basin streamflows – such as the case in the application to the GRB is demonstrated. If there are more than one leading PC that capture a significant part of the spatial variance, then this framework can be applied to all the significant leading PCs and the estimated categorical forecasts from each of the PCs optimally combined following Rajagopalan et al. (2002).

7.2.3. Decision Support System

The multimodel ensemble streamflow forecast method was integrated with a decision support model of the GRB to form a Decision Support System (DSS) to generate ensembles of decision variables. The skills in the streamflow forecasts seem to transfer quite well to the decision variables, as seen by their skilful forecasts. Positive skill score of decision variables highlights the influence of forecasted streamflows compared to the climatological streamflows in driving the model. The better performance of decision variables especially with January 1st forecasts, which uses only climate information, provides four month lead time allowing water managers to modify/make better decisions in spring season. The lower performance of streamflow forecasts is not linearly transformed onto decision variables, i.e., in several months, a few decision variables derived from both January 1st and April 1st forecasts exhibited approximately similar performance. Also, the nonlinear transferability skill is observed between streamflow forecasts and decision variables, i.e., negative skill of streamflow forecasts resulted in positive skill of decision variables, and vice versa. However, there are few variables which are not influenced by skill in streamflows, for example, filling the Blue Mesa reservoir by July end, maintaining reservoir elevation at its maximum in Morrow Point and Crystal reservoirs. All three different streamflow scenarios (i.e., actual, forecasted, climatological) met the above criteria resulting the same value of decision variable, and consequently undefined skill scores. This suggests ‘carry over storage’ influence and less influence of streamflow magnitudes on the decision variables.

There have been few attempts at evaluating the streamflow forecast skills in a decision making context. Hamlet et al. (2002) shown the influence of long-lead streamflow forecast in terms of better management of releases and increased power production on the Columbia River Basin. Grantz et al. (2006) investigated the streamflow forecast skill on a simplistic decision framework on the Truckee and Carson River basins. This research demonstrates the utility of ensemble streamflow forecasts in a full fledged decision making context.

7.2.4. Streamflow Scenarios for Long-term Planning

A new and novel approach was presented, in which the strong aspects (i.e., the state representation) of paleo reconstructed flows and the observational flows (i.e., magnitude) are combined. In this approach, blocks of paleo reconstructed flows are bootstrapped and the state information (i.e., wet or dry) of each year in the block is selected. The flow magnitudes are then generated from the observational data keeping the year to year (i.e., lag-1) correlation. This combined approach has the ability to generate a rich variety of streamflow scenarios and more importantly sequences of wet and dry conditions which are key to water resources system operation. The paleo reconstructions were wetter than average compared to the observational record. As a result, the combined approach generated wetter sequences on average.

7.3. Future Work

There are several areas of the proposed research that can be significantly improved, which are listed below.

1. Role of vegetation feedbacks on the spring melt (e.g., Wang et al., 2005) together with soil moisture effects (i.e., quantified by the PDSI), snow pack ripening, spring (daily) wind patterns, air temperature, relative humidity, melt patterns in association with topography and shading factors (Lundquist and Flint, 2005), and cloud cover need to be investigated to better understand the streamflow mechanism. This can provide additional skilful predictors for multimodel streamflow forecast.
2. Improved objective criteria for selecting the multimodels, combining their ensemble forecasts and dealing with multicollinearity need to be developed. The methods developed are quasi-objective.
3. Application of the nonparametric logistic regression (Loader, 1999) and optimal ways (Rajagopalan et al., 2002) to combine to categorical forecasts from multimodels need to be explored to improve the categorical streamflow forecasts.
4. The decision model in RiverWare requires monthly streamflows. A simple disaggregation method is proposed and implemented for the disaggregation of seasonal streamflow forecast to monthly flows. Robust nonparametric disaggregation methods recently developed (Prairie et al., 2006b) should be used for better representation of the monthly forecasts.

5. Although most of the key decision rules of the water resources management in the GRB have been included in the development of the DSS, other operational rules could be included in the DSS to make it more realistic.
6. The block bootstrap approach to resample paleo reconstructions to generate system state (wet or dry) was used. However, if longer lengths of scenarios are required, e.g., 90 years, then blocks of 90 years have to be resampled from the paleo record. This would greatly reduce the variety of the sequence. To address this, the state transitions for each year have to modeled as a nonhomogeneous Markov chain with the transition probabilities estimated from kernel estimators (Lall et al., 1996; Rajagopalan et al., 1996). The transition probabilities can be used to generate the sequence of states, which now will produce a much richer variety.
7. The streamflow simulation on long-time scales using the paleo data involves bootstrapping observational flow record. As a result flows not seen in the historical record are not generated. Traditional parametric methods can be used (Salas, 1985) or local polynomial based modification of the KNN1 (Prairie et al., 2006) can also be used. Nonetheless, the approach developed in this research provides a firm start point.

REFERENCES

- Aguado, E., D. R. Cayan, L. G. Riddle, and M. Roos (1992), Climatic fluctuations and the timing of West Coast streamflow. *Journal of Climate*, 5, 1468-1483.
- Allan, R. J., J. A. Lindesay, and D. E. Parker (1996), *El Nino Southern Oscillation and Climatic Variability*, CSIRO, Collingwood, Australia.
- Bates, J. M., and C. W. J. Granger (1969), The combination of forecasts, *Operational Research Quarterly*, 20, 451-468.
- Barnett, T., R. Malone, W. Pennell, D. Stammer, B. Semtner, and W. Washington (2004), The effects of climate change on water resources in the west: introduction and overview, *Climatic Change*, 62, 1-11.
- Bjerknes, J. (1969), Atmospheric teleconnections from the equatorial Pacific, *Monthly Weather Review*, 97, 163–172.
- Bradley, A. A., T. Hashino, and S. S. Schwartz (2003), Distributions-oriented verification of probability forecasts for small data samples, *Weather and Forecasting*, 18, 903–917.
- Bradley, R. S. (1976), *Precipitation history of the Rocky Mountain States*, Westview Press, Boulder, CO.
- Bras, R.L., and I. Rodriguez-Iturbe (1985), *Random Functions and Hydrology*, Addison Wesley, Reading, Massachusetts.
- Brown, D. P., and A. C. Comrie (2004), A winter precipitation ‘dipole’ in the western United States associated with multidecadal ENSO variability, *Geophysical Research Letters*, 31, L09203, doi:10.1029/2003GL018726.

- Burn D. H. (1994), Hydrologic effects of climatic change in west-central Canada, *Journal of Hydrology*, 160, 53-70.
- Cayan, D. R. (1996), Climate variability and snow pack in the western United States, *Journal of Climate*, 9, 928-948.
- Cayan D. R., and J. O. Roads (1984), Local relationships between United States West Coast precipitation and monthly mean circulation parameters, *Monthly Weather Review*, 112, 1276-1282.
- Cayan, D. R., and D. H. Peterson (1989), The influence of North Pacific atmospheric circulation on streamflow in the west, in *Aspects of Climate Variability in the Pacific and the Western Americas*, *Geophysical Monograph Series*, volume 55, edited by D. H. Peterson, pp. 365-374, AGU, Washington, D. C.
- Cayan, D. R., and R. H. Webb (1992), El Niño/Southern Oscillation and streamflow in the western United States, in *El Nino-Historical and Paleoclimatic Aspects of the Southern Oscillation*, edited by H. F. Diaz and V. Markgraf, pp. 29-68, Cambridge Univ. Press, Cambridge.
- Cayan, D. R., M. D. Dettinger, H. F. Diaz, and N. Graham (1998), Decadal variability of precipitation over western North America, *Journal of Climate*, 11, 3148–3166.
- Cayan, D. R., K. T. Redmond, and L. G. Riddle (1999), ENSO and hydrologic extremes in the western United States, *Journal of Climate*, 12, 2881-2893.
- Cayan, D. R., S. A. Kammerdiener, M. D. Dettinger, J. M. Caprio, and D. H. Peterson (2001), Changes in the onset of spring in the western United States, *Bulletin of the American Meteorological Society*, 82, 399–416.

- Changnon, D., T. B. McKee, and N. J. Doesken (1993), Annual snowpack patterns across the Rockies: Long-term trends and associated 500-mb synoptic patterns, *Monthly Weather Review*, *121*, 633-647.
- Christensen, N. C., A. W. Wood, N. Voisin, D. P. Lettenmaier, and R. N. Palmer (2004), The effects of climate change on the hydrology and water resources of the Colorado River Basin, *Climatic Change*, *62*, 337-363.
- Clark, M. P., M. C. Serreze, and G. J. McCabe (2001), Historical effects of El Nino and La Nina events on the seasonal evolution of the montane snowpack in the Columbia and Colorado River Basins, *Water Resources Research*, *37*, 741-757.
- Clark, M. P., and L. E. Hay (2004), Use of medium-range numerical weather prediction model output to produce forecasts of streamflow, *Journal of Hydrometeorology*, *5*, 15-32.
- Clark, M. P., and A. G. Slater (2006), Probabilistic quantitative precipitation estimation in complex terrain, *Journal of Hydrometeorology*, *7*, 3-22.
- Clemen R. T. (1989), Combining forecasts: A review and annotated bibliography, *International Journal of Forecasting*, *5*, 559-583
- Craven, P., and G. Whaba (1979), Optimal smoothing of noisy data with spline functions, *Numerische Mathematik*, *31*, 377-403.
- Cook, E. R., K. Briffa, S. Shiyatov, and V. Mazepa (1990), Tree-ring standardization and growth-trend estimation, in *Methods of Dendrochronology: Applications in the Environmental Sciences*, edited by E. R. Cook and L. A. Kairiukstis, pp. 104-123, Springer, New York.

Cook, E. R., C. A. Woodhouse, C. M. Eakin, D. M. Meko, and D. W. Stahle (2004), Long-term aridity changes in the western United States, *Science*, 306, 1015–1018.

Day, G. N. (1985), Extended streamflow forecasting using NWSRFS, *Journal of Water Resources Planning and Management*, 111, 157-170.

Dai, A., K. E. Trenberth, and T. Qian (2004), A global dataset of Palmer Drought Severity Index for 1870–2002: Relationship with soil moisture and effects of surface warming, *Journal of Hydrometeorology*, 5, 1117-1130.

Dettinger, M. D., and D. R. Cayan (1995), Large-scale atmospheric forcing of recent trends toward early snowmelt runoff in California, *Journal of Climate*, 8, 606-623.

Dettinger, M.D., D. R. Cayan, H. F. Diaz, and D. Meko (1998), North-south precipitation patterns in western North America on interannual-to-decadal time scales, *Journal of Climate*, 11, 3095-3111.

Dettinger, M. D., D. R. Cayan, M. K. Meyer, and A. E. Jeton (2004), Simulated hydrologic responses to climate variations and change in the Merced, Carson, and American River Basins, Sierra Nevada, California. 1900-2099, *Climatic Change*, 62, 283-317.

Dracup, J. A., and E. Kahya (1994), The relationships between U.S. streamflow and La Niña events, *Water Resources Research*, 30, 2133-2142.

Emmert, J. D. (2005), Network Stochastic Programming for Valuing Reservoir Storage, M.S. thesis, Univ. of Colorado at Boulder, Boulder, CO.

Eschenbach, E., T. Magee, E. Zagona, M. Goranflo, and R. Shane (2001), Goal programming decision support system for multiobjective operation of reservoir systems, *Journal of Water Resources Planning and Management*, 127, 108-120.

- Garen, D. C. (1992), Improved techniques in regression-based streamflow volume forecasting, *Journal of Water Resources Planning and Management*, 118, 654–670.
- Gershunov, A., and T. P. Barnett (1998), ENSO influence on intraseasonal extreme rainfall and temperature frequencies in the contiguous United States: observations and model results, *Journal of Climate*, 11, 1575-1586.
- Grantz, K., B. Rajagopalan, M. Clark, and E. Zagona (2005), A technique for incorporating large-scale climate information in basin-scale ensemble streamflow forecasts, *Water Resources Research*, 41, W10410, doi:10.1029/2004WR003467.
- Grantz, K., B. Rajagopalan, E. Zagona, and M. Clark, (2006), Water management applications of climate-based hydrologic forecasts: Case study of the Truckee-Carson River Basin, Nevada, *Journal of Water Resources Planning and Management* (accepted).
- Fritts, H. C., (1976), *Tree Rings and Climate*, Elsevier, New York.
- Hagedorn, R., F. J. Doblas-Reyes, and T. N. Palmer (2005), The rationale behind the success of multi-model ensembles in seasonal forecasting. Part I: Basic concept, *Tellus A*, 57, 219-233.
- Hamill, T. M., (2001), Interpretation of rank histograms for verifying ensemble forecasts, *Monthly Weather Review*, 129, 550-560.
- Hamlet, A. F., and D. P. Lettenmaier (1999a), Effects of climate change on hydrology and water resources in the Columbia River basin, *Journal American Water Resources Association*, 35, 1597–1623.

- Hamlet, A. F., and D. P. Lettenmaier (1999b), Columbia River streamflow forecasting based on ENSO and PDO climate signals, *Journal of Water Resources Planning and Management*, 125, 333-341.
- Hamlet, A. F., D. Huppert, and D. P. Lettenmaier (2002), Economic value of long-lead streamflow forecasts for Columbia River hydropower, *Journal of Water Resources Planning and Management*, 128, 91-101.
- Helsel, D. R., and R. M. Hirsch (1995), *Statistical Methods in Water Resources*, Elsevier Science, Amsterdam.
- Hidalgo, H. G., T. C. Piechota, and J. A. Dracup (2000), Alternative principal components regression procedures for dendrohydrologic reconstructions, *Water Resources Research*, 36, 3241–3249.
- Hidalgo, H. G. and J.A. Dracup (2003), ENSO and PDO effects on hydroclimatic variations of the Upper Colorado River Basin, *Journal of Hydrometeorology*, 4, 5-23.
- Higgins, R. W., A. Leetmaa, and V. E. Kousky (2002), Relationships between climate variability and winter temperature extremes in the United States, *Journal of Climate*, 15, 1555–1572.
- Higgins, R. W., H.-K. Kim, and D. Unger (2004), Long-lead seasonal temperature and precipitation prediction using tropical pacific SST consolidation forecasts, *Journal of Climate*, 17, 3398–3414.
- Hoerling, M. P., A. Kumar, and M. Zhong, (1997), El Nino, La Nina and the nonlinearity of their teleconnections, *Journal of Climate*, 10, 1769-1786.
- Hoeting, J. A., D. M. Madigan, A. E. Raftery, and C. T. Volinsky (1999), Bayesian model averaging: A tutorial (with discussion), *Statistical Science*, 14, 382-401.

- Horel, J. D., and J. M. Wallace (1981), Planetary scale atmospheric phenomena associated with the Southern Oscillation, *Monthly Weather Review*, 109, 813-829.
- Hosmer, D. S., and S. Lemeshow (1989), *Applied Logistic Regression*, Wiley, New York.
- Hou, D., E. Kalnay, and K. K. Droegemeier (2001), Objective verification of the SAMEX'98 ensemble forecast, *Monthly Weather Review*, 129, 73-91.
- Hwang, Y., (2005), Impact of input uncertainty in ensemble streamflow generation, Ph.D. thesis, Univ. of Colorado at Boulder, Colorado.
- Kahya, E., and J. A. Dracup (1993), U.S. streamflow patterns in relation to the El Niño/Southern Oscillation, *Water Resources Research*, 29, 2491-2504.
- Kahya, E., and J. A. Dracup (1994), The Influences of Type 1 El Niño and La Niña events on streamflows in the Pacific Southwest of the United States, *Journal of Climate*, 7, 965-976.
- Kalnay, E., et al., (1996), The NCEP/NCAR 40-Year Reanalysis project, *Bulletin of the American Meteorological Society*, 77, 437-471.
- Klein, W. H., (1963), Specifications of precipitation from the 700-millibar circulation, *Monthly Weather Review*, 91, 527-536.
- Klein, W. H., C. W. Crockett, and J. F. Andrews (1965), Objective prediction of daily precipitation and cloudiness, *Journal of Geophysical Research*, 70, 801-813.
- Klein, W. H., and H. J. Bloom (1987), Specification of monthly precipitation over the United States from the surrounding 700 mb height field, *Monthly Weather Review*, 115, 527-536.
- Koutsoyiannis, D., (2001), Coupling stochastic models of different timescales, *Water*

Resources Research, 37, 379-391.

Krishnamurti, T. N., C. M. Kishtawal, T. E. LaRow, D. R. Bachiochi, Z. Zhang, C. E. Williford, S. Gadgil, and S. Surendran (1999), Improved weather and seasonal climate forecasts from multi-model superensemble, *Science*, 285, 1548–1550.

Krishnamurti, T. N., C. M. Kishtawal, Z. Zhang, T. E. LaRow, D. R. Bachiochi, C. E. Williford, S. Gadgil, and S. Surendran (2000), Multi-model ensemble forecasts for weather and seasonal climate, *Journal of Climate*, 13, 4196–4216.

Lall, U. (1995), Recent advances in nonparametric function estimation: Hydraulic applications, *Rev. Geophys.*, 33, 1093-1102.

Lall, U., and A. Sharma (1996), A nearest neighbor bootstrap for resampling hydrologic time series, *Water Resources Research*, 32, 679-693, 1996.

Lall, U., B. Rajagopalan, and D. G. Tarboton (1996), A Nonparametric wet/dry spell model for resampling daily precipitation, *Water Resources Research*, 32, 2803-2823.

Lettenmaier, D. P., and T. Y. Gan (1990), Hydrologic sensitivities of the Sacramento-San Joaquin River basin, California, to global warming. *Water Resources Research*, 26, 69-86.

Leung, L. R., Y. Qian, X. Bian, W. M. Washington, J. Han, and J. O. Roads (2004), Mid-century ensemble regional climate change scenarios for the western United States, *Climatic Change*, 62, 75-113.

Lins, H. F., and P. J. Michaels (1994), Increasing U.S. streamflow linked to greenhouse gas forcing, *Eos, Trans. Amer. Geophys. Union*, 75, 281-285.

Loader, C. (1999), *Local Regression and Likelihood*, Springer, New York.

- Lundquist, J., and A. Flint, 2005: 2004 onset of snowmelt and streamflow: How shading and the solar equinox may affect spring runoff timing in a warmer world, *Journal of Hydrometeorology* (in press).
- Madigan, D., and A. E. Raftery (1994), Model selection and accounting for model uncertainty in graphical models using Occam's window, *Journal of American Statistical Association*, 89, 1535–1546.
- Magee, T. M., and H. M. Goranflo (2002), Optimizing daily reservoir scheduling at TVA with RiverWare, in *Proceedings of the Second Federal Interagency Hydrologic Modeling Conference*, Las Vegas, NV.
- Mantua, N. J., S. R. Hare, Y. Zhang, J. M. Wallace, R. C. Francis (1997), A Pacific interdecadal climate oscillation with impacts on salmon production, *Bulletin of the American Meteorological Society*, 78, 1069–1079.
- Maurer, E. P., D. P. Lettenmaier, and N. J. Mantua (2004), Variability and potential sources of predictability of North American runoff, *Water Resources Research*, 40, W09306, doi:10.1029/2003WR002789.
- McCabe, G. J. (1994), Relationships between atmospheric circulation and snowpack in the Gunnison River Basin, Colorado, *Journal of Hydrology*, 157, 157-175.
- McCabe, G. J. (1996), Effects of winter atmospheric circulation on temporal and spatial variability in annual streamflow in the western United States, *Journal of Hydrological Sciences*, 41, 873-887.
- McCabe, G. J., and D. R. Legates (1995), Relationships between 700 hPa height anomalies and April 1 snowpack accumulations in the western USA, *International Journal of Climatology*, 15, 517-530.

- McCabe, G. J., and M. D. Dettinger (1999), Decadal variations in the strength of ENSO teleconnections with precipitation in the western United States, *International Journal of Climatology*, *19*, 1399-1410.
- McCabe, G. J., and M. D. Dettinger (2002), Primary modes and predictability of year-to-year snowpack variations in the western United States from teleconnections with Pacific Ocean climate, *Journal of Hydrometeorology*, *3*, 13-25.
- McCabe, G. J., and D. M. Wolock (2002), A Step increase in streamflow in the conterminous United States, *Geophysical Research Letters*, *24*, 2185-2188.
- Meko, D. M., C. W. Stockton, and W. R. Boggess (1995), The tree-ring record of severe sustained drought, *Water Resources Bulletin*, *31*, 789–801.
- Mote, P. W. (2003), Trends in snow water equivalent in the Pacific Northwest and their climatic causes, *Geophysical Research Letters*, *30*, 1601-1604.
- Nash, L. N. and P. H. Gleick (1991), Sensitivity of streamflow in the Colorado basin to climatic changes, *Journal of Hydrology*, *125*, 221-241.
- Newman, M., G. P. Compo, and M. A. Alexander (2003), ENSO-forced variability of the Pacific Decadal Oscillation, *Journal of Climate*, *16*, 3853-3857.
- Payne, J. T., A. W. Wood, A. F. Hamlet, R. N. Palmer, and D. P. Lettenmaier (2004), Mitigating the effects of climate change on the water resources of the Columbia River basin. *Climatic Change*, *62*, 233-256.
- Piechota, T. C., J. A. Dracup, and R. G. Fovell (1997), Western US streamflow and atmospheric circulation patterns during El Niño-Southern Oscillation, *Journal of Hydrology*, *201*, 249–271.

- Piechota, T. C., F. H. S. Chiew, J. A. Dracup, and T. A. McMahon (1998), Seasonal streamflow forecasting in eastern Australia and the El Nino-Southern Oscillation, *Water Resources Research*, 34, 3035-3044.
- Piechota, T. C., H. Hidalgo, and J. Dracup (2001), Streamflow variability and reconstruction for the Colorado River Basin, in *Proceedings of the EWRI World Water & Environmental Resources Congress*, Orlando, Florida.
- Porporato, A., and L. Ridolfi (1997), Nonlinear analysis of river flow time sequences, *Water Resources Research*, 33, 1353-1368, 10.1029/96WR03535.
- Porporato, A., and L. Ridolfi (2001), Multivariate nonlinear prediction of river flows, *Journal of Hydrology*, 248, 109-122.
- Prairie, J., B. Rajagopalan, T. Fulp, and E. Zagona (2005), Statistical nonparametric model for natural salt estimation, *Journal of Environmental Engineering*, 131, 130-138.
- Prairie, J., B. Rajagopalan, T. Fulp, and E. Zagona (2006a), Modified K-NN model for stochastic streamflow simulation, *Journal of Hydrologic Engineering*, 11, 371-378.
- Prairie, J., B. Rajagopalan, U. Lall (2006b), A stochastic nonparametric technique for space-time disaggregation of streamflows, *Water Resources Research* (accepted).
- Raftery, A. E., D. Madigan, and J. A. Hoeting (1997), Bayesian model averaging for regression models, *Journal of American Statistical Association*, 92, 179-191.
- Rajagopalan, B., and U. Lall (1995), Seasonality of precipitation along a meridian in the western United States, *Geophysical Research Letters*, 22, 1081-1084.

Rajagopalan, B., U. Lall, and D. G. Tarboton (1996), A Nonhomogeneous Markov model for daily precipitation simulation, *Journal of Hydrologic Engineering*, 1, 33-40, 1996.

Rajagopalan, B. and U. Lall (1999), A k-nearest-neighbor simulator for daily precipitation and other weather variables, *Water Resources Research*, 35, 3089-3101.

Rajagopalan, B., U. Lall, and S. Zebiak (2002), Optimal categorical climate forecasts through multiple GCM ensemble combination and regularization, *Monthly Weather Review*, 130, 1792-1811.

Rao, C. R., and H. Toutenburg (1999), *Linear models: least squares and alternatives*, Springer, New York.

Rasmussen, E. M. (1985), El Nino and variations in climate, *American Scientist*, 73, 168-177.

Ray, A. J. (2004), Linking climate to multi-purpose reservoir management: Adaptive capacity and needs for climate information in the Gunnison basin, Colorado, Ph.D. thesis, Univ. of Colorado at Boulder, CO.

Redmond, K. T., and R. W. Koch (1991), Surface climate and streamflow variability in the western United States and their relationship to large-scale circulation indices, *Water Resources Research*, 27, 2381-2399.

Regonda, S., B. Rajagopalan, M. Clark, and J. Pitlick (2005a), Seasonal cycle shifts in hydroclimatology over the Western US, *Journal of Climate*, 18, 372-384.

- Regonda, S., B. Rajagopalan, U. Lall, M. Clark and Y. Moon (2005b), Local polynomial method for ensemble forecast of time series, *Nonlinear Processes in Geophysics*, 12, 397-406.
- Regonda, S. K., B. Rajagopalan, M. Clark, and E. Zagana (2006), A multimodel ensemble forecast framework: Application to spring seasonal flows in the Gunnison River Basin, *Water Resources Research*, 42, W09404, doi:10.1029/2005WR004653.
- Reid, D. J. (1968), Combining three estimates of gross domestic product, *Economica*, 35, 431-444.
- Robertson, A. W., and M. Ghil (1999), Large-Scale weather regimes and local climate over the western United States, *Journal of Climate*, 12, 1796-1813.
- Roos, M. (1987), Possible changes in California snowmelt pattern, *Proc., Fourth Pacific Climate Workshop*, Pacific Grove, CA, 22-31.
- Roos, M. (1991), A trend of decreasing snowmelt runoff in northern California. *Proc., 59th Western Snow Conference*, Juneau, AK, 29-36.
- Ropelewski, C. F., and M. S. Halpert (1986), North American precipitation and temperature patterns associated with the El Nino/Southern Oscillation (ENSO), *Monthly Weather Review*, 115, 2352-2362.
- Salas, J. D. (1985), Analysis and modeling of hydrologic time series, in *Handbook of Hydrology*, edited by D. R. Maidment, pp: 19.1-19.72, McGraw-Hill, New York.
- Santos, E. G., and J. D. Salas (1992), Stepwise disaggregation scheme for synthetic hydrology, *Journal of Hydraulic Engineering*, 118, 765-784.

Serreze, M. C., M. P. Clark, R. L. Armstrong, D. A. McGinnis, and R. S. Pulwarty (1999), Characteristics of the western United States snowpack from snowpack telemetry (SNOWTEL) data, *Water Resources Research*, 35, 2145-2160.

Sharma, A. and R. O'Neill (2002), A nonparametric approach for representing interannual dependence in monthly streamflow sequences, *Water Resources Research*, 38,1100, doi:10.1029/2001WR000953.

Sivakumar B., A. W. Jayawardena and T. M. K. G. Fernando (2002), River flow forecasting: use of phase-space reconstruction and artificial neural networks approaches, *Journal of Hydrology*, 265, 225-245.

Slack, J. R., and J. M. Landwehr (1992), Hydro-Climatic Data Network: A U.S. Geological Survey streamflow data set for the United States for the study of climate variations, 1974-1988, *U.S. Geological Survey Rep.*, pp 92-129.

Singhrattna, N., B. Rajagopalan, M. Clark and K. Krishna Kumar (2005), Forecasting Thailand summer monsoon rainfall, *International Journal of Climatology*, 25, 649-664.

Stewart, I. T., D. R. Cayan, and M. D. Dettinger (2004), Changes in snowmelt runoff timing in western North America under a 'Business As Usual' climate change scenario, *Climatic Change*, 62, 217-332.

Stewart, I. T., D. R. Cayan, and M. D. Dettinger (2005), Changes toward earlier streamflow timing across western North America, *Journal of Climate*, 18, 1136-1155.

Stockton, C. W., and G. C. Jacoby (1976), Long-term surface-water supply and streamflow trends in the Upper Colorado River Basin, *Lake Powell Res. Proj. Bull.* 18, Natl. Sci. Found., Arlington, Va.

- Stokes, M. A., and T. L. Smiley (1968), *An Introduction to Tree-Ring Dating*, Univ. of Ariz. Press, Tucson.
- Swetnam, T. W., M. A. Thompson, and E. K. Sutherland (1985), *Using Dendrochronology to Measure Radial Growth of Defoliated Trees*, *Agric. Handb.*, vol. 639, For. Serv., U.S. Dep. of Agric., Washington, D. C.
- Tarboton, D.G., A. Sharma, and U. Lall (1998), Disaggregation procedures for stochastic hydrology based on nonparametric density estimation, *Water Resources Research*, 34, 107-119.
- Tamea, S., F. Laio, and L. Ridolfi (2005), Probabilistic nonlinear prediction of river flows, *Water Resources Research*, 41, W09421, doi:10.1029/2005WR004136.
- Thomson, D. J., 1995: The seasons, global temperature, and precession, *Science*, 268, 59-68.
- Trenberth, K. E. (1997), The definition of El Niño, *Bulletin of the American Meteorological Society*, 78, 2771–2777.
- Valencia, D. R., and J. C. Schaake (1973), Disaggregation processes in stochastic hydrology, *Water Resources Research*, 9, 580-585.
- Vanrheenen, N. T., A. W. Wood, R. N. Palmer, and D. P. Lettenmaier (2004), Potential implications of PCM climate change scenarios for Sacramento-San Joaquin River basin hydrology and water resources, *Climatic Change*, 62, 257-281.
- Viessman, W., Jr., C. Welty (1985), *Water Management: Technology and Institutions*, Harper & Row, New York.
- Von Storch, H., and F. W. Zwiers (1999), *Statistical Analysis in Climate research*, Cambridge Univ. Press, Cambridge.

- Vogel, R.M. and A.L. Shallcross (1996), The moving blocks bootstrap versus parametric time series models, *Water Resources Research*, 32, 1875-1882.
- Vorosmarty, C. J., P. Green, J. Salisbury, and R.B. Lammers (2000): Global water resources: Vulnerability from climate change and population growth, *Science*, 289, 284-288.
- Wahl, K. L., 1992: Evaluation of trends in runoff in the western United States: Managing water resources during global change, *Proc. Annual Conf. and Symp.*, Reno, NV, American Water Resources Association, 701–710.
- Walpole, R. E., R. H. Myers, S. L. Myers, K. Ye, and K. Yee (2002), *Probability and Statistics for Engineers and Scientist*, Prentice Hall, Upper Saddle River, N.J.
- Wang, W., B. T. Anderson, N. Phillips, R. K. Kaufmann, C. Potter, and R. B. Myneni (2005), Feedbacks of vegetation on summertime climate variability over the North American grasslands: 1. Statistical Analysis, *Earth Interactions* (in press).
- Weare, B. C., and M. A. Hoeschele (1983), Specification of monthly precipitation in the western United States from monthly mean circulation, *Journal of Applied Meteorology*, 22, 1000-1007.
- Wheeler, K., T.M. Magee, T. Fulp, and E. Zagona (2002), Alternative Policies on the Colorado River, in *Proceedings of Natural Resources Law Center Allocating and Managing Water for a Sustainable Future: Lessons From Around the World*, Boulder, CO.
- Wilks, D. S. (1995), *Statistical Methods in the Atmospheric Sciences*, Academic Press, San Diego.

- Wood, A. W., L. R. Leung, V. Sridhar, and D. P. Lettenmaier (2004), Hydrologic implications of dynamical and statistical approaches to downscaling climate model outputs. *Climatic Change*, 62, 189-216.
- Woodhouse C. A., S. T. Gray, and D. M. Meko (2006), Updated streamflow reconstructions for the Upper Colorado River Basin, *Water Resources Research*, 42, W05415, doi:10.1029/2005WR004455.
- Yarnal B., and H. F. Diaz (1986), Relationships between extremes of the Southern Oscillation and the winter climate of the Anglo-American Pacific coast, *Journal of Climatology*, 6, 197-219.
- Yates, D., S. Gangopadhyay, B. Rajagopalan, and K. Strzepek (2003), A technique for generating regional climate scenarios using a nearest neighbor bootstrap, *Water Resources Research*, 39, 1199, doi:10.1029/2002WR001769.
- Zagona, E., T. Fulp, R. Shane, T. Magee, and H. Goranflo (2001), RiverWare: A Generalized Tool for Complex Reservoir Systems Modeling, *Journal of the American Water Resources Association*, 37, 913-929.
- Zagona, E., T. Magee, H. M. Goranflo, T. Fulp, D. K. Frevert, and J. L. Cotter (2006), RiverWare, in *Watershed Models*, edited by V. P. Singh and D. K. Frevert, pp 527-548, Taylor & Francis group, Boca Raton, Florida.